

A Systematic Literature Review of Rotating Detonation Engines (RDE's) & Potential Scalability for Use in Non-Rocket Based Applications

a project presented to
The Faculty of the Department of Aerospace Engineering
San José State University

in partial fulfillment of the requirements for the degree
Master of Science in Aerospace Engineering

by

Ian A. Vaca

May 2023

approved by

Dr. Periklis Papadopoulos
Faculty Advisor



San José State
UNIVERSITY

© 2022
Ian A. Vaca
ALL RIGHTS RESERVED

Abstract

The goal of this paper is to explore an emerging technology in the field of aerospace propulsion, discuss the fundamentals of detonation, analyze the current state of Rotating Detonation Engine (RDE) technology and pinpoint its current limitations via a comprehensive systematic literature review. Secondly, this paper will explore the viability of scalability of the technology via computational fluid dynamics (CFD) simulations in Ansys Fluent.

Acknowledgements

I would like to thank my graduate advisor Dr. Periklis Papdopoulos, my colleague Samuel Zuniga, my classmate Justin Williams, my Mother and Father for their encouragement, my best friend, Ezequiel Wangaard for his support, and finally my girlfriend Isabelle Marques.

Table of Contents

| | |
|----------------------------------|---------|
| 1.0 Introduction | Page 1 |
| 2.0 Systematic Literature Review | Page 33 |
| 3.0 Ansys Fluent Background | Page 57 |
| 4.0 RDE Computational Model | Page 59 |
| 5.0 Analysis & Discussion | Page 80 |
| 6.0 Conclusions & Future Work | Page 82 |

Figures

Figure 1 Specific impulse vs Mach number for various engine types 1

Figure 2 Specific impulse vs Mach number for various engine types 1

Figure 3 NASA technology readiness level TRL scale

Figure 4 Holzwarth explosion turbine

Figure 5 Deflagration to detonation transition

Figure 6 Humphrey cycle p-v diagram

Figure 7 Brayton cycle p-v diagram

Figure 8 Thermodynamic cycle comparison

Figure 9 ZND wavefront diagram with structure

Figure 10 Long-EZ PDE national air force museum

Figure 11 Voitsekhovskiy's stationary spin detonation apparatus

Figure 12 Wang's pre-detonation tube apparatus

Figure 13 NETL'S water-cooled rotating detonation engine

Figure 14 James Koch rotating detonation engine University of Washington

Figure 15 RDE cutaway diagram

Figure 16 RDE thermal gradient view

Figure 17 RDE cutaway with fuel manifold

Figure 18 Systematic review flowchart with steps

Figure 19 Unrolled RDE flow-field from numerical solution

Figure 20 RDE-powered GTD-350 Soviet turboshaft engine

Figure 21 Contour plot for static pressure with 40 injectors

Figure 22 Contour plot for static temperature with 40 injectors

Figure 23 Solving time for mesh reusage vs without mesh reusage

Figure 24 3-Dimensional RDE annulus unrolled into 2-dimensional sheet

Figure 25 3 Different ideal injection conditions

Figure 26 Computational setup in a 2-dimensional simplified RDE chamber

Figure 27 Time-accurate simulation temperature with time-averaged streamline

Figure 28 Ansys Fluent fluid dynamics software automobile flow visualization

Figure 29 NASA CEA program problem selection

Figure 30 NASA CEA program pressure and temperature input

Figure 31 NASA CEA program fuel selection

Figure 32 NASA CEA program oxidizer selection

Figure 33 Ansys Fluent GUI

Figure 34 Ansys Fluent graphical user tree

Figure 35 Ansys Fluent RDE mesh

Figure 36 Ansys Fluent pulse detonation tube mesh

Figure 37 Ansys Fluent pulse detonation tube residuals

Figure 38 Ansys Fluent RDE initial residuals

Figure 39 Ansys Fluent 2nd RDE simulation 50% complete residuals

Figure 40 Ansys Fluent 2nd RDE simulation 50% complete temperature

Figure 41 Ansys Fluent 2nd RDE simulation 50% complete pressure

Figure 42 Ansys Fluent 2nd RDE simulation 100% complete residuals

Figure 43 Ansys Fluent 2nd RDE simulation 100% complete temperature

Figure 44 Ansys Fluent 2nd RDE simulation 100% complete pressure

Figure 45 RDE residual graph mesh scaling

Figure 46 RDE residual graph mesh scaling 0.5x

Figure 47 RDE residual graph mesh scaling 2x

Figure 48 Ansys Fluent RDE scaling 0.5x simulation 100% temperature

Figure 49 Ansys Fluent RDE scaling 0.5x simulation 100% pressure

Figure 50 Ansys Fluent RDE scaling 2x simulation 100% temperature

Figure 51 Ansys Fluent RDE scaling 2x simulation 100% pressure

Figure 52 NASA Marshall Space Flight Center RDE hot-fire testing

Variables

F = Force in Newtons

Th = Thrust in Newtons

V = Velocity in meters per second

Ve = Exhaust Velocity in meters per second

a = acceleration in meters per second squared

g0 = acceleration due to gravity 9.8 meters per second squared

Isp = Specific Impulse in seconds

m = mass in kilograms

M = Mach number

P = Pressure in Pascals

T = Temperature in Kelvin

u = wave velocity in meters per second

Y = Mass fraction of reactants

R = specific gas constant

Ea = activation energy

1.0 Introduction

1.1.1 Motivation

Propulsion system technology is one of the key factors that either serves to advance the aerospace industry forward or limit its potential. Current rocket-based propulsion systems utilize extremely large amounts of fuel whether that be of a solid, liquid, or hybrid nature. Over time, especially as the aerospace industry becomes privatized, this method of space exploration (primarily launch vehicle applications), is not sustainable given the gargantuan financial cost of fuel and the destructive effects that these launches cause to the environment. If we are to move towards a more sustainable future and provide more viable methods of space exploration (opposed to the conventional combustion engine), alternative methods of propulsion must be explored by current scientists and engineers. One of the emerging technologies that shows a very promising potential in terms of efficiency and viability is the Rotating Detonation Engine, otherwise known as an RDE.

RDE's, an excellent candidate for advancing the science of propulsion system technology, have the potential to provide more usable thrust while at the same time consuming less fuel. Different variations of this engine exist, the Pulsed Detonation Engine (PDE), and the Oblique-Wave Detonation Engine (OWDE), all of which use the same phenomena of detonation, contrary to combustion, to produce thrust. The basic concept of a detonation engine is as follows: an ignition of the gaseous fuel is used to cause a detonation whose force provides thrust output from an engine. In the case of the pulsed detonation engine, ignition occurs at repeated instances in a pulsed fashion. However, in the case of a rotating detonation engine, the ignition occurs once and the detonation is sustained. This phenomenon of a sustained detonation wave occurs because the wave travels circumferentially or azimuthally in an annulus (circular

channel), given the proper setup and timing of the engine is in place. The implications of a useful RDE in the real world would mean a potential 25% efficiency increase when compared to conventional combustion engines. Even more, these engines provide the possibility of unlocking hypersonic velocities upwards of Mach 17 for experimental aircraft.

With all this in consideration, RDE's present as a viable pathway for pushing past the stagnancy of the most utilized aerospace propulsion systems, conventional combustion engines. It is important to mention that the entire reason this efficiency is possible is because of the RDE's ability to exhibit a virtual lack of pressure loss in the engine during its operation. In an RDE, the engine has the ability to build its own pressure by a process known as pressure gain combustion. This is far different from what occurs in a conventional turbine engine, where there is in fact a pressure loss. As a result, the RDE's will naturally be more efficient than traditional combustion engines. This principle will be discussed at greater detail to provide further understanding by exploring detonation phenomena. Below is a common graph that compares common propulsion types while looking at their Isp or specific impulse, which is a measure of efficiency. Next, in the figure below, we see that PDE's which are engines exhibiting a pulsed form of detonation fall on this measure at approximately ~9000s. As RDE's contain self-sustaining detonation waves, their efficiency is theoretically even higher than where PDE's lie on this chart. This comparison provides some context for the technological potential that exists here.

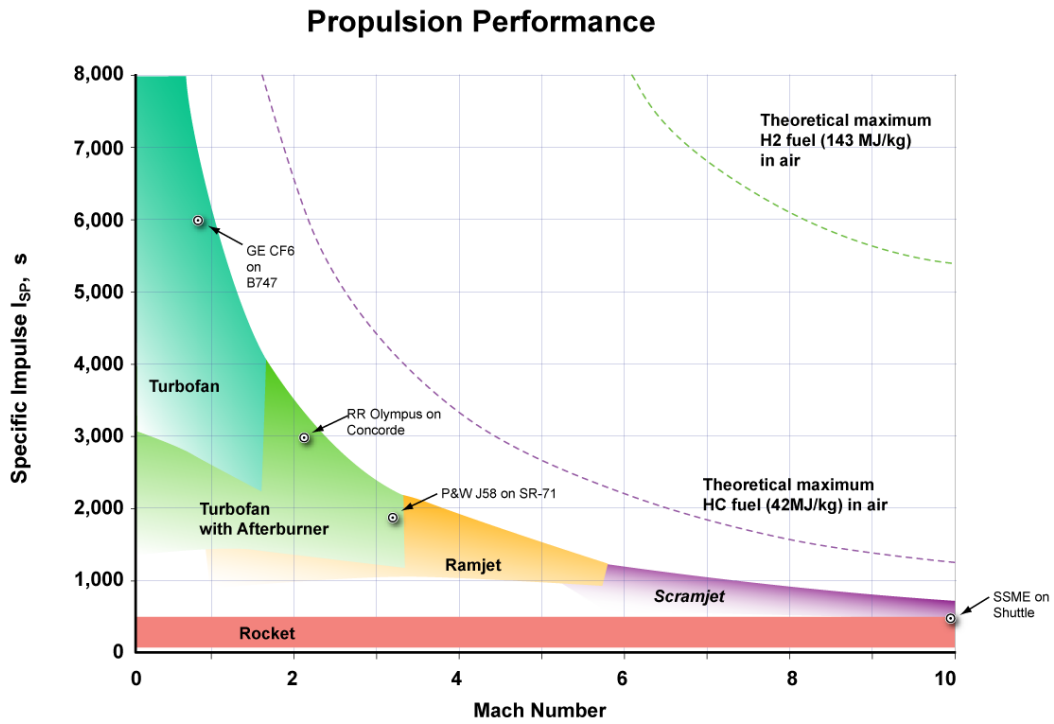


Figure 1 Specific impulse vs Mach number for various engine types 1 [1].

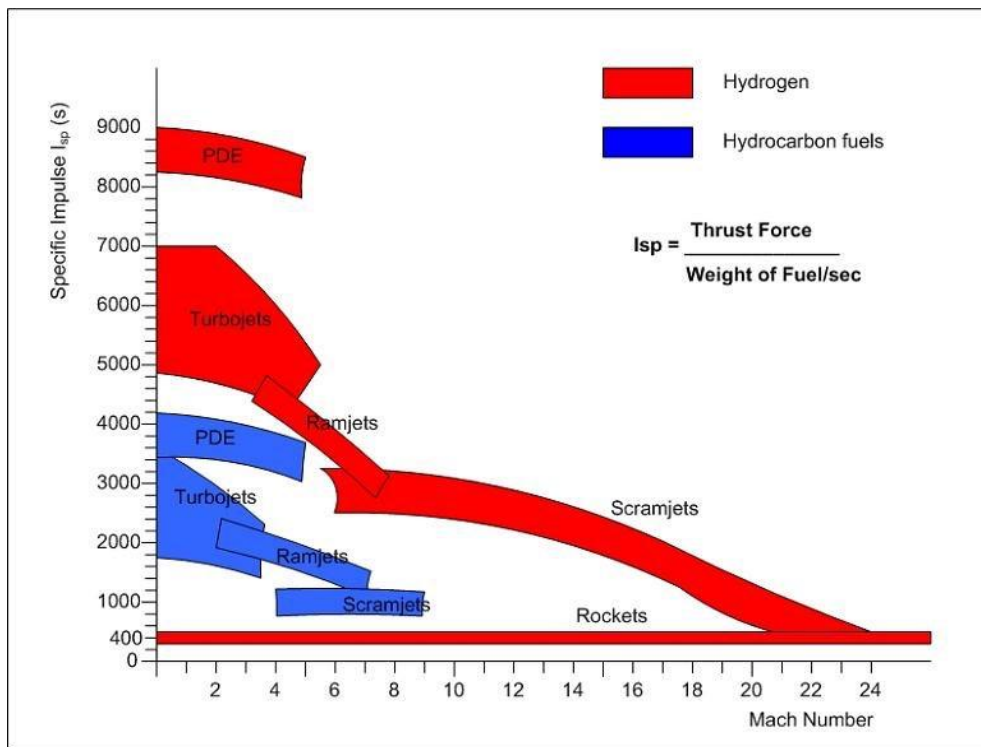


Figure 2 Specific impulse vs Mach number for various engine types 1 [2].

Next, with a basic understanding of the potential benefits of this more recent and novel propulsion system, it is important to qualify exactly where the technology is at. In order to do this, it will provide cause for a need to discuss the current progress of RDE's, the existing challenges faced, and the next steps to arrive at a fully realized system. One way to characterize the RDE in this manner is to determine and then apply an estimated TRL or Technology Readiness Level. "Technology Readiness Levels (TRL's) are a type of measurement system used to assess the maturity level of a particular technology", NASA TRL. The technology in question is evaluated against given criteria for levels 1 through 9, with 9 being the highest (flight-proven). TRL 9 is our objective, but arriving there takes years of iterations, tweaking the design, and revised experiments. To arrive at the end goal we must first know where in fact we are.

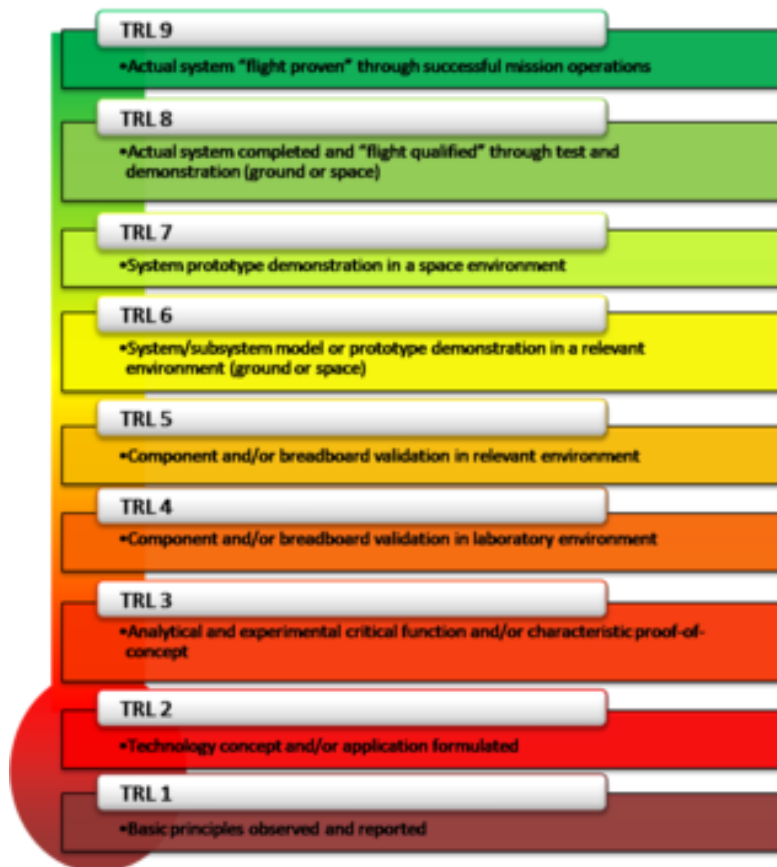


Figure 3 NASA technology readiness level TRL scale [3].

Finally, is this new technology scalable? According to existing literature, this has not been explored. Some basic analyses must be conducted to determine this and fully understand the subject of ‘scalability’ as it applies to RDE propulsion systems. This will first explore the current integration of the technology and additional viable use cases as applied to different applications or spacecraft, ideally of smaller size than has currently been exhibited or explored. For example, if the RDE has the ability to be downsized and retain its overall efficiency where parameters such as theoretical specific impulse (Isp) are virtually unaffected, it can propel smaller spacecraft such as large satellites, cubesats, or be a means of spacecraft attitude control.

$$I_{sp} = V_e / g_0 \quad (1.1)$$

If true, this could create a great paradigm shift in the aerospace industry, by decreasing fuel cost for these applications and spurring the discovery of even more fuel-efficient engines.

1.1.2 Background & Detonation Phenomenon

As mentioned, this project has been broken into two separate parts. The initial plan was to complete an entirely research-based project. However, given that it might not fulfill the requirements of AE 295, a new project was devised with the faculty advisor that will include the need for some analysis. This section of the paper will include a comprehensive systematic review of the literature that currently exists on the topic of Rotating Detonation Engines RDE’s, their viable status as a useful technology, and their potential applications.

Let’s take a step back to understand how Rotating Detonation Engines came about. As mentioned, RDE’s are a relatively new and emerging technology within the sector of aerospace propulsion. These specific engines are lumped together with related engine types such as Pulsed Detonation Engines PDE’s and Oblique-Wave Detonation Engines OWDE’s. Each of these

engines are unique in the following way: they utilize the phenomena of detonation as a form of energy-force conversion rather than the conventional phenomena of combustion. This process can also be referred to as *pressure-gain combustion*. All three of the aforementioned methods of propulsion utilize this process. Pressure gain combustion can be defined as: “A fundamentally unsteady process whereby gas expansion by heat release is constrained, causing a rise in stagnation pressure and allowing work extraction by expansion to the initial pressure” [4]. This refers to the key differentiating factor between RDE’s and combustion engines: a virtual lack of pressure loss for the RDE. This concept has existed for some time and has been implemented in a variety of engines dating back to the Holzwarth Explosion Turbine in 1914 [5].

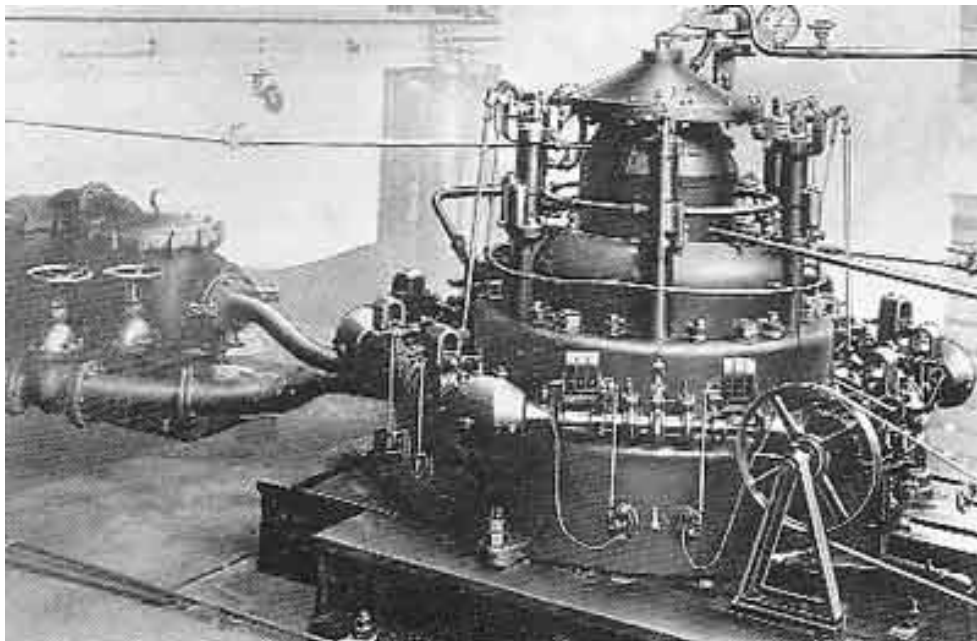


Figure 4 Holzwarth explosion turbine [5].

It is important to further define the features that distinguish detonation engines from typical aerospace propulsion systems (combustion engines). The defining characteristic is the use of detonation in substitution of deflagration. Deflagration is the method of subsonic combustion (less than Mach 1) that propagates through the medium via heat transfer, which is a

relatively slow process. There exists an entire host of advantages as well as disadvantages to this method, such as:

1. being more stable in nature (easier to control)
2. having a lower overall fuel efficiency
3. being a constant pressure process

This is without question a technology of TRL 9 as combustion engines have been flight-proven on rockets such as NASA's Saturn V back in the 60's all the way up to SpaceX's Falcon 9 of the present day.

On the other end of the spectrum there exists detonation, which differs from deflagration in some key aspects making it more attractive in certain respects, but at the same time causing special considerations to be taken. Detonation is supersonic combustion (greater than Mach 1) that propagates through the medium via shock waves. Some characteristics that describe this phenomenon are:

1. chaotic in nature (difficult to control)
2. a higher overall efficiency (less fuel consumption)
3. a constant pressure process (adiabatic)

These two processes are closely related as there exists what is called a deflagration-to-detonation transition, otherwise known as a DDT. "Deflagration to detonation transition is the general process by which a subsonic wave (deflagration or flame) becomes a supersonic combustion wave (detonation)" [4]. Below is an illustration of what this looks like in a laboratory environment. Notice the uniformity of the shock compared to the flame.

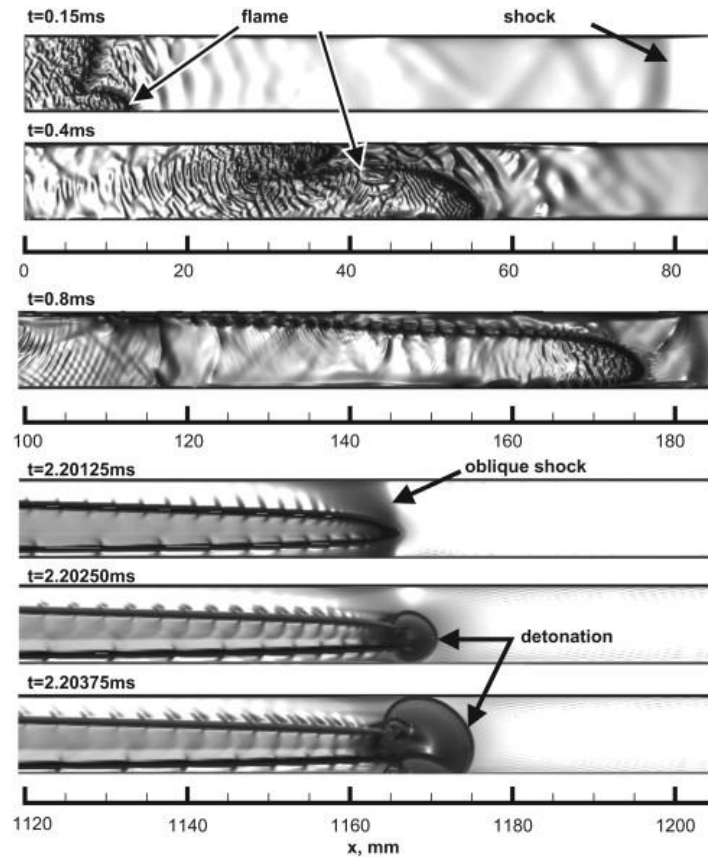


Figure 5 Deflagration to detonation transition [7].

Current theoretical models and experimental results show that the detonation process can yield a higher efficiency (up to $\sim 25\%$) when compared to combustion engines depending on the injection scheme being modeled or utilized [8]. This potential alone is the primary reason that exists for the need for further development of this engine. Accomplishing a quarter increase in efficiency will have huge implications for the field of aerospace, the energy sector, and more specifically for propulsion technology.

When it comes to detonation, it is highly complex, and very difficult to model exactly, similar to the unsolved case of turbulent flow when examining the Navier Stokes equations. As necessary, detonation has been described by several theoretical models in order to simplify existing uncertainties for the sake of a more rudimentary analysis. Some of the theoretical

models that attempt to characterize detonation are the ZND Theory and the Chapman-Jouguet Condition [9], which will be explored further. First, it is important to note that typical detonation (modeled in Pulsed Detonation Engines or PDE's) utilizes the Humphrey cycle. This is in contrast to the Brayton cycle utilized by typical combustion processes. The Humphrey Cycle PV diagram illustrated below, can be thought of as a 'modified Brayton Cycle' [10]. The main difference is that the constant pressure heat addition is replaced by one of constant volume [10].

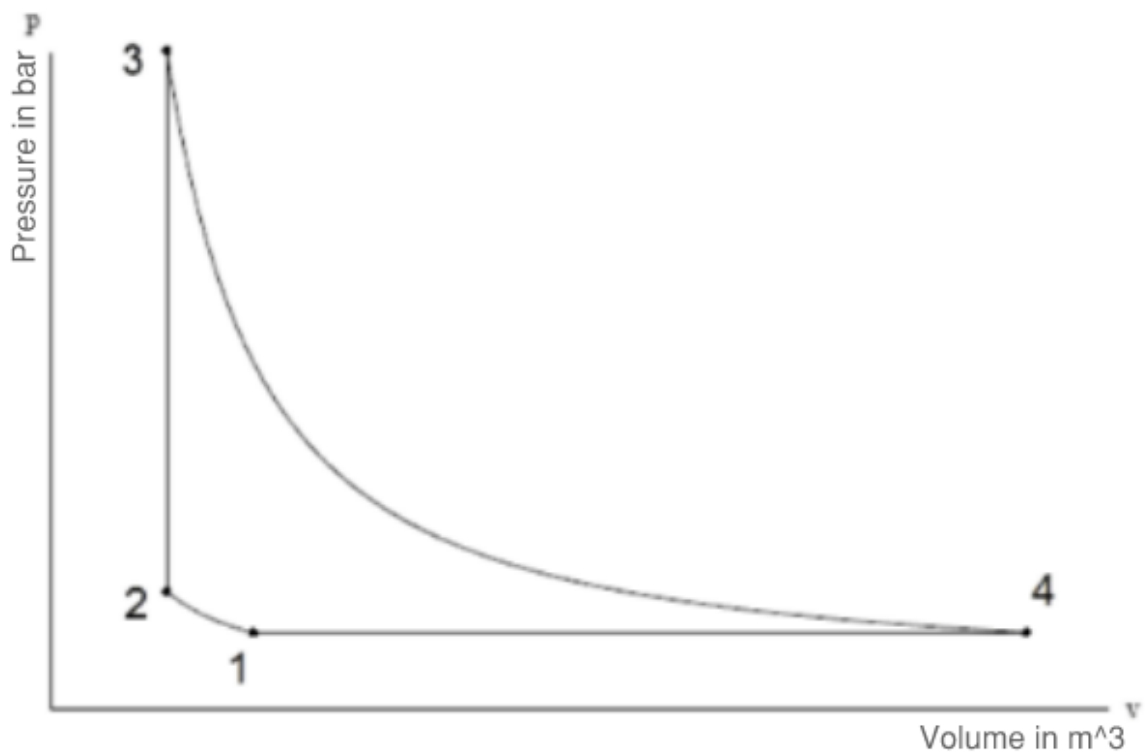


Figure 6 Humphrey cycle p-v diagram [10].

The following explanation helps to explain the transition from various states along the P-V Diagram. From states 1 to 2 there is reversible, adiabatic (isentropic) compression. From states 2 to 3 there is constant-volume heat addition. From states 3 to 4 there is reversible, adiabatic (isentropic) expansion. Finally, returning to state 1 from 4 there is constant-pressure

heat rejection. Let's now explore the idealized Brayton Cycle below:

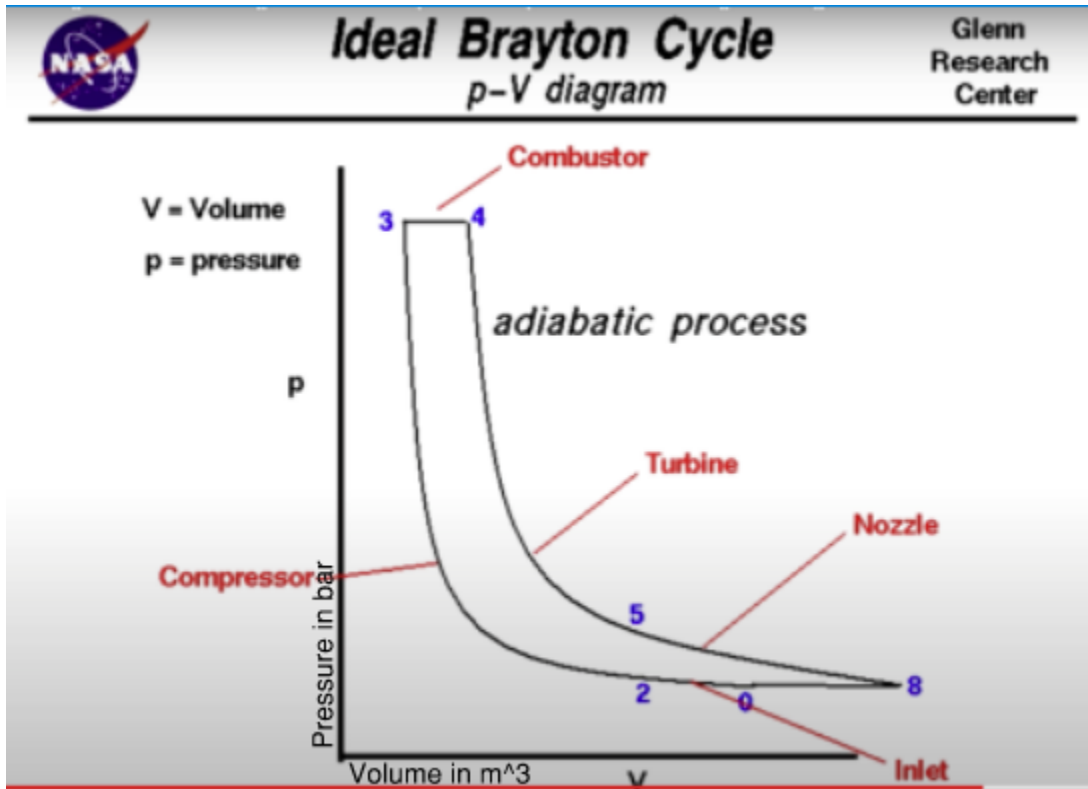


Figure 7 Brayton cycle p-v diagram [11].

The following explanation helps to explain the transition from various states along the P-V Diagram. First, from states 1 to 2 there is adiabatic compression. Second, from states 2 to 3 there is isobaric heat addition. Third, from states 3 to 4 there is adiabatic expansion. Finally, returning from state 4 to 1 we have isobaric heat rejection. The main difference between these two cycles is that the Humphrey Cycle, utilized in rotating detonation engines, is the pressure gain discussed earlier seen in Figure 6. This is not seen in the conventional Brayton cycle used in combustion engines. Because of the pressure loss in a Brayton cycle, there is a need for a compressor in combustion engines, this need does not exist with RDE's. This differentiating factor that characterizes this non-conventional propulsion technique is what causes an overall

increase in efficiency, theoretically. The problem at hand is being able to harness that extra energy and keep the engine (detonation waves) operating in a stable fashion, non-destructively.

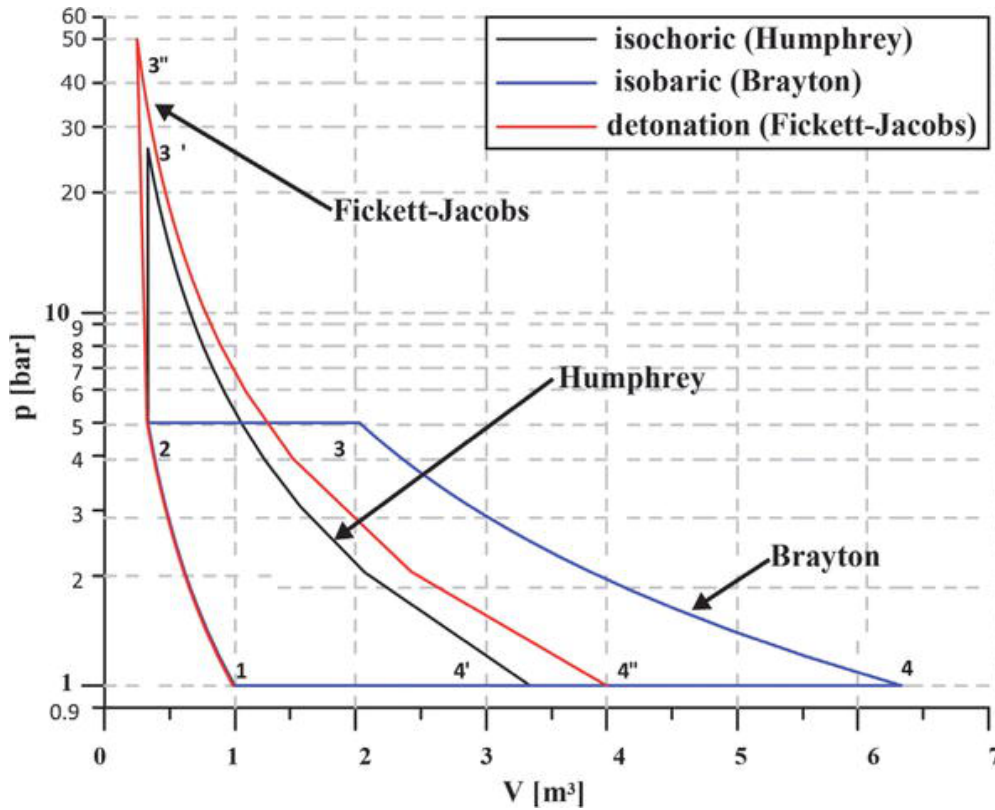


Figure 8 Thermodynamic cycle comparison [12].

Finally, RDE's utilize a cycle that differs ever so slightly from the Humphrey Cycle. The main difference in characterization between PDE's and RDE's when looking at engine cycles and P-V Diagrams is that RDE's are characterized by self-propagating or sustained detonation waves. This contrast with a pulsed form of detonation means that an even higher pressure cycle is displayed by the engine, otherwise known as the Fickett-Jacobs cycle. The need for purging in an RDE is absent, but required for PDE's. Another important aspect of the above graph to note is that in the Fickett-Jacobs curve, there is no change in Volume from phases 2 to 3 making it similar to the Humphrey cycle, but different from the Brayton cycle.

| Fuel | Brayton (%) | Humphrey (%) | Fickett-Jacobs (%) |
|--|-------------|--------------|--------------------|
| Hydrogen (H ₂) | 36.9 | 54.3 | 59.3 |
| Methane (CH ₄) | 31.4 | 50.5 | 53.2 |
| Acetylene (C ₂ H ₂) | 36.9 | 54.1 | 61.4 |

Table 1.1 Cycle fuel efficiency comparison with fuel types [12].

$$\eta_B = 1 - \frac{1}{\left(\frac{p_2}{p_1}\right)^{\frac{k-1}{k}}} \quad (1.4)$$

$$\eta_H = 1 - k \frac{T_1}{T_2} \frac{\left(\frac{T_{3'}}{T_2}\right)^{\frac{1}{k}}}{\frac{T_{3'}}{T_2} - 1} \quad (1.5)$$

$$\eta_F = 1 - k \frac{1}{\left(\frac{p_3}{p_1}\right)^{\frac{k-1}{k}}} \frac{\left(\frac{T_{3'}}{T_2}\right)^{\frac{1}{k}} - 1}{\frac{T_{3'}}{T_2} - 1} \quad (1.6)$$

Above are the fuel efficiency equations for the Brayton, Humphrey, and FJ Cycles [12]. Looking at the difference in fuel efficiencies at the different cycles discussed, it is clear that the Fickett-Jacobs cycle exhibits the highest efficiency with an average overall ~23% increase of fuel-efficiency when compared to the Brayton cycle. In other words, RDE's in theory are approximately 23% more efficient than traditional combustion engines given the above fuel types of Hydrogen, Methane, and Acetylene. This does not include potential experimental mixtures, which may yield an even higher efficiency. Thus, there is now an approximation for calculating the total Work performed due to a self-propagating detonation.

Furthermore the Fickett Jacobs cycle is based on the Chapman-Jouguet Condition, which approximates the velocity of the detonation wave in the following way. The Chapman-Jouguet Condition states that: “the detonation propagates at a velocity at which the reacting gasses just reach sonic velocity (in the frame of the leading shock wave) as the reaction ceases” [13]. Below are some of the basic equations that serve to approximate this velocity relationship:

$$\mu = \gamma \frac{\tilde{p}}{\tilde{v}}. \quad (1.7)$$

$$M_2 = \frac{u_2}{c_2} = 1 \quad (1.8)$$

$$\tilde{p}_{\pm} = 1 + \alpha(\gamma - 1) \left\{ 1 \pm \left[1 + \frac{2\gamma}{\alpha(\gamma^2 - 1)} \right]^{\frac{1}{2}} \right\} \quad (1.9)$$

$$\tilde{v}_{\pm} = 1 + \frac{\alpha(\gamma - 1)}{\gamma} \left\{ 1 \mp \left[1 + \frac{2\gamma}{\alpha(\gamma^2 - 1)} \right]^{\frac{1}{2}} \right\} \quad (1.10)$$

$$\mu_{\pm} = \gamma + \alpha(\gamma^2 - 1) \left\{ 1 \pm \left[1 + \frac{2\gamma}{\alpha(\gamma^2 - 1)} \right]^{\frac{1}{2}} \right\} \quad (1.11)$$

$$M_{1\pm} = \left[1 + \frac{\alpha(\gamma^2 - 1)}{2\gamma} \right]^{\frac{1}{2}} \pm \left[\frac{\alpha(\gamma^2 - 1)}{2\gamma} \right]^{\frac{1}{2}} \quad (1.12)$$

This model was originally formulated as applied to an infinitesimally thin detonation, however, later a physical interpretation (one-dimensional model) of this theorem came about

known as the ZND Detonation Model, proposed during World War II by Zeldovich, Neumann, and Doring. The ZND Model is as follows:

1. “An infinitesimally thin shock wave compresses the explosive to a high pressure called the Von Neumann Spike”
2. “At the Von Neumann spike point the explosive still remains unreacted”
3. “The spike marks the onset of the zone of exothermic chemical reaction, which finishes at the Chapman-Jouget State”
4. “Finally, the detonation products expand backward”

It is important to note that for a self-propagating detonation (that is, those utilized in RDE's), the shock relaxes to a speed given by the Chapman-Jouget condition (mentioned earlier), which causes all chemical energy to be harnessed by the detonation process and propagate the shock wave forward. Finally, when performing experiments to test the ZND Theorem in the 60's, the structures are often three-dimensional, not one-dimensional, and must be accounted for by the Wood-Kirkwood Detonation Theory, which can describe this process multidimensionally.

The ZND structure

Zel'dovich, von Neuman, Döring

shock followed by a fast flame

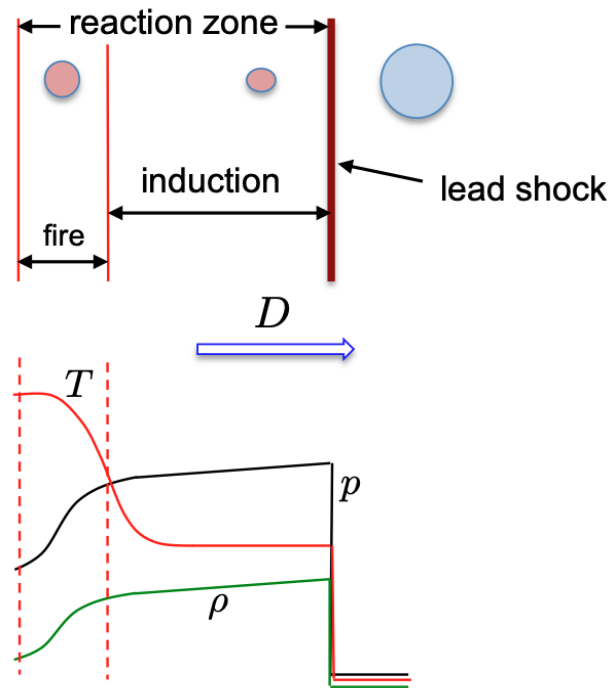


Figure 9 ZND wavefront diagram with structure [14].

Above in Figure 9 is a diagram that illustrates the wavefront described by the ZND Theorem in a 2-dimensional view [14]. The wavefront diagram is in line with a Temperature, Pressure, and Density ρ graph to show how these parameters vary along the length of this wavefront. First, there is the fire and induction, which make up the reaction zone. Directly after the induction zone, as the wave moves from left to right, is the leading shock of a detonation wave.

1.1.3 Detonation Engines, A History of Experimentation

There exists a brief history of detonation engines without a discussion of which would be detrimental to this research. In terms of the historical timeline of detonation engines and their use, the first flight-proven concept is relatively recent considering the year is currently 2022. About 14 years ago in 2008, the Air Force Research Laboratory first utilized a Pulse Detonation Engine to power the flight of a Scaled Composites Long-EZ [15]. This method of detonation is rudimentary at best, given the fact that a pulsed configuration requires constant purging of the engine and the detonation wave is not sustained or as self-propagating as discussed earlier. This ends up not being nearly as efficient, including extra steps to the sequence of operation of the engine as well as additional components. PDE's, although promising, proved to be a less-than ideal way to propel an aircraft because of the added complexity.



Figure 10 Long-EZ PDE national air force museum [16].

Most likely, the very first instance of the continuous detonation engine concept is seen to have been developed by a scientist with the name Voitsekhovsky. In the *Journal of Applied Mechanics and Technical Physics*, his paper entitled: “*Stationary Spin Detonation*,” a continuous detonation was achieved by utilizing an oxy-acetylene fuel mixture in a low-pressured disk-shaped chamber. Voitsekhovsky conducted this experiment at the Institute of Hydrodynamics at the Soviet Academy of Sciences. Although a bit more rudimentary and not exactly a rotating detonation engine, this achievement was a milestone that marked the beginning of this type of research and experimentation of sustained detonations. These experiments dated all the way back to the 1960’s [17].

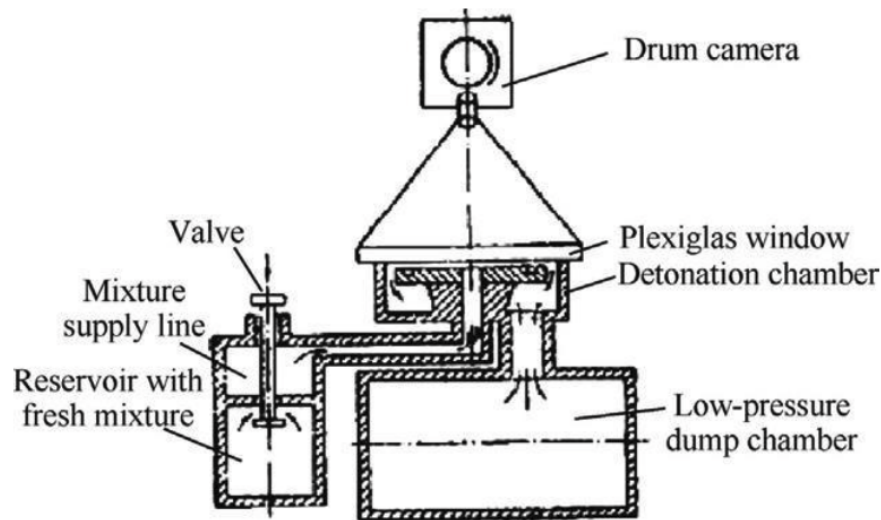


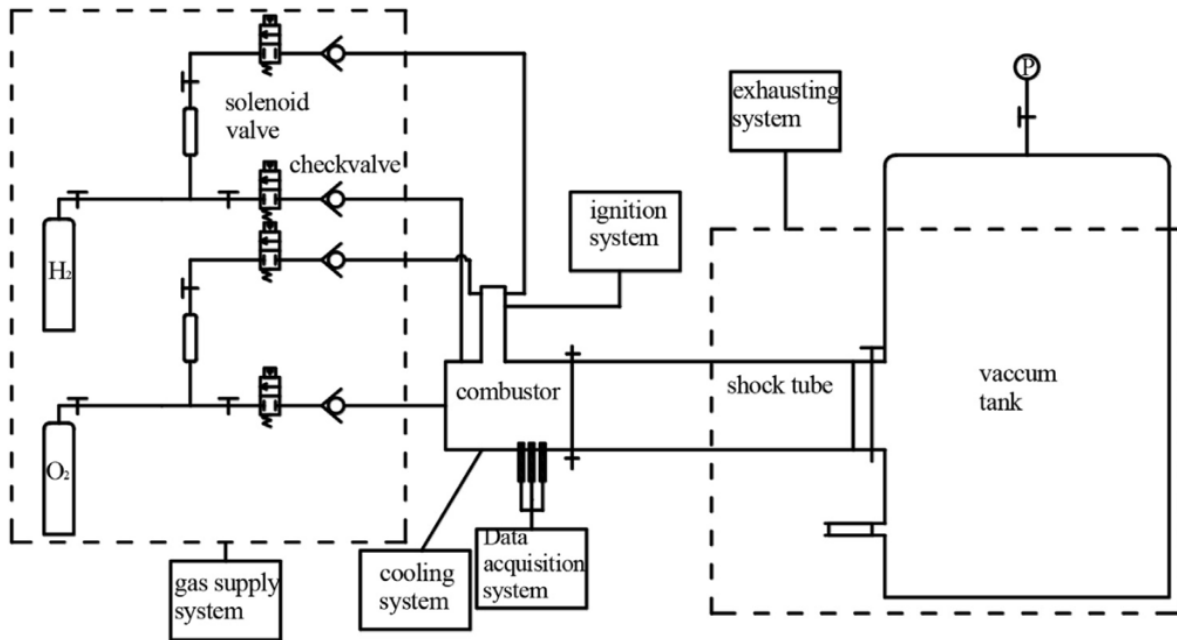
Figure 11 Voitsekhovsky’s stationary spin detonation apparatus [17].

One of the more notable researchers who devised and performed experiments of this caliber from a similar background was a man by the name of Bykovski. Bykovski was able to successfully perform these experiments at the Institute of Hydrodynamics in Russia in a cylindrical chamber or annulus as is a characteristic of the RDE. Fuel types were varied along with oxidizer to produce a number of different sustained results of stable detonation waves. The

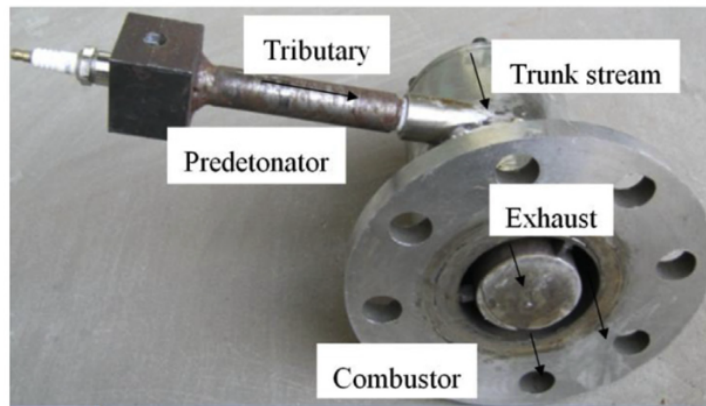
slow, but steady progression of rudimentary design to proof-of-concept RDE experiments was encouraging to see throughout this era of scientific advancement. The years in which the Bykovski experiments took place were primarily in the early 2000's.

Next, there has been a substantial amount of research and experimentation done in China by a researcher with the name Yuhui Wang at Peking University. Throughout many trials Jianping and his team were able to produce and sustain detonation waves successfully in a circular chamber (annulus). This was done utilizing a mixture of hydrogen/oxygen for fuel and allowed operating conditions for wave propagating velocities of over 2000 m/s. One of the key results of this experimentation was the discovery of advantages to utilizing a pre-detonator channeled apparatus for directing the detonation wave into the main chamber of the engine. Ultimately it was discovered that there is a period of time between the maturation of the detonation wave and the time, which the detonation wave is initiated. This is the reason they had found for the case of a pre-detonation chamber being utilized in the rotating detonation engine, Wang and Liu. Below is a figure including the plumbing and instrumentation diagram or P&ID for the detonation engine, including the pre detonation chamber. This provides an excellent framework and context for future research and design work of even better rotating detonation engines. This research took place concurrently with similar discoveries being made by Liu, also a Chinese researcher.

Finally, another notable discovery in China was made by Zheng. Utilizing orifices with slot-like formation, injection methods were simulated with a conventional spark plug. These experiments yielded close to a 95% success rate of creating the detonation wave. Just about one of the hardest processes in the sequence of operation of an RDE [19].



(a) Experimental system



(b) Combustor

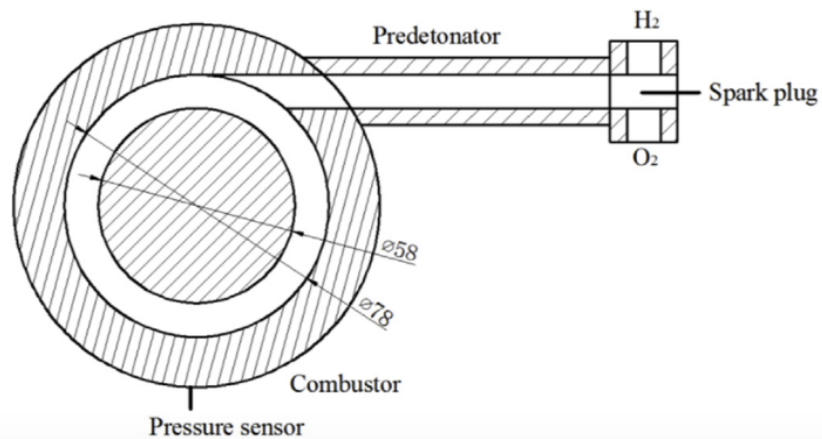


Figure 12 Wang's pre-detonation tube apparatus [20].

Another individual with very successful experimentation of RDE's is Wolanski, a scientist with a team of researchers in Poland at the University of Warsaw. Utilizing a typical cylindrical chamber, successful detonations were produced and sustained in a laboratory environment. These experiments were on a small scale with the largest diameter being 200mm. Fuel types experimented with include: acetylene, ethane, hydrogen, propane, and methane with oxygen [21]. Wolanski goes on to investigate a rotating detonation engine in the configuration of a turbojet by replacing the typical combustor with a detonation wave combustor. This is one of the first applications of the technology that we serve in the form of a viable propulsion system which is already flight-proven [21].

In addition, two very notable groups that are on the cutting edge of aerospace and rocket propulsion today involved in the design and development of RDE's have been Pratt & Whitney as well as Aerojet Rocketdyne. Pratt & Whitney, headquartered in East Hartford, Connecticut is specifically known for their advancements in aircraft engines for both civil and military applications. They have dabbled in the field of RDE's and have successfully demonstrated a modular concept of hardware integration for these engines with successful firings and sustained detonation of various fuel types. Aerojet Rocketdyne has had similar success with a modular hardware concept configuration as well displaying sustained detonation cycles in their prototype engines. Finally, the AFRL (Air Force Research Labs) have had extensive collaboration with a number of universities in more recent events, which are listed later on.

Up until the present time, one of the more successful experiments of a generic rotating detonation engine has been conducted by the U.S. Naval Research Laboratory [22]. Kailasanath, one of the greater known names in the more recent work of detonation engine technology, goes into the experimentations in much greater detail. This is by far the most successful model that

has been replicated in the real world, and it will be discussed further in the systematic review. Another very notable author in the field of detonation-powered propulsion is Thomas A. Kaemming with Innovative Scientific Solutions in Dayton, Ohio. Kaemming provides a very insightful overview of the technology as well as a method for modeling its performance using a reduced order approach [23,24]. Reduced order models exist to scale down the complexity or granularity of the solution. Below is pictured the DOE's water-cooled RDE:



Figure 13 NETL'S water-cooled rotating detonation engine [25].

When reading through the literature, another name for the engine configuration in question is: Continuous Rotating Detonation Engine (CRDE). The operation of these engines can be briefly described and characterized in the following ways: Utilizes a detonation wave or waves that travels circumferentially or azimuthally around a circular channel known as an annulus. Form of pressure gain combustion that “effects a rise in effective pressure across the

combustor by utilizing the same fuel as a typical constant pressure combustor” [26]. Fuel and oxidizer are injected into the channel via small openings to be detonated by use of an ignition source. After the first detonation/ignition, the detonations are “self-sustaining”. Some of the advantages of this type of engine include: no moving parts, single ignition sequence required, waves cycle around the chamber (no need for purging like in a PDE). There is less complexity involved, no compressor required, and a smaller combustion chamber can be used.

In the present era of academia, many of the advancements with RDE technology that have been publicized take place in scholarly settings of higher education such as research-focused departments in Universities. In order to provide a brief summary, some of these Universities are:

1. University of Cincinnati - Air Force Research Laboratory
2. University of Central Florida - Air Force Research Laboratory
3. University of Alabama Huntsville
4. University of Washington in Seattle, WA
5. Peking University in China

Going back to the subject of engine operation, as a reminder, this method of propulsion produces axial thrust, therefore it is imperative to maintain optimal operating conditions inside the annular channel so that the detonation waves continue to propagate throughout and not dissipate or cancel themselves out. One example of this is keeping the detonation waves ‘in-phase’ with each other so they do not operate in a destructive manner. James Koch, a researcher with University of Washington displays and discusses a type of “Mode-Locking” in his paper: “Mode-Locked Rotating Detonation Waves: Experiments and a Model Equation” [27].

This may provide a means of fine-tune control for the operation of detonation, something which had previously been seen as an uncontrollable phenomena.

In conclusion, the primary advantage that this type of propulsion system has over the conventional is that of a “self-sustaining” thrust. The system only needs to be initiated once and the detonation waves travel circumferentially or azimuthally until they slowly dissipate and decompose over time. This facet alone of the design saves time and stress on the engine when compared to a traditional combustion engine. Not to mention the fact that there is virtually no pressure loss compared to combustion.

To summarize, there are a number of current challenges and hangups with this technology that must be overcome in order to achieve longer periods of sustained detonation. Most of the experimentations exhibiting sustained detonations have been relatively short, especially when compared to traditional combustion engines and other flight-proven technology. A number of these challenges include:

1. Intense heat transfer into walls by turbulence and shock waves during detonation
2. Pressure losses in fuel feeding system, not easily sustained
3. Insufficient fuel / oxidizer mixing in the detonation process before injection

These are all according to the literature (Zuniga, SJSU) [28]. There are extremely high temperatures in the engine that transfer to the walls, one potential solution for this can be solved by more studies in the area of materials engineering. Regarding the pressure losses, a pressure-feeding device will most likely need to be devised. With a modular approach to the hardware, this could be realized in a more straightforward manner. Finally, regarding the insufficient fuel and oxidizer mixing prior to the injection and detonation process, a device must also be proposed to properly mix fuel and oxidizer, verify mixing, and inject into the detonation

chamber. This has been explored recently according to an AIAA Propulsion and Energy journal article exploring the design and experiments of a physical continuous rotating detonation engine, detailing fuel mixing [29]. Of course, all these solutions sound relatively straightforward in theory, but prove to be much more involved in simulations and in experimental practice. These will be explored at greater length in the systematic literature review, Section 2.0.

1.2 Proposal

1.2.1 Systematic Literature Review Proposal

The goal of this project is to address two separate objectives. First and foremost, there is the need to provide the reader and greater scientific community with a baseline in terms of today's detonation engine technology, what has been successfully accomplished in the field, the current limitations that exist, and the potential next steps that need to be taken in order to realize this propulsion system. This will be done via a systematic literature review of rotating detonation engine technology.

1.2.2 Sizing & Scalability Analysis Proposal

Secondly, in order to fulfill the analytical requirement of the Master's Project, the scalability of the rotating detonation engine will be explored. Scalability is the ability of the technology, in this instance a propulsion system, to be physically shrunk down and replicated at a smaller (or larger) scale. The reason of interest would be as an application for non-rocket based applications like satellites, including cubesats. Other than the cost-savings due to efficient use of fuel, this is an area of interest for the reason that it could provide cubesats the ability to travel further distances than previously thought possible.

1.3 Methodology

1.3.1 Systematic Literature Review Methodology

In order to accomplish this a Systematic Literature Review of the current literature will be conducted. The different phases of this review will include a breakdown of the rotating detonation engine in order to address how it operates, the phenomena involved, and the various considerations that must be taken to bring about a functioning prototype. Next, successful and unsuccessful experimentation and simulations will be carefully examined in order to determine what works and what does not. Finally, the current limitations of the technology will be outlined and as a result a pathway for next steps will be determined to guide future endeavors.

1.3.2 Sizing & Scalability Analysis Methodology

Regarding the second purpose of analysis to determine scalability of the technology, a simulation will be devised to be run in ANSYS Fluent, an aerospace industry-popularized fluid dynamics modeling software, to provide a baseline for conventional engine size and performance. Once this baseline simulation is achieved, the setup parameters will be scaled down to emulate an engine the size of a 1U form-factor, with the intention for potential use on a cubesat as a propulsion system. Results of both simulations will be analyzed and compared with data that already exists to confirm or deny the ability of the RDE to be scaled successfully.

1.4 Mechanical Overview of the Rotating Detonation Engine

Before beginning the systematic literature review or the rotating detonation engine CFD analysis, the mechanical construction of RDE's must be explained. To understand exactly how Rotating Detonation Engines operate, it is necessary to first fully understand the design and construction of such an engine. This section will explore the mechanical design of the RDE engine and detail its operation in a sequenced fashion, that can serve as a rough template for laboratory experiments. More importantly, a discussion of the RDE design is necessary before even considering any modeling or simulation aspects of its operation. What provides the greatest understanding in this case will be looking specifically at diagrams of the RDE in a traditional mechanical form, a schematic diagram, and finally a thermal visualization to understand where fuel flows and detonations take place in the engine.

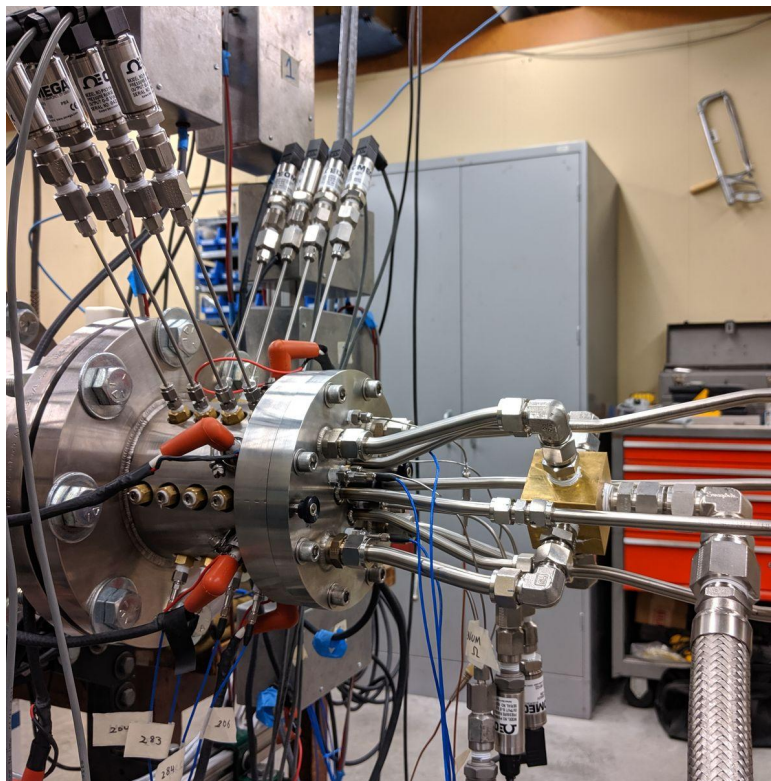


Figure 14 James Koch rotating detonation engine University of Washington [30].

In Figure 14, James Koch's RDE at the University of Washington, we have a basic photograph of a fully functional and operational rotating detonation engine that has been constructed, simulated, and tested at the University of Washington. This particular engine was featured in popular mechanics in order to help popularize the notion that much more efficient propulsion systems are probable and necessary steps forward to continue and sustain spaceflight. The rotating detonation engine at University of Washington was constructed by a researcher by the name of James Koch, who has run successful tests and simulations of the engine and displayed what has been coined as "mode-locking". This "mode-locking" refers to the ability to maintain the phase of multiple detonation waves that are rotating circumferentially around the annulus so that they do not act destructively nor do they produce bifurcations. Bifurcations in this case refers to the splitting division of one detonation wave into multiple waves. This is natural at the beginning of the detonation process, but must be prevented in order to maintain the aforementioned mode-locking. Although visually complex the engine can be explained diagrammatically.

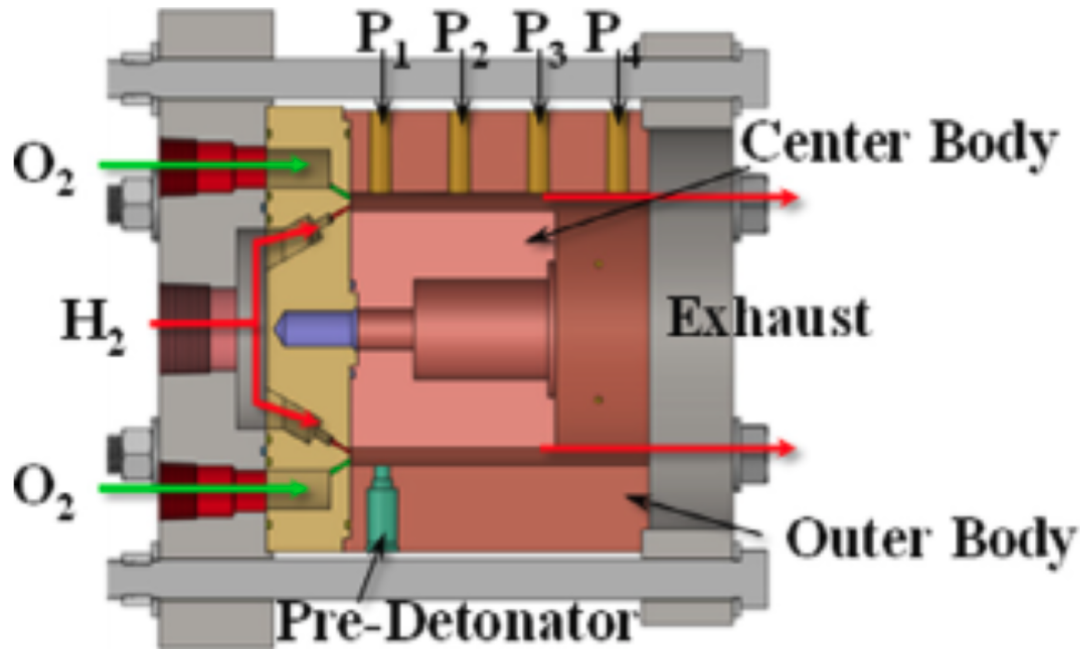


Figure 15 RDE cutaway diagram [31].

In Figure 15 RDE cutaway diagram [31], there is shown a sliced-view cross-section of a conventional rotating detonation engine with components, fuel, and characteristics labeled accordingly. The diagram comes from a study performed by the several researchers at the Central University of Florida Propulsion and Energy Research Laboratory. These experiments utilized a 3" RDE modeled after the Air Force Research Laboratory (Edwards Air Force Base) engine. This model incorporates H₂ and O₂ jets in an impinged formation that make up the propellant injectors. The injectors for fuel and oxidizer can be seen clearly on the left side of the diagram, both of which feed directly into the annulus, which is where the denotations travel circumferentially in the engine. P₁ thru P₄ annotate the pressure sensors or pressure transducers that are recording the pressure inside the annulus, and finally the exhaust is seen as the center chamber.

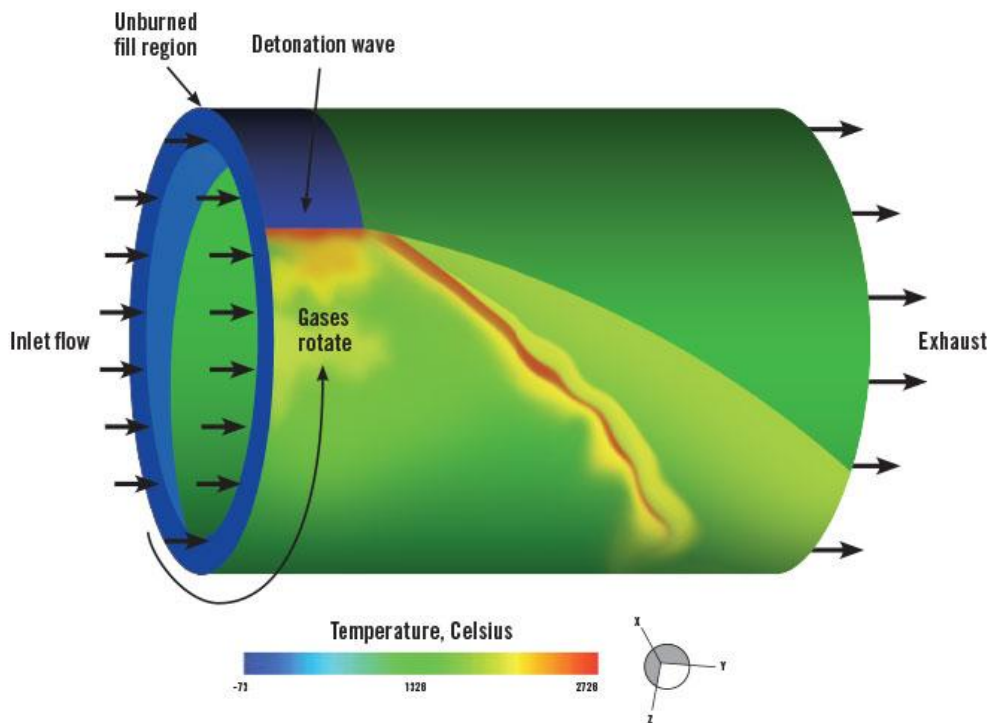


Figure 16 RDE thermal gradient view [32].

In Figure 16 Rotating Detonation Engine Thermal View [32], there is a thermal temperature gradient view of a rudimentary rotating detonation engine. This image comes from Aerojet Rocketdyne’s Advanced Program Rocket Shop in Alabama. Examining the engine view, we first notice that the side profile denotes a primary flow from left at the inlet to right at the exhaust. The direction of rotation of gasses in this case is counterclockwise, but in this type of engine will always be dependent on the injection setup at the inlet. In addition to the circumferential rotation, the gasses of detonation also travel in a lateral direction from left to right. Notice that the exhaust is expelled through the annulus or cylindrical portion of the engine and not the center channel as is the case with a typical combustion engine. The reason for the cylindrical design is as follows according to the researchers at Aerojet Rocketdyne: “Detonation combustion needs to occur in a space where its volume remains constant, which is why the

design is cylindrical; in deflagration combustion, the volume of the combustion has room to expand.” [32].

The view above does not include a nozzle on the engine, this is something that makes the RDE a bit modular. “Like all jet-thrust reaction-based engines, the exhaust from a RDE may be channeled through a nozzle to increase thrust. Outlet and nozzle designs have varied across different RDEs. Many have not attached any nozzle, whilst some have chosen to utilize an aerospike” [12]. A number of researchers touch on this subject in Ian Shaw’s paper of which he details a Theoretical Review of Rotating Detonation Engines [12]. Some designs tend to have the fuel and oxidizer mix right at the inlet of the detonation channel, while others are premixed and injected as a mixture into the detonation chamber. Numerous studies have been conducted both numerical and experimental exploring the advantages and disadvantages of both of these methods. In the case of the figure below, Figure 17, the entire fuel and oxidizer injection system is made up of several modular parts, the feed lines, the oxidizer and fuel manifold, and the fuel injection plate. Probably one of the biggest shortcomings with the technology today is the injection scheme or method used to ignite these RDE engines. There is still much work to be done in this area.

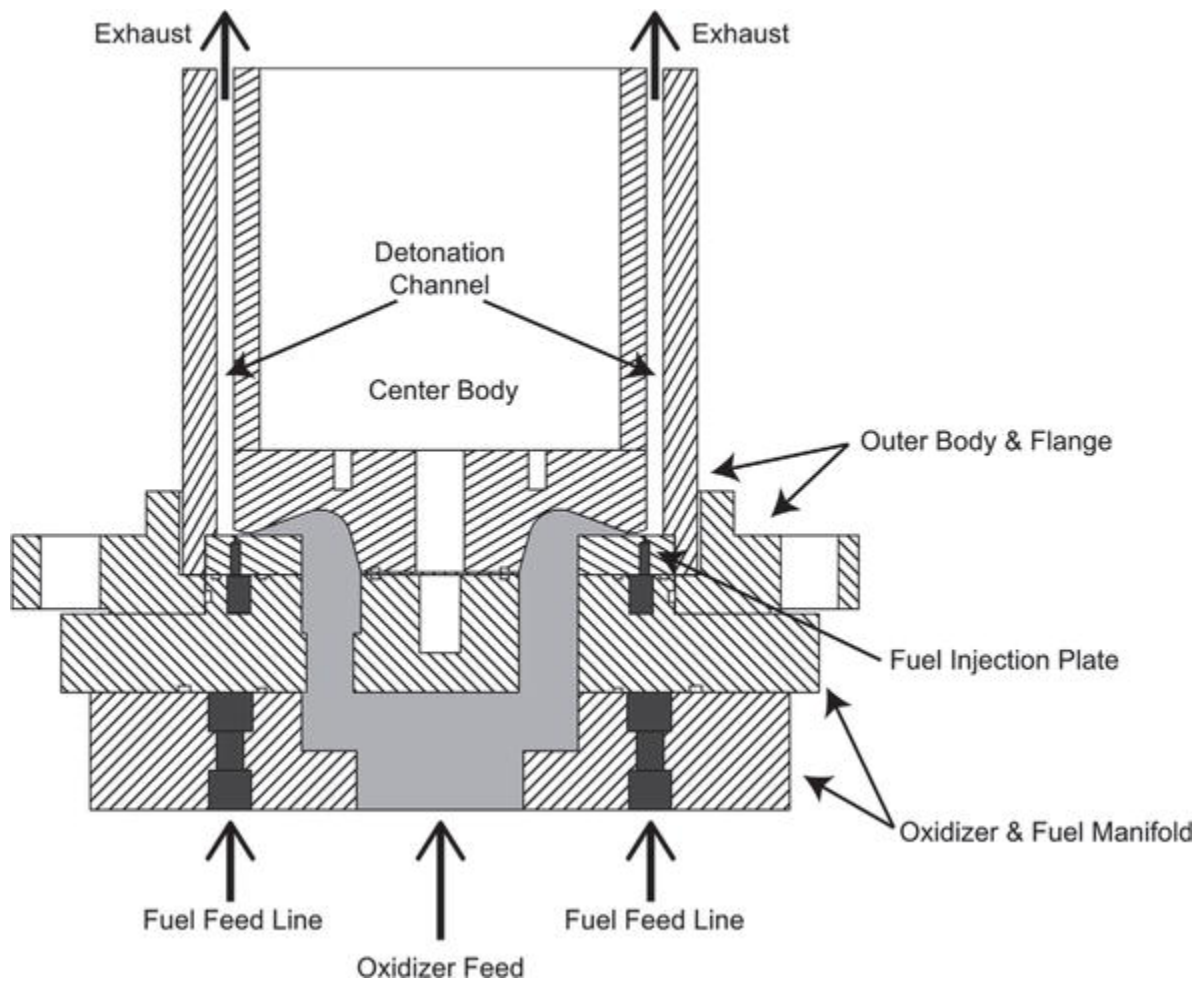


Figure 17 RDE cutaway with fuel manifold [12].

2.0 Systematic Literature Review

The purpose of a Systematic Review is to explore and select current scientific literature that fits a specific criteria in order to produce a compilation of state of the art progress in a given topic. These particular types of reviews are highly popular in the medical field, but can be applied to just about any other research area or discipline. As defined in the Medical Community, “A systematic review is a summary of the medical literature that uses explicit and reproducible methods to systematically search, critically appraise, and synthesize on a specific issue” [33]. Below is displayed an example of the type of questions that must be asked in every systematic review in the form of a flowchart [34]:

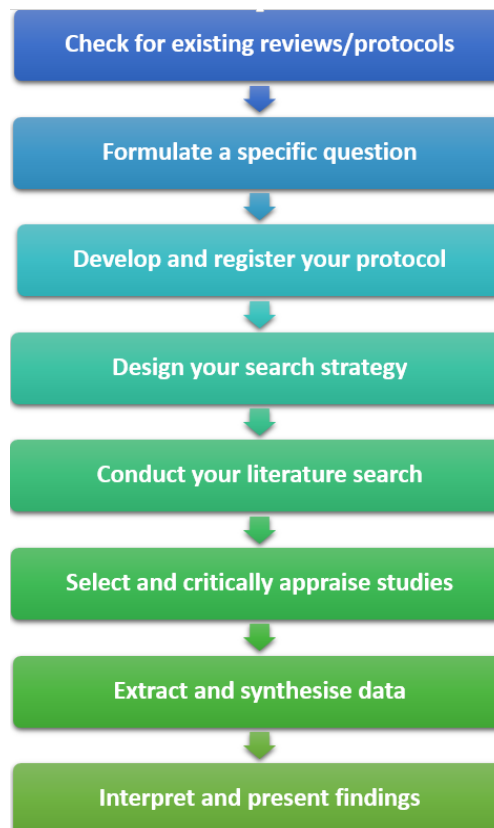


Figure 18 Systematic review flowchart with steps [34].

After first checking existing reviews/protocols, it is discovered that a small number of papers exist for the purpose of providing status reports and current technological accomplishments in terms of rotating detonation engines. Among these are mainly the work of Kailas Kailasanath who had been heavily invested in the field of detonation as applied to aerospace propulsion systems [8,35,36]. Kailasanath's most recent status report [8] is dated back to 2011, over 10 years ago as this paper is being written. Therefore, it is necessary to explore the literature further to determine what more recent advancements have taken place regarding the technology.

The next step in the process we arrive at is formulating a specific question, which will be based on the objective. In the specific case of this review, the objective is to characterize rotating detonation engine technology and determine the most recent advancements made, be that in real-time experimentation and post-experimental analysis or in computerized simulations. Considering this, the research question will be: "Where does Rotating Detonation technology currently stand and what are the limitations?" This question will be referred to as the Research Question. Although a broad question, given that this particular study is quite niche, this will provide structure to guide the search and selection of papers.

Now that a question has been formulated, related inclusive criteria must be selected in order to properly direct the selection of available papers to populate the so-called 'literature repository'. When using the Research Question to guide our search, another important factor to consider is the credibility of the authors. That is, it will prove more useful to gather papers from a well-published author who has established good rapport in the field. As is implied with any author who is well-written it is also important that this author has spent sufficient time researching rotating detonation engines and their viability as a propulsion system. For the sake

of this review, a period of 10 years will be chosen as a required time spent in the field for papers of greater heritage. Kailas Kailasanath is one of the few researchers whose work fits this criteria with publications on detonation ranging from as far back as 1983 to as recent as 2018. Of course, this last criteria must be omitted when compiling more recent advancements in the field. It is inevitable that there will be a hand-off of this sort of research from the previous generation to the current and evaluating where progress currently stands is vital to maintaining the momentum of rotating detonation engine development.

Kailas Kailasanath began his studies with looking at detonation, however, he is still able to provide the reader with an excellent technological baseline as of the year 2017 (about 5 years ago at the time of this paper) in the *55th AIAA Aerospace Sciences Meeting* with his addition: "*Recent Developments in the Research of Rotating Detonation Wave Engines*". [37] In this journal article, Kailasanath is able to briefly summarize state of the art achievements surrounding RDE or RDWE technology. He begins to note some of the more recent researchers who "jump started" work in the RDE field as the technology had already been around for approximately 50 years. Among some of these are Eidelman, Bussing, and Pappas. These researchers primarily focused on the pulsed detonation engine type configuration and explored performance estimates and nozzle types for this use case. As mentioned previously, the first scientist to implement the cylindrical annular combustion chamber for a continuous detonation was Voitsekohvsky. The study explored a variety of gaseous and liquid fuels as well as discovering critical chamber dimensions for detonation. This is also where we begin to see the effect of injection and mixing: "the quality of liquid fuel spray and mixing had a significant effect on the stability and limits of detonative combustion" [37].

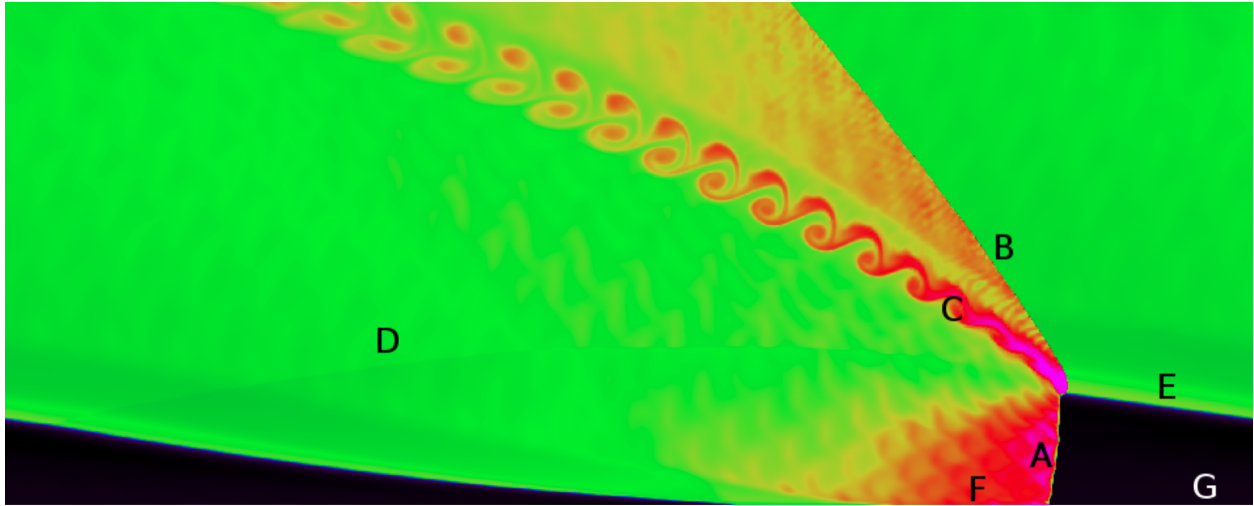


Figure 19 Unrolled RDE flow-field from numerical solution [37].

Next, most notable are the numerical investigations into rotating detonation engines which provide us with better descriptions and understanding of the flow field and overall performance of the engine. Most easily performed simulations tend to be two-dimensional, however, three-dimensional simulations add a level of accuracy but also complexity. At the time of Kailasanath's summary, one of the researchers involved in characterizing the flow field in an RDE is Hishida. Hishida's work in computational simulations discovered that there exists what is known as the Kelvin-Helmholtz instability on the interface of the combustible fuel mixture. "The Kelvin-Helmholtz instability is a fluid instability when there is a velocity shear in a single continuous fluid or velocity difference across the interface between two fluids" [38]. In Figure 19 above, Unrolled RDE Flow-Field from Numerical Solution, we see the Kelvin-Helmholtz instability notated by C. This figure provides a visual understanding as to what is occurring inside the annulus as if it were a sheet of paper "unrolled" onto a two-dimensional plane. To further demonstrate, below is a legend to the marked artifacts in the simulation:

- A - Detonation Wave
- B - Oblique Shock Wave

- C - Slip Line between New and Old Detonation Products
- D - Secondary Shock Wave
- E - Mixing Region between Premixed and Detonated Gasses
- F - Blocked Injection Micronozzles
- G - Unreacted Mixture

Exploring the key parameters and performance tellers of RDE engines, we come across the topic of pressure, specifically Delta P or pressure change. This is of great interest given that these engines exhibit pressure gain rather than pressure loss. The primary concern here is the difference in two separate pressures, the stagnation and back pressure or the pressure at the inlet micronozzles and the pressure at the chamber exit. Two different simulations were run in a parametric study [39] where first: stagnation pressure was held constant and back pressure was varied, and second, back pressure was held constant and stagnation pressure was varied. All in all, the numerical simulations exhibited a pressure ratio varied from 2.5 to 20. This in turn, yielded a variation in detonation velocity from 1875 m/s to 1920 m/s.

Turning the discussion to measurable quantities that are indicative of performance indicators, the dialogue would not be complete without an examination of mass flow rate and thrust. Mass flow rate is almost entirely dependent on the stagnation pressure, where the thrust force is dependent on both stagnation and back pressure. However, the specific impulse of any engine of ISP is dependent not on the magnitude of either pressure but the relative difference or pressure ratio itself. Looking back to some previous statements made on the efficiency of an RDE, the estimated increase of efficiency over typical combustion is approximately 25%. However, there is a steep increase from PDE technology (pulsed detonations) to RDE technology (continuous detonations). According to Heiser and Pratt [40], the estimated specific impulse for

an RDE at ideal sea level conditions with a typical fuel-air mixture is 6250 seconds. Although a very high ISP, there is the opportunity to bring this even higher with specific mixing techniques, fuel-type variation, and injection schemes.

Kailasanath goes on further to provide a comprehensive analysis of notable research conducted in three main continents, Europe, Asia, and North America. These areas are where the primary substantial advancements have been made. Among the countries in Europe where progress has been made include France, Poland, and Germany. In Asia, the primary countries are Japan, China, and Korea. Finally, in North America, most advancements have taken place at various research institutions, government agencies, and universities in the United States of America.

First, in Europe, France is a country that has exhibited great initiative in the realm of RDE testing and development, specifically a company known as MBDA which primarily manufactures missile systems. The main effort has been to develop detonation wave engines for use in high-velocity environments such as guided systems. They have successfully built and tested a fully operational rotating detonation engine, dubbing the new RDE-powered missile replacement “Perseus”. The current estimates show a potential greater than 60% weight savings in the launch mass, which has substantial implications for future guided missile systems. The company even has a patent for a “detonation-based gas-turbine engine”.

Next, in France, there are the CNRS or Center National de la Recherche Scientifique laboratories and the LCD or Laboratory of Combustion and Detonation that have contributed to current advancements. At this research center, scientists were able to successfully construct and test an RDE with sustained continuous detonations. One of the main discoveries made during

experimentation was that there is a relationship between the number of detonation waves and the mass flow of the propellants in the engine.

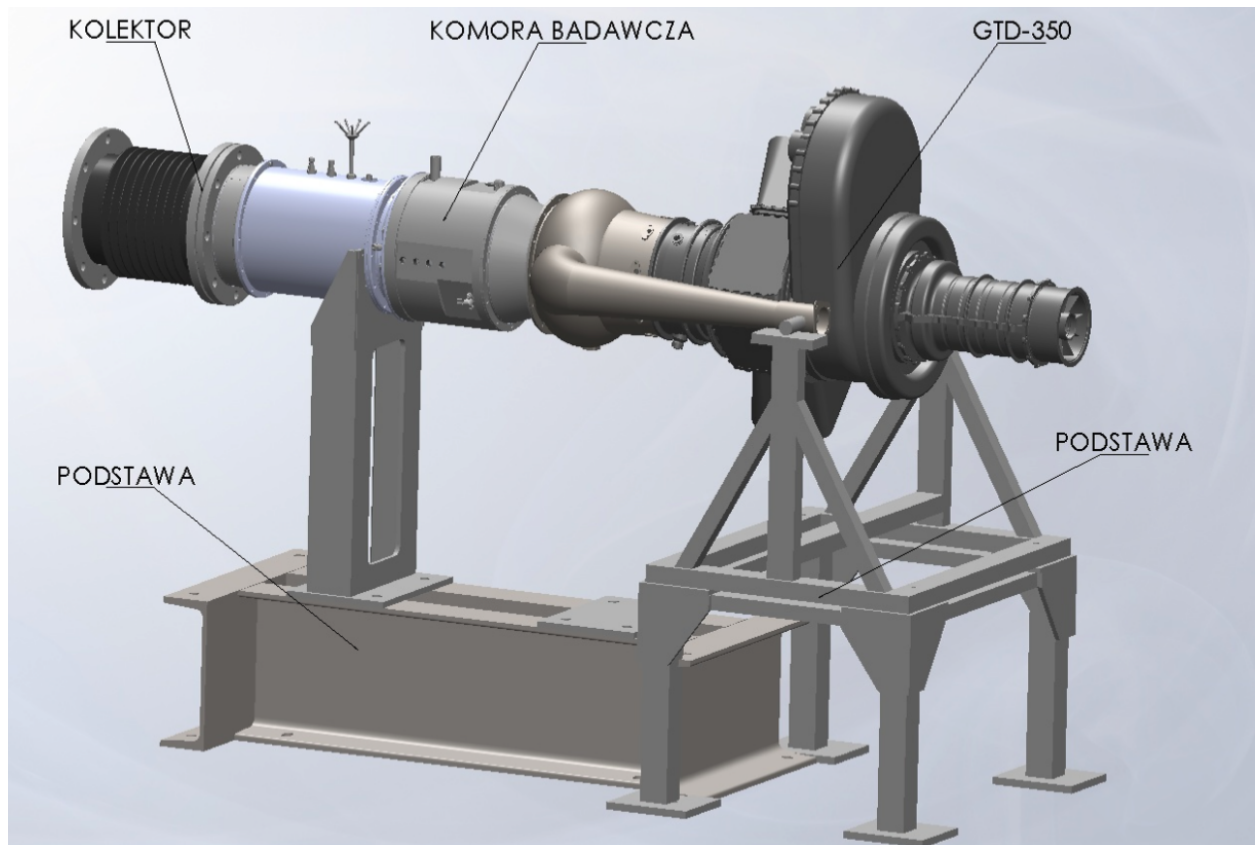


Figure 20 RDE-powered GTD-350 Soviet turboshaft engine [36].

Continuing with the exploration of European countries there is Poland, which has had great efforts, specifically at the Warsaw University of Technology and the Warsaw Institute of Aviation. Wolanski was mentioned in the previous sections regarding his advancements in developing a rotating detonation engine for a rocket-based application. In addition to this, Poland is known for successfully converting a GTD-350 turbojet engine, a Soviet gas-turbine turbojet engine into a detonation powered device with an RDE combustor. Finally, Germany is reported to have made a number of contributions to the technology, however, the primary findings have been undisclosed to a number of scientific communities or public journals.

In China, the majority of scientific accomplishments related to RDE technology have been demonstrated by China and Japan, but there are other countries making advancements such as Singapore and South Korea. In China, the most popular research institutions that fit this criteria are Peking University, Beijing Institute of Technology, and Northwestern Polytechnic University. This was mainly discussed previously, but Peking University has provided a look at the application of a pre-detonator also known as an initiator pictured in Figure 12. by J.P. Wang's research paper. The inclusion of this device has exhibited a higher rate of successive continuous detonation waves in the chamber.

In addition to this, Peking University has done extensive research into numerical simulations of RDE technology. The biggest discovery made was relating to the relationship of stagnation pressure and transition. They noticed that during simulations, when a change in stagnation pressure was initiated, conversely the axial velocity at the head end of the rotating detonation engine also changed. As a result, the axial velocity would tend to drop while the pressure increased at the head until reaching a stable state with little to no variation. The so-called "adjusting time" for this to take place was discovered to be approximately 2 times the cycle period of a detonation wave traveling around the chamber. Next, they explored the effect of different exhaust nozzle shapes/types on engine performance computationally. The three nozzle types simulated were converging, diverging, and Laval. The best performing out of these three was found to be the Laval nozzle. Axial flow is an important achievement in these simulations as it is imperative for fuel efficiency that the highest amount of rotational flow possible is converted into axial momentum. This ensures that flow does not act destructively and cause efficiency loss in the engine.

Finally, in North America, specifically in the United States, there has been a large number of scientists, researchers, students, and institutions contributing to technological advancements of RDE's. Among these institutions include: AFRL Air Force Research Laboratory Wright Patterson AFB Air Force Base, NRL Naval Research Laboratory, Aerojet Rocketdyne, Purdue University, University of Pennsylvania, GE, GHKN Energy, University of Texas Arlington, and University of Cincinnati.

The Air Force Research Laboratory has constructed a fully operational rotating detonation engine and has even devised a method of manufacturing to include a quartz window on the side of the detonation chamber to allow for visualization of the detonation waves. This window into the visual artifacts of continuous detonation allows for direct comparison to numerical simulations for the sake of confirmation of result validity. The AFRL was able to directly compare experimentation visualization results of detonation in the chamber to computation results from the NRL. The results were rudimentary at best, however, there are better technologies to visualize such flow artifacts such as Schlieren imagery. This is a topic of discussion that needs to be explored further.

Aerojet Rocketdyne, as mentioned previously, has performed extensive research in this area and has constructed a fully modular RDE. Their tests have exhibited successful continuous detonation results in collaboration with Purdue University and University of Pennsylvania. Utilizing a hydrogen, ethane, and methane fuel types there has been exhibited a non-axial exit flow which further confirmed simulations done by the NRL. Furthermore, at the University of Texas Arlington, it was discovered that the direction of detonation wave propagation can be controlled by varying the ignition process. This currently has a wide range of ambiguous results and further research must be done to determine what exactly the direct relationship is between

injection and wave propagation. The University of Cincinnati has also observed via experimentation a number of instability modes in the combustor itself, this is discussed further in their research paper entitled Rotating Detonation Combustor Research at the University of Cincinnati [41].

In summary, the technological limitations of rotating detonation engines fall into the main category of the inability to sustain a long-term detonation cycle in the annulus of a rotating detonation engine. This stems first and foremost from the injection schemes utilized during testing, and secondly from the fuel and oxidizer mixtures being experimented with in the lab setting. Although setting up these experiments is expensive, intricate, and time-consuming, there is the possibility of exploring these effects via conducting computational fluid dynamics simulations. Of course, this case is also quite time consuming, but with the proper processing in place proved less expensive and intricate than when compared to constructing an entire rotating detonation engine and test stand.

Next, it makes sense to explore numerical CFD simulations of RDE engines that have already been performed and explore how those results compare to real world experiments and hypotheses. A couple notable numerical simulations are worth discussing that are fairly recent and valid for the purposes of exploring CFD for RDE's. Among these viable candidates, one paper comes to mind that explores numerical calculations of Rotating Detonation Chambers published in the Journal of Power Technologies in 2017 by Zhenda Shi and Jan Kindracki [42]. Both researchers are from the Institute of Heat Engineering at Warsaw University of Technology in Poland. "This paper mainly focuses on research into the behavior of stable continuously rotating detonation in premixed combustion cases". The reason for this is that Ansys Fluent is not exactly designed for detonation cases and has trouble reinitiating the detonation cycle after

waves have either decayed or collided with each other. This would be an issue if the detonation model was based on a non-premixed fuel-air combustion case. Both the boundary conditions and mesh cells were varied in this study producing a range of results to increase validity. Vital to any study is selecting the proper numerical method to model the calculation, to simulate the detonation occurring in the chamber accurately. Let's outline the necessary numerical parameter selections that were made for this study:

- Energy equation
- k - epsilon turbulence model
- "Explicit temporal discretization of all solved equations"
- "Second order numerical scheme"

These selections ensure that detonation waves are not 'smoothed' during calculation and that sufficient granularity in results are obtained.

Taking a look at the premixed combustion case, it is clear that simulation is much more straightforward and easily examined. The results exhibited "successful reactivated detonation after collision". Immediately after a detonation is initiated, there are two waves that travel in a destructive manner (opposing motion) to each other. The opposing detonation wave rotating motion continues until only one wave is left rotating. This occurs within approximately 20 milliseconds. The Y^+ value used for these calculations was from 200 to 250 with inclusion of 40 individual injectors. "The Y^+ value is a non-dimensional distance (based on local cell fluid velocity) from the wall to the first mesh node" [43]. This is a pretty standard mesh resolution, however, with higher resolution meshes (lower range Y^+ values), we see an increase in the granularity of the detonation structure. For example, the ideal grid size Y^+ value range was seen

to exist from 45 to 115. Below are pictured, some of the results obtained by Shi and Kindracki in Figure 21 and 22 Contour plot results for pressure and temperature with 40 injectors [40].

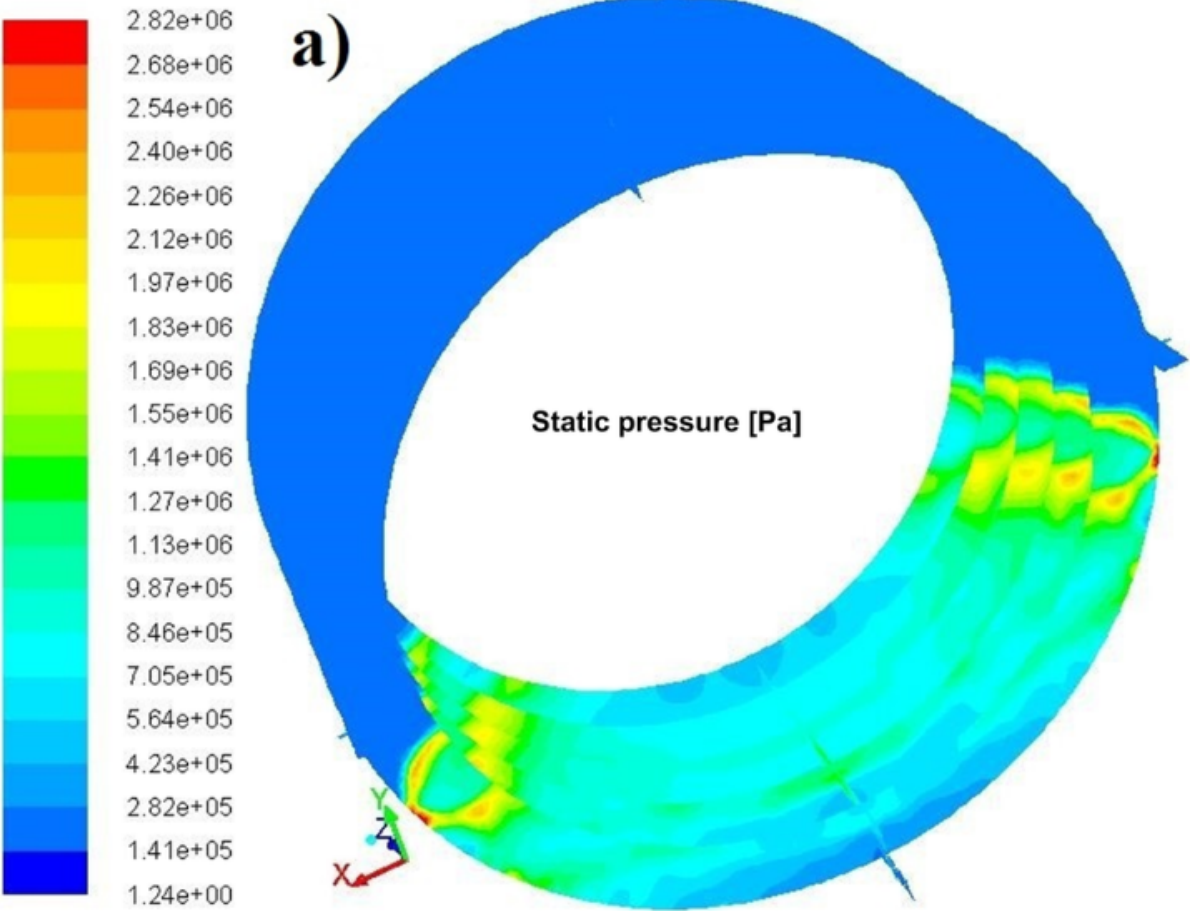


Figure 21 Contour plot for static pressure with 40 injectors [40].

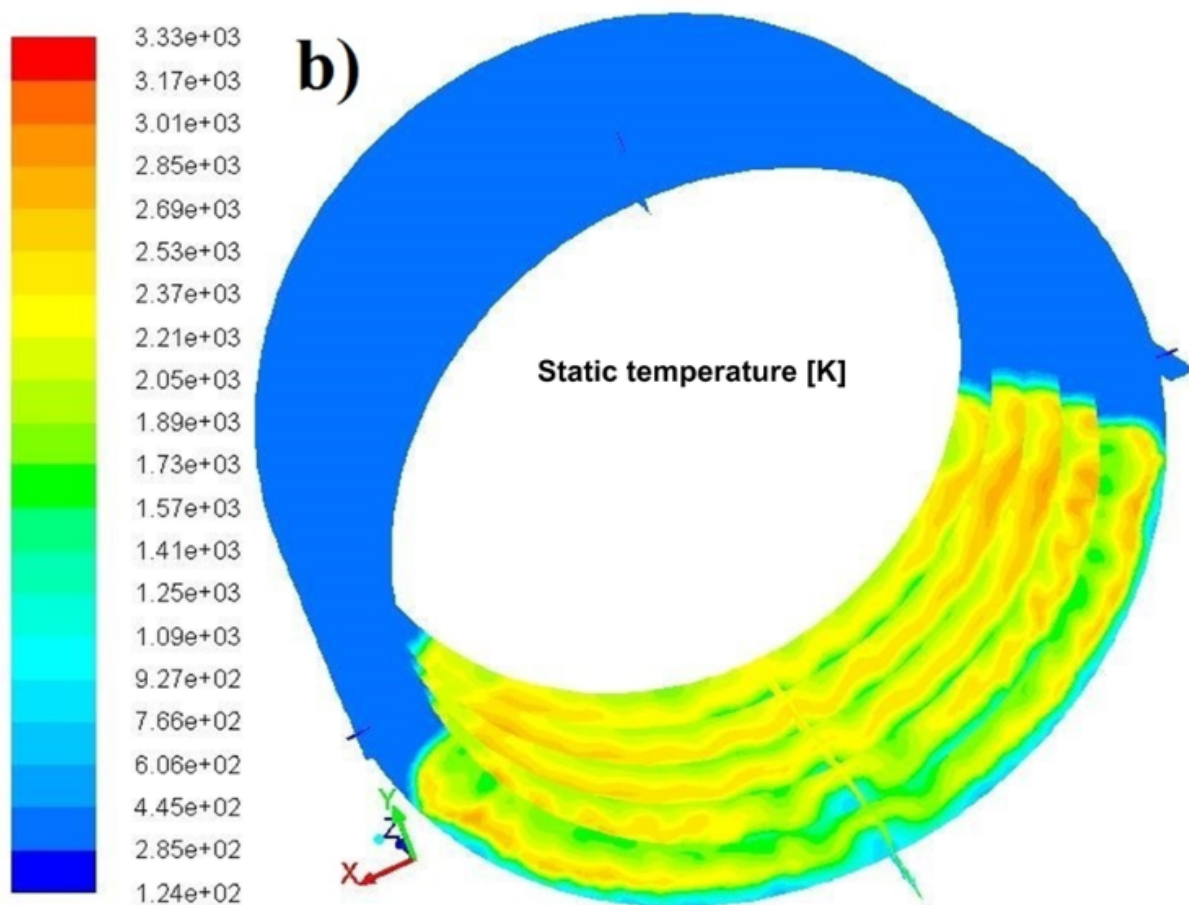


Figure 22 Contour plot for static temperature with 40 injectors [40].

Overall, the two key parameters of importance that determine whether or not conditions for ‘stable’ detonation wave propagation exist are the chamber configuration and the boundary conditions. The results are as follows... After completing all numerical investigations for both the premixed and non-premixed combustion cases, it was discovered that the premixed case would not sustain a stable detonation. The possible solutions to this problem are to either size up the chamber (one of the first comments seen in regard to sizing) or to decrease the mixture density and couple the setup with a higher mass flow rate on the injection side. The second option was taken as the chamber size was fixed to a relatively small size. Testing the other use

case, it was discovered that stable detonation is much easier to achieve when the fuel mixture is lean rather than when it is rich or stoichiometric. The grid construction is extremely important to achieving valid, repeatable results for both cases. It is suggested that a hexahedron structured mesh be used with a larger concentration of grid density near the region of mixing. The only way to sustain detonation in the non-premixed case is when refilling and reactivation are a seamless process. Another very vital result was the discovery of a range of mass flow rates for which stable detonation can be initiated. These are important discoveries to be aware of for both future simulations and future experiments as well.

Next, Craig Nordeen is another notable fluid dynamicist researcher with contributions to share in the realm of rotating detonation engine studies, specifically numerical simulations and CFD results. Dr. Nordeen's paper entitled: *Thermodynamics of a Rotating Detonation Engine*, is a highly detailed walkthrough of the thermodynamic phenomena that occur inside of a rotating detonation engine by way of computer simulation [44]. The paper includes a validation of the US Naval Research Laboratory's RDE numerical simulation as well as a deeper dive into the results, a post-processing to provide discussion and definition of the characteristics exhibited by the engine. One of the key discussions that Nordeen mentions is that of the concept of rothalpy. Rothalpy is also known as rotational stagnation enthalpy, according to Wikipedia [45]. Together, the simulation is based around a combination of the concepts of rothalpy as well as the ZND Zel'dovich-von Neumann-Döring detonation theory, as discussed previously. These help to define the constraints of the detonation wave behavior throughout the study.

The method outlined is that of the Heuristic Method, for how to accomplish this simulation. Heuristic method is defined as "an approach to problem-solving using a calculated

guess derived from previous experiences' [46]. There are 8 detailed, repeatable steps total in the process outlined by Nordeen and they are as follows:

1. *"A time-averaged computational fluid dynamics solution is processed from the time-accurate solution of a 2-D numerical simulation."*
2. *"A Galilean transformation of coordinates produces a velocity field in the rotating frame of reference."*
3. *"Streamlines in the rotating frame of reference are computed from the resulting relative velocity field."*
4. *"Integrating along the streamlines creates pathlines in the fixed frame of reference."*
5. *"Basic properties of density, momentum, reaction progress, pressure, and temperature are interpolated along the streamlines."*
6. *"Thermodynamic cycle properties along the streamlines, such as rothalpy and entropy, are computed from the basic field properties."*
7. *"A one-dimensional, geometry-independent, steady-state analytical thermodynamic cycle is constructed based on an interpretation of the numerical simulation."*
8. *"The analytical model cycle is compared to the simulation cycle and judged by two criteria:*
 - a. *Does the analytical model explain or predict features of the numerical simulation within a reasonable limit?*
 - b. *Does the analytical model predict thermal efficiency or specific impulse with reasonable accuracy?"* [44]

The paper goes on to mention the Naval Research Laboratory's numerical simulations of RDE's, specifically the fact that the test cases are of the nature of a premixed stoichiometric hydrogen-air fuel mixture in the software. The traditional method of approaching this simulation is to convert it from a 3-dimensional model to a 2-dimensional model. In its most basic form an RDE is a cylinder, however, for the purposes of reducing complexity, it is traditionally seen in these types of simulations that the cylinder is unwrapped into a 2-dimensional flat shape. This allows solutions to converge giving us tangible results. As with any computational fluid dynamics problem, complexity can spiral out of control quickly and computational expense can increase drastically (solving time and processor requirements), so it is imperative that a balance be found between an accurate solution and adequate detail of that solution. One method of accomplishing this is through various methods of mesh manipulation such as the one seen in Figure 23 below:

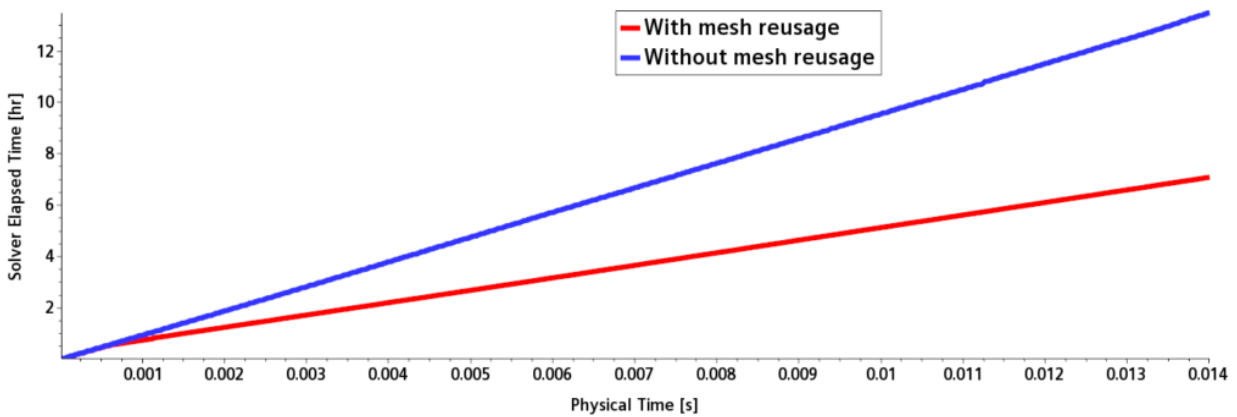


Figure 23 Solving time for mesh reuse vs without mesh reuse [47].

Finally, there is a highly informative research paper on the investigation of the rotating detonation engine also done by a fellow Aerospace Engineering graduate student at San Jose State University by the name of Samuel Zuniga. The author provides an investigation into the details of detonation theory as a preface to the numerical investigation provided at the end.

Similarly to the planned methodology in this paper, the author explores how to produce CFD analysis of an RDE in an Ansys simulation. In order to initialize the software analysis for the rotating detonation engine and validate results are accurate, it was necessary to produce a simulation of a pulse detonation engine PDE case. This reduced complexity, but a similar use case was used to model the environment, process, and chemicals used to apply to the more complex case. The primary mechanism used in both cases is that of a hydrogen-air mixture. The main foundational factors necessary for this CFD as with any are: “geometry, grid dependence, required schemes, and problem initiation” [28]. The analysis is that of a 2-dimensional nature to reduce complexity.

“Two-dimensional unsteady Euler equations with source terms due to chemical reactions” were used in the analytical modeling done by Ansys [28]. A structured mesh was used varying grid size based on previous numerical studies. The walls were modeled as periodic conditions, with the pressure outlet located at the exit end of the device. “The injector can be modeled as either an ideal or non-ideal case. In the ideal case, it is modeled by using a user-defined function. In the non-ideal case, the injectors are modeled individually throughout the inlet wall region” [28]. The start of any CFD simulation is of course the 3-dimensional Navier Stokes Equations as seen here:

$$\frac{d}{dt} \int_V \mathbf{W} dV + \oint_C [\mathbf{F} - \mathbf{G}] d\mathbf{A} = \int_V \mathbf{S} dV \quad (2.1)$$

In order to convert from a 2-dimensional to a 3-dimensional case, it is assumed that the transport properties are negligible (do not exist or have no effect). These properties are viscosity, thermal diffusion, and mass diffusion. In addition to these assumptions it is necessary to assume turbulence also has no effect for the sake of reducing complexity. The resulting setup is a

simulation that is one-step, irreversible, and Arrhenius. Total enthalpy H , exponential factors K and A , activation energy, specific gas constant, mass fraction of the reactants, and temperature are all required variables for the simulation. Furthermore, to reduce complexity the hydrogen-air reaction thermodynamic properties are considered to be held constant. ZND and CJ conditions must be verified with a “one-step stoichiometric hydrogen-air mechanism”. A structured mesh was used with a 0.1mm spacing length. All boundary conditions were initialized by modeling the walls as adiabatic boundaries, that is they are unchanging. The bottom boundary, however, was the pressure outlet, therefore, symmetrical. The outlet of course was modeled as standard ambient conditions, 1 atm, etc. The mass fraction in this case for a hydrogen-air stoichiometric mixture is in fact 1.0, which keeps things relatively straightforward. Below is a table outlining the initial conditions for the burned and unburned gas, Table 2.1.

| Initial Conditions (Burned Gas) | | |
|-----------------------------------|----------|----------------------|
| P_0 | 90 [atm] | Initial Pressure |
| T_0 | 3500 [K] | Initial Temperature |
| X_{H_2O} | 0.25480 | H_2O Mass Fraction |
| X_{N_2} | 0.74520 | N_2 Mass Fraction |
| Initial Conditions (Unburned Gas) | | |
| P_0 | 1 [atm] | Initial Pressure |
| T_0 | 300 [K] | Initial Temperature |
| X_{H_2} | 0.02852 | H_2 Mass Fraction |
| X_{O_2} | 0.22640 | O_2 Mass Fraction |
| X_{N_2} | 0.74510 | N_2 Mass Fraction |

Table 2.1 Ansys Fluent initial conditions for hydrogen-air gas mixture [28].

The solver was selected to be density-based. The primary attributes of the solution were:

- Axis-symmetric
- Laminar
- Transient
- Time step = $1 \cdot 10^{-7}$ s
- Courant # = 0.5
- Second order upwind scheme for spatial discretization
- Implicit formulation for temporal discretization
- ROE flux difference splitting scheme

The results yielded for temperature, pressure, and velocity of conditions within the detonation tube all proved to be very similar to NASA's CEA (Chemical Equilibrium with Applications) software for validation. The average Temperature was 2783 Kelvin, Pressure was $1.49 \cdot 10^6$ Pascals, and Velocity was 2015 meters per second. The results from NASA's CEA benchmark came to an average Temperature of 2947 Kelvin, Pressure of $1.59 \cdot 10^6$ Pascals, and Velocity of 1968 meters per second, all within +/- 10% error of the achieved solution in Ansys. These results from this pulse detonation case provided a baseline for detonation before moving to the rotating detonation engine simulation. Next the paper moves on to the RDE simulation case.

To begin with the setup process, the majority of the substance parameters, ambient conditions, initial conditions, and boundary conditions remain the same as the pulse detonation simulation with the exception of a few. As discussed, the rotating detonation engine requires a 3-dimensional simulation as the detonation wave moves throughout the annulus in an x, y, z axis. But, for the sake of simplicity and computational time and resources, the RDE is "unrolled" into a 2-dimensional sheet as seen in the Figure below:

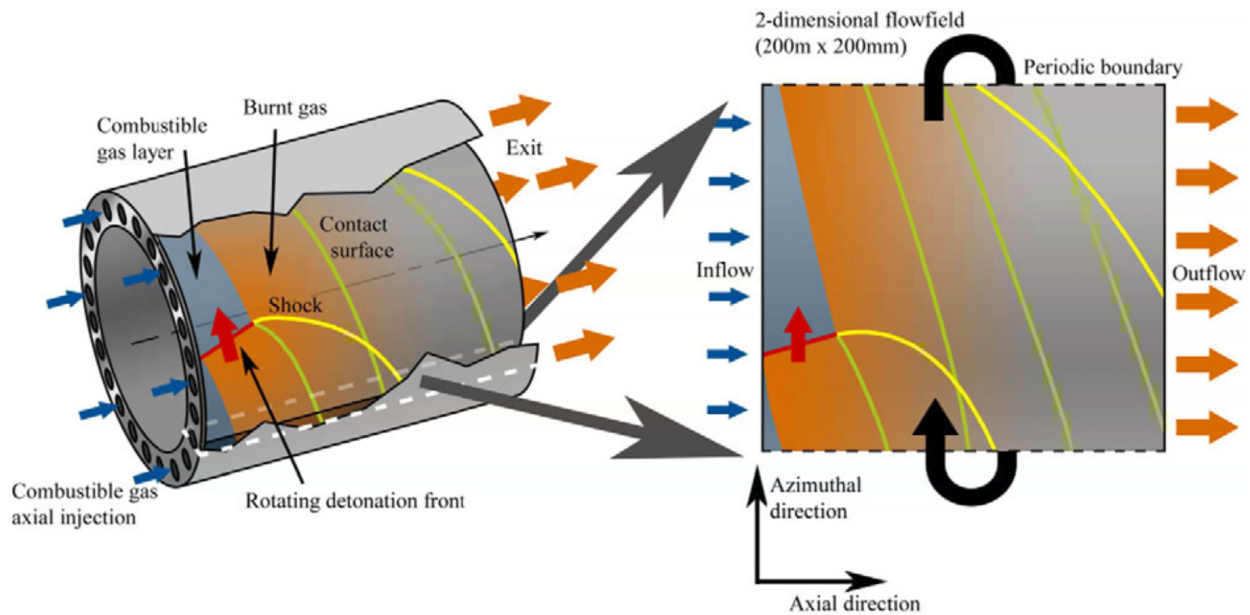


Figure 24 3-Dimensional RDE annulus unrolled into 2-dimensional sheet [48].

It turns out that, unrolling the annulus and simulating the detonation wave propagation in a 2-dimensional manner does not have a drastic effect on the results achieved when compared with previous 3-dimensional simulations. The stoichiometric hydrogen-oxygen mixture with a one-step mechanism remains the same. The chamber entrance is described by a slip rigid wall boundary condition, while the exit is described by a pressure outlet boundary condition; the upper and lower bounds are described by periodic boundary conditions. The crucial piece here is the simulation of the tangential injection into the annulus. “A one-dimensional Chapman-Jouguet detonation is patched in the domain for a short distance from the head left end, with a strong tangential velocity to ignite the flow into a detonation in one direction”.

The next discussion is between the non-ideal injection approach and ideal injection approach. In the non-ideal injection approach, multiple injectors are placed along the combustion chamber (annulus in this case) with the addition of a mixture plenum. This is contrasted by the ideal injection approach, which does not physically model the individual

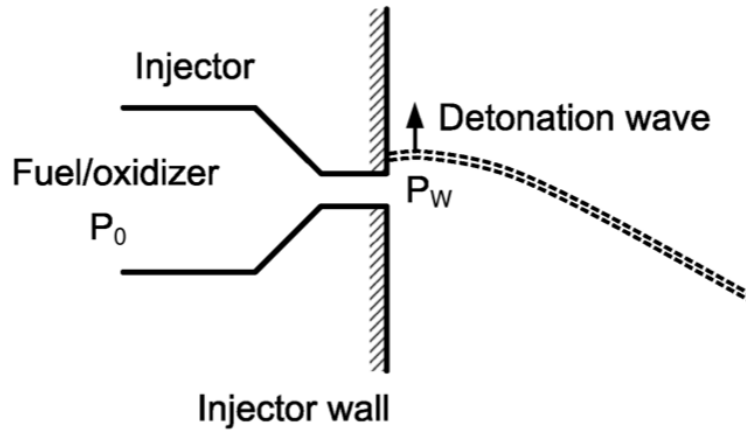
injectors, but instead provides a continuous detonable mixture into the combustion chamber. According to Wolanski in his publication “*Detonative Propulsion*”, the mixture must be generated continuously in order to sustain detonation in the chamber. “As was mentioned before, both fuel and oxidizer are supplied by different injection holes (or slits) and they have to mix inside the chamber to form a detonable mixture just before one revolution of the detonation wave. This condition is crucial for supporting the continuous and steady rotation of the detonation wave” [21].

There are 3 different injection conditions that can be modeled for the ideal injection case.

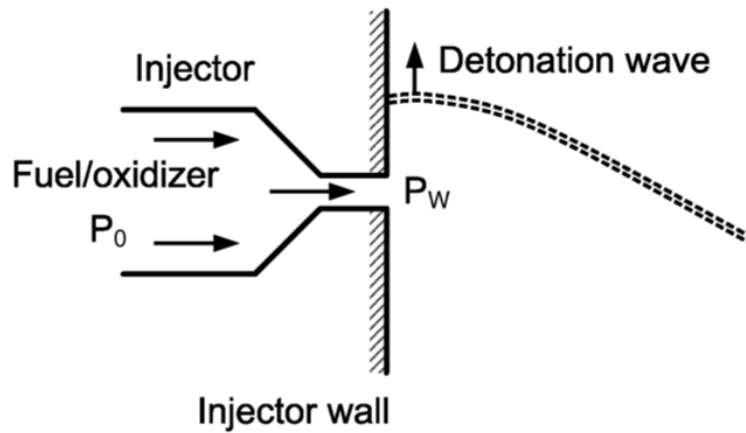
The cases are as follows:

1. No Injection Flow Supplied
2. Subsonic Injection Flow Supplied
3. Supersonic Injection Flow Supplied

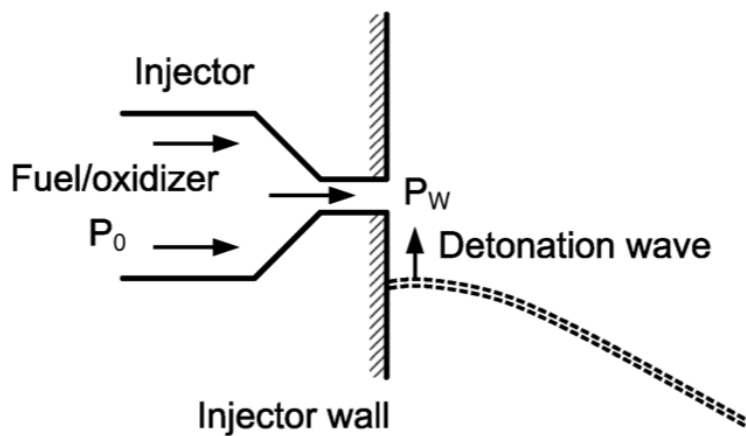
In the first condition, the wall pressure is greater than the injection pressure. In the second condition, the wall pressure is less than the injection pressure, but greater than the critical pressure. In the third condition, the wall pressure is less than critical pressure. These different conditions can be seen below in Figure 25 as discussed in Yi and Wolanski’s paper that explores the propulsive performance characteristics of rotating detonation engines [48]. Notice that $P_w > P_o$ in the first case with no injection flow supplied. In the second case with subsonic injection flow, $P_o > P_w > P_{cr}$. Finally, in the third case that reflects supersonic injection flow, $P_w < P_{cr}$. This is further detailed in the figures below. There is also a corresponding unique temperature relationship for each of the injection cases below.



a) No injection: $p_w \geq p_0$



b) Subsonic injection: $p_0 > p_w > p_{cr}$



c) Sonic injection: $p_w \leq p_{cr}$

Figure 25 3 Different ideal injection conditions [48].

Next, a detailed discussion of the boundary conditions and grid characteristics is necessary to replicate any results found in this report. The pressure outlet (exhaust) was modeled with standard atmospheric conditions and the walls were modeled as ‘translational periodic’. The grid was defined with a 0.1 mm spacing length and the mesh was set to be adaptive. This was done because of the complexities added by the shockwaves within the propagating detonation wave in the combustion chamber. The most complex portion involved generating a new surface to ‘patch’ the solution to the detonation wave. The Chapman-Jouguet velocity was ‘patched’ in the tangential direction to ensure correct and proper propagation of the detonation wave in the combustion chamber, or in this case within the 2-dimensional unrolled annulus combustion chamber ‘sheet’ [28]. As mentioned previously, stoichiometric hydrogen-air mixture in the plenum was setup to have a Pressure of 1.013×10^6 Pascals and a Temperature of 300 Kelvin. Lastly, the combustion chamber area was initialized at standard atmospheric temperature and pressure, the inlet was initialized as a velocity inlet, and the inlet boundary condition required setup with a user-defined function. This is also referred to in short as a UDF.

Finally, the expected results were as follows: A detonation wave will propagate from left to right on the ‘unrolled’ annulus or 2-dimensional combustion chamber ‘sheet’ in a tangentially slanted manner as seen in the below Figure 26 Computational Setup in a Two-Dimensional Simplified RDE Chamber from Yi and Wolanski’s paper entitled: *Propulsive Performance of a Continuously Rotating Detonation Engine* [48]. Details of the boundaries, surfaces, shockwave, and the detonation wave itself can be seen in this Figure 26.

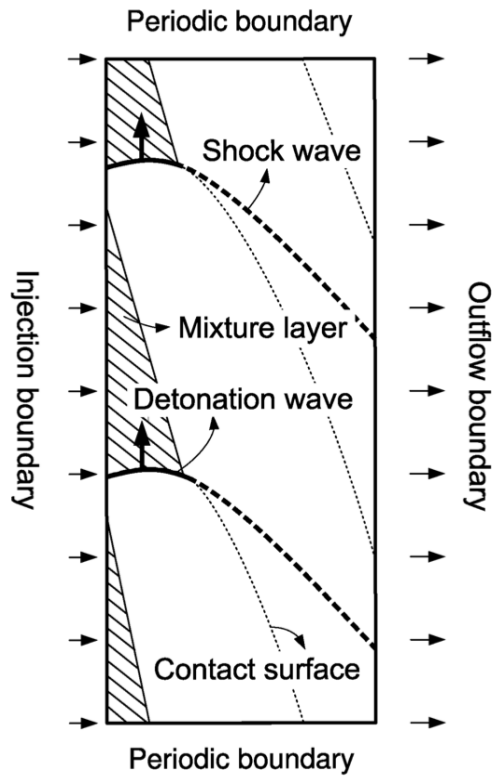


Figure 26 Computational setup in a 2-dimensional simplified RDE chamber [48].

The final results should look similar to the below in Nordeen's Ph.D dissertation, *Thermodynamics of a Rotating Detonation* from the University of Connecticut [27].

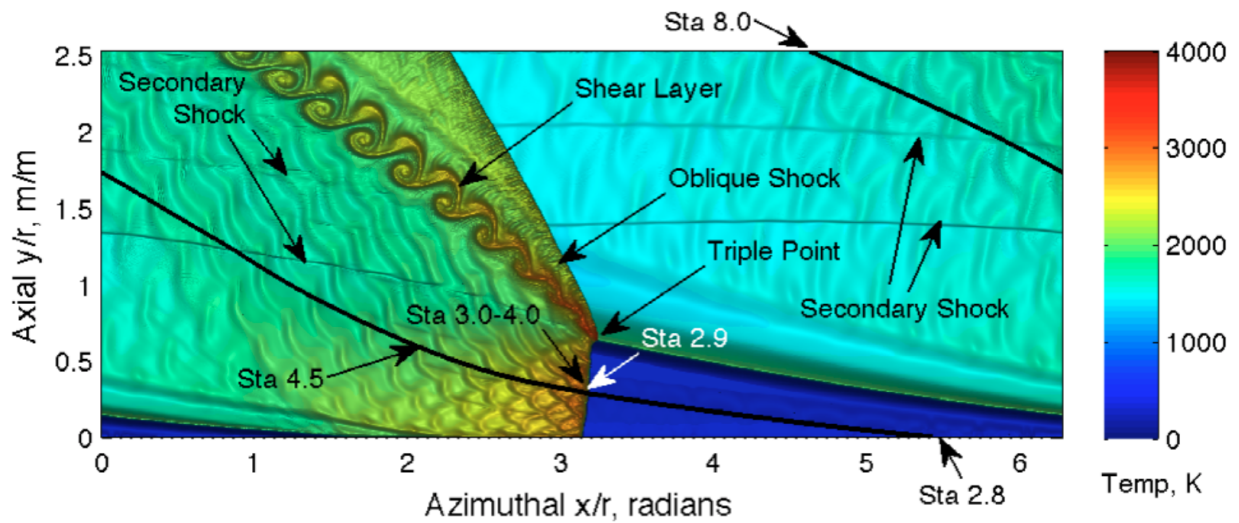


Figure 27 Time-accurate simulation temperature with time-averaged streamline [44].

3.0 Ansys Fluent Software Background

In this section, we will outline the basic requirements and necessary steps for running a thermal and computational fluid dynamics CFD simulation, specifically, one that will allow for determination of scalability of rotating detonation engine technology. The first step will require setting a performance and sizing baseline by configuring engine geometry in a computational aided design CAD program and then importing that geometry into the fluid dynamics software. The next step is to vary size by scaling the engine and run subsequent simulations to compare both performance parameters and efficiency results between the different models and to determine whether there is any loss or gain in scaling the size larger or smaller than the baseline model. However, before any of the above steps can be performed, we must provide a background on the software programs that are going to be used in this analysis process.

ANSYS Fluent, a highly sophisticated CFD software will be used for all computational simulations relating to initial rotating detonation engine performance and efficiency determination, sizing, and scalability analysis. In order to construct the engine geometry, Solidworks, an aerospace industry widely used CAD software will be utilized.

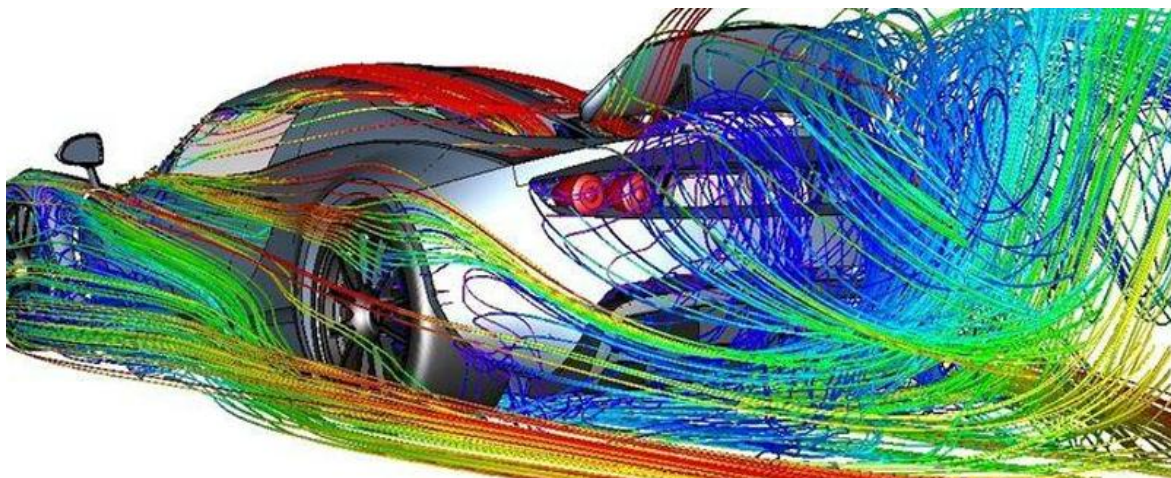


Figure 28 Ansys Fluent fluid dynamics software automobile flow visualization [49].

Ansys offers a multitude of different software packages for specialized applications such as fluid simulation, mechanical finite element analysis FEA, 3D computer aided design CAD, 3D product simulation, electromechanical, etc. Ansys Fluent, the fluid dynamics software package is described as “the industry-leading fluid simulation software known for its advanced physics modeling capabilities and industry leading accuracy” [49]. CFD software such as Ansys Fluent is utilized by a whole host of individuals such as students, engineers, professors, researchers, and industry professionals. It has proven to be highly effective for cutting-edge research, validating experimental results, and expediting innovation in the aerospace industry as well as other areas including the automotive industry. A generic snapshot of the software’s capabilities can be seen in Figure 28 where there is an aerodynamics flow visualization of air over an automobile.

4.0 RDE Computational Model

The modeling process will be heavily based on Zuniga's methodology as mentioned in Section 2.0, Systematic Literature Review. Problem setup will be nearly identical with the exception of varying the engine size multiple times and observing performance parameters at their respective simulations. Post-processing analysis will be done in order to compare the different engine sizes and determine the best performing size. All in all, this section will detail the Ansys Fluent CFD software via explaining the mathematical relationships and assumptions used by the program to describe flow dynamics, setup of the RDE simulation model, and the viable, repeatable results that have been obtained.

How to properly set up a cfd simulation will include a focus on the following attributes:

- *Geometry*
- *Mesh: Y+ value*
- *Numerical Method*
- *Boundary conditions*
- *Initial conditions*
- *Environment*
- *Fuel/Oxidizer Mixture*
- *Post-Processing Techniques & Calculations*

4.1 Mathematical Relationships & Assumptions

The main foundation of any computational fluid dynamics software program is its mathematical basis, that is what mathematical formulas are used in order to model the flow dynamics. The vital starting point for all CFD programs is of course the Navier Stokes Equations. This set of equations, although very complex and to this day remain unsolved,

explain the motion of viscous fluids via conservation of momentum and conservation of mass of the fluid substance. Pressure, temperature, and density sometimes serve as a supporting set of factors included with the base equations [50]. These equations can be seen below in Equation 4.1 along with descriptors of the vectors in Equation 4.2. This is the most general form, that is, the three-dimensional integral form [28].

$$\frac{d}{dt} \int_V \mathbf{W} dV + \oint_C [\mathbf{F} - \mathbf{G}] d\mathbf{A} = \int_V \mathbf{S} dV \quad (4.1)$$

$$\mathbf{W} = \begin{Bmatrix} \rho \\ \rho u \\ \rho v \\ \rho w \\ \rho \mathbf{E} \end{Bmatrix}, \mathbf{F} = \begin{Bmatrix} \rho v \\ \rho v u + p \hat{i} \\ \rho v v + p \hat{j} \\ \rho v w + p \hat{k} \\ \rho v \mathbf{E} + p v \end{Bmatrix}, \mathbf{G} = \begin{Bmatrix} 0 \\ \tau_{xi} \\ \tau_{yi} \\ \tau_{zi} \\ \tau_{ij} v_j + q \end{Bmatrix} \quad (4.2)$$

These equations become simplified with a major key assumption: the transport effects are nullified and can be ignored. Transport effects are This means that the fluid properties of viscosity, thermal conduction, and mass diffusion will not have an effect on the simulation, meaning that $G = 0$, thus, all tao terms go to zero. Another necessary simplification made for the simulation is the neglect of turbulence and its effects on the results. These assumptions can be made when referencing Shao and Wang's research on numerical techniques involving determination of rotating detonation engine performance [51]. The resulting mathematics lead to the unsteady Euler equations that can describe the fluid dynamics after all aforementioned effects have been ignored. These equations can be seen below in Equation 4.3, along with descriptors of the vectors in Equation 4.4 and Equation 4.5.

$$\frac{d\mathbf{Q}}{dt} + \frac{d\mathbf{F}_1}{dx} + \frac{d\mathbf{F}_2}{dy} = \mathbf{S} \quad (4.3)$$

$$\mathbf{Q} = \begin{bmatrix} \rho \\ \rho u \\ \rho v \\ \rho E \\ \rho Y \end{bmatrix}, \quad \mathbf{F}_1 = \begin{bmatrix} \rho u \\ \rho u^2 + p \\ \rho uv \\ \rho uH \\ \rho uY \end{bmatrix} \quad (4.4)$$

$$\mathbf{F}_2 = \begin{bmatrix} \rho v \\ \rho uv \\ \rho v^2 + p \\ \rho vH \\ \rho vY \end{bmatrix}, \quad \mathbf{S} = \begin{bmatrix} 0 \\ 0 \\ 0 \\ 0 \\ \dot{w} \end{bmatrix} \quad (4.5)$$

Equally as important, are some additional equations that describe the chemical reaction taking place during the detonation. The next few equations will outline this.

Below is the equation for mass production rate:

$$\dot{w} = \frac{dY}{dt} = -K\rho Y e^{-\frac{E_a}{RT}} = AT^n e^{-\frac{E_a}{RT}} \quad (4.6)$$

Below is the equation for total Energy:

$$E = \frac{p}{(\gamma - 1)\rho} + qY + \frac{1}{2}(u^2 + v^2) \quad (4.7)$$

Below is the equation for enthalpy:

$$H = E + \frac{p}{\rho} \quad (4.8)$$

The next portion will continue to focus on the chemical equilibrium equations. NASA Glenn Research Center has a very important and valuable resource known as the NASA CEA software [52]. CEA stands for Chemical Equilibrium with Applications. This program

“chemical equilibrium compositions and properties of complex mixtures”, commonly used in rocket-based chemistry applications. NASA’s CEA program does have an option for a Chapman-Jouguet Detonation problem type which fits the criteria of this problem. Next, the temperature and pressure range can be selected as well as the fuel and oxidizer type. Temperature range of 3000 K to 4000 K was selected with a Pressure range of 80 atm to 90 atm. Fuel type was selected to be H₂ with Air H₂O as the oxidizer. As this is a stoichiometric mixture, the mixing ratio phi was selected to be 1.0. The comprehensive results of this CEA simulation can be seen in Appendix III. These screenshots of the program can be seen below in Figure 29 thru Figure 32 [53]. This step was important to provide a baseline prior to the detonation simulations to be performed in Ansys Fluent.

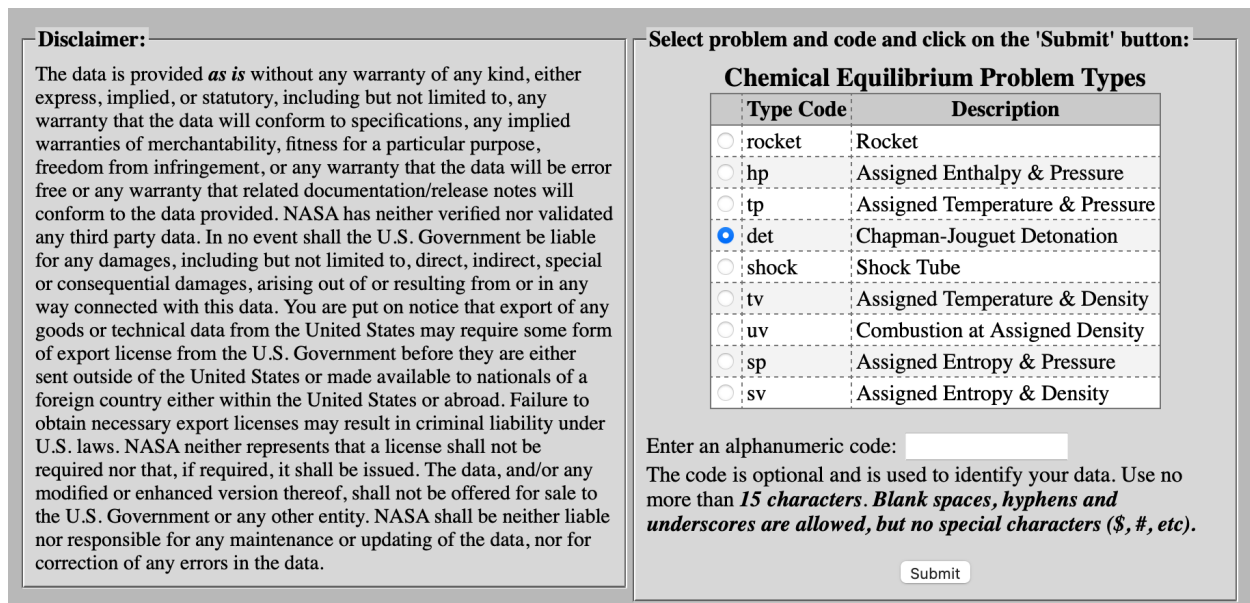


Figure 29 NASA CEA program problem selection [53].

For a refresh on Chapman-Jouguet Detonation Theory with visual representation, please revisit section 1.1.2, which detailed detonation phenomena and the various theories used to describe it, including ZND Theory.

| Temperature | | Pressure | |
|--|--|--|--|
| Enter Low/High/Interval values for no more than 24 datapoints. | 1. <input type="text"/> 13. <input type="text"/> | Enter Low/High/Interval values for no more than 24 datapoints. | 1. <input type="text"/> 13. <input type="text"/> |
| Low Value: <input type="text" value="3000"/> | 2. <input type="text"/> 14. <input type="text"/> | Low Value: <input type="text" value="80"/> | 2. <input type="text"/> 14. <input type="text"/> |
| High Value: <input type="text" value="4000"/> | 3. <input type="text"/> 15. <input type="text"/> | High Value: <input type="text" value="100"/> | 3. <input type="text"/> 15. <input type="text"/> |
| Interval: <input type="text" value="100"/> | 4. <input type="text"/> 16. <input type="text"/> | Interval: <input type="text" value="2"/> | 4. <input type="text"/> 16. <input type="text"/> |
| <input type="button" value="Clear Low/High/Int. Fields"/> | 5. <input type="text"/> 17. <input type="text"/> | <input type="button" value="Clear Low/High/Int. Fields"/> | 5. <input type="text"/> 17. <input type="text"/> |
| | 6. <input type="text"/> 18. <input type="text"/> | | 6. <input type="text"/> 18. <input type="text"/> |
| | 7. <input type="text"/> 19. <input type="text"/> | | 7. <input type="text"/> 19. <input type="text"/> |
| | 8. <input type="text"/> 20. <input type="text"/> | | 8. <input type="text"/> 20. <input type="text"/> |
| | 9. <input type="text"/> 21. <input type="text"/> | | 9. <input type="text"/> 21. <input type="text"/> |
| | 10. <input type="text"/> 22. <input type="text"/> | | 10. <input type="text"/> 22. <input type="text"/> |
| | 11. <input type="text"/> 23. <input type="text"/> | | 11. <input type="text"/> 23. <input type="text"/> |
| | 12. <input type="text"/> 24. <input type="text"/> | | 12. <input type="text"/> 24. <input type="text"/> |
| | <input type="button" value="Clear Numbered Fields"/> | | <input type="button" value="Clear Numbered Fields"/> |
| Select one: <input checked="" type="radio"/> K <input type="radio"/> C <input type="radio"/> F <input type="radio"/> R | | Select one: <input checked="" type="radio"/> atm <input type="radio"/> bar <input type="radio"/> mmHg <input type="radio"/> psia | |
| *Ref: NASA RP1311 Part II (Users Manual), Section 2.4.10 | | *Ref: NASA RP1311 Part II (Users Manual), p. 13, Section 2.4.8 | |

Figure 30 NASA CEA program pressure and temperature input [53].

Select one of the following:

Select one of the following compounds for *simple* (1-component) fuels, or select a mixture using the periodic table:

CH4 H2 Use Periodic Table (mixtures)

- The species listed above are assumed to be **pure**. If your reactant is not shown here, or you need to blend one or more compounds, use the Periodic Table.
- Please note that any fuel combinations using the Periodic Table will cancel out a current simple-fuel selection.**
- Be careful to select the appropriate compounds. Some compounds are represented in the CEA database in more than one form. For example, H2 refers to gas while H2(L) is liquid.
- To specify reactants without distinguishing between 'fuels' and 'oxidants', select '**None**' from the Oxidizer Selection page, and CEA will be instructed to skip the Oxidizer Selection Form.

Enter Reactant Temperature(K), if needed:

Please specify how to define reactant mixtures (*both Fuels & Oxidizers*): wt% mole

Figure 31 NASA CEA program fuel selection [53].

Select one of the following:

Select one of the following compounds for *simple* (1-component) oxidizers, or select a mixture using the periodic table:

Air CL2 F2 N2O O2

Enter Oxidizer Temperature(K), if needed:

Use Periodic Table (mixtures) None

- Use the Periodic Table if your oxidizer does not appear above or you need a mixture of two or more compounds.
- **Please note that selecting oxidizer(s) using the Periodic Table cancels out any simple-oxidizer selection.**
- If you do not want your analysis to distinguish between fuels and oxidizers, select **None**.
- Select your reactants carefully, since some compounds are represented in the CEA Database in more than one form. For example, H2O refers to water vapor while H2O(L) is liquid.

Figure 32 NASA CEA program oxidizer selection [53].

With the inputs mentioned in the paragraph above, NASA's CEA program spit out the following results: $P/P1 = 1.131$, $T/T1 = 1.034$, $M/M1 = 1.000$, $\text{Rho}/\text{Rho}1 = 1.094$, Detonation Mach Number = 1.085, Detonation Velocity = 3219.7 m/s. Below is a graph of the range of values created from importing these solution vectors into MATLAB. Note that traditional detonation velocities can be around 1700 m/s but can reach into the 3000 m/s range [54]. Further iterations of this NASA CEA Chapman-Jouguet detonation case needed to be produced in order to validate the results.

In the next NASA CEA Chapman-Jouguet iteration the inputs were varied slightly to measure the overall effect of slight fluctuations in the detonation combustion chamber or annulus of the RDE. The inputs to the function were selected as follows. The temperature and pressure range can be selected as well as the fuel and oxidizer type. Temperature range of 2500K to 3500K was selected with a Pressure range of 70 atm to 80 atm. Fuel type was selected to be H2 with Air H2O as the oxidizer as was done in the first scenario. As this is a stoichiometric mixture, the mixing ratio phi was selected to be 1.0 for the second case. The comprehensive results of this CEA simulation can be seen in Appendix C - NASA CEA Test 2. NASA's CEA

program then output the following results: $P/P_1 = 1.345$, $T/T_1 = 1.128$, $M/M_1 = 1.010$, $Rho/Rho_1 = 1.2.41$, Detonation Mach Number = 1.241, Detonation Velocity = 3351.2 m/s. It is seen that the second test case produced better results with higher detonation velocity.

4.2 Ansys Fluent Initialization

The program used in the rotating detonation engine model simulation is Ansys Fluent. Below is pictured in Figure 33 a screenshot of the program environment and graphical user interface (GUI). The details of the user interface and program will be explored in this section.

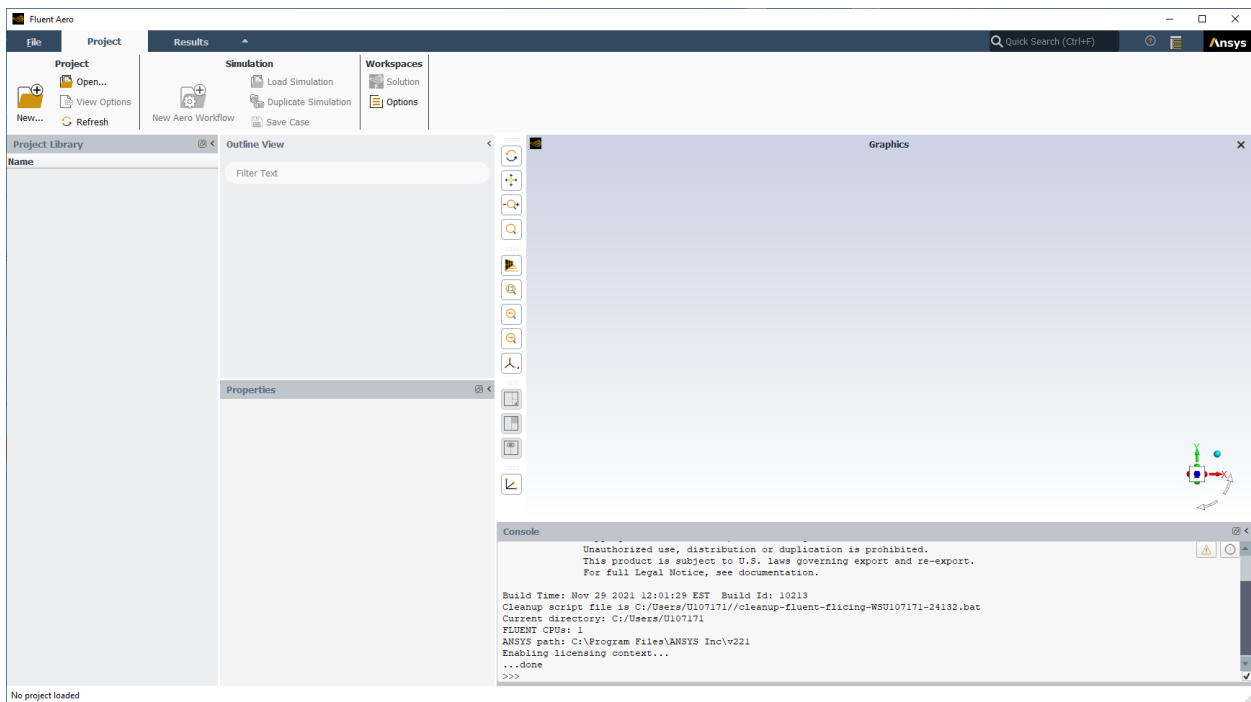


Figure 33 Ansys Fluent GUI [49].

The Ansys Fluent program includes a user interface graphical tree on the left-hand side which includes three different sections: setup, solution, results. The initial setup of the program includes these items in the tree: general, models, materials, cell zone conditions, boundary conditions, mesh interfaces, dynamic mesh, reference values, reference frames, and named

expressions. The main focus of our study will include the setup and solution sections, including models, materials, boundary conditions, and mesh interfaces for setup as well as methods, calculation activities (solution animation), and run calculation for the solution section. This graphical tree can be seen below in Figure 34:

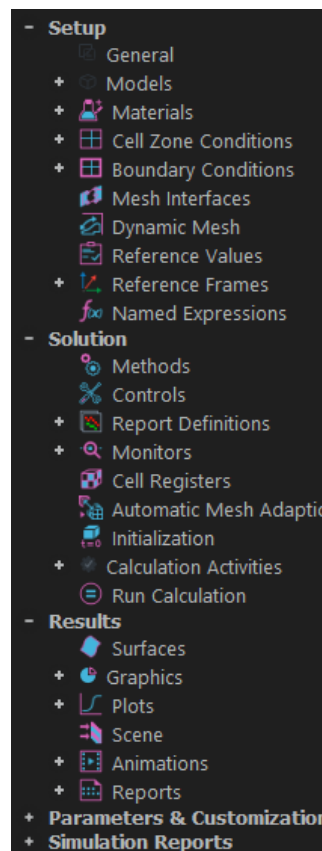


Figure 34 Ansys Fluent graphical user tree [49].

In order to produce viewable results, the solutions tab must be explored further. Located underneath the solutions tab is the calculation activities section which includes solution animations. In addition to the standard residuals graph which includes the parameters:

continuity, x-velocity, y-velocity, and energy, it is important to display temperature and pressure. This can be done by selecting a new contour for a solution animation and then choosing the parameter of interest, in this case one for pressure and one for temperature are created. Furthermore, the mesh surfaces of interest can be selected or deselected to show pressure and temperature on the respective surfaces. For the RDE simulation model, Ansys Fluent was successfully able to produce HSF animation files for each of these parameters on all surfaces.

4.3 RDE Simulation Model

Section 4.3 will outline the rotation detonation engine simulation model including the input parameters, initial conditions, boundary conditions, fuel and oxidizer types, solution methods, and calculation details. For the primary focus of study, the non-ideal injector case was utilized, that is, many injectors spaced out evenly on the bottom portion of the combustion chamber pointing upward. The fuel mixture remains a stoichiometric hydrogen-air combo.

Starting with initial and boundary conditions, to reiterate, the combustion chamber (3-dimensional cylinder) was unrolled and modeled as a 2-dimensional sheet. The lower boundary is where the non-ideal injectors are placed while the remaining walls are defined as periodic boundaries (translational), which are no slip stationary walls. This bottom boundary was set as a User-Defined Function (UDF), borrowed from Samuel Zuniga [28]. Both the inlet and outlets were set to reference atmospheric conditions, while the inlet was set to be defined as a velocity inlet in Fluent and the outlet was similarly set to a pressure outlet. Furthermore, the velocity inlet was defined with the following: a Velocity Magnitude of 317m/s, a Temperature of 250 Kelvin, a Supersonic/Initial Gauge Pressure of 535282 Pascals, and an Outflow gauge

pressure of 101325 Pascals (atmospheric). The pressure outlet settings reflected were a Gauge Pressure of 0 Pascals, and a Mach Number of 0.6.

Next, for the solution methods, the following is true. Formulation was chosen as implicit, Flux Type to be Roe-FDS, Spatial Discretization Gradient as Least Squares Cell Based, and Spatial Discretization Flow as Second Order Upwind. A current Number of 0.05 was used for the initial simulation model.

Finally, the details of the Run Calculation are outlined as the following. The Time Advancement Type is Fixed, Method is User-Specified, the Number of Time Steps is 500, the Time Step Size is $1e-6$, Max Iterations/Time Step is 10, Reporting Interval is 1, and the Profile Update Interval is also 1. The last portion of interest is related to the Results section which focuses on the post-processing techniques of the solution in Ansys Fluent. This will be focused on in the Initial Results Section.

Next, is the initial 2-D Unrolled RDE mesh, which had a spacing of 0.1 mm with adaptive attributes. Here the boundary conditions can be seen on the lower and upper walls of the unrolled combustion chamber mesh. The size of this mesh will be varied in subsequent Fluent simulations to explore the scalability of the rotating detonation engine, that is, how are the resulting performance parameters affected by scaling up the size of the combustion chamber and scaling down the size of the combustion chamber. The initial mesh was referenced from Zuniga's work [28].

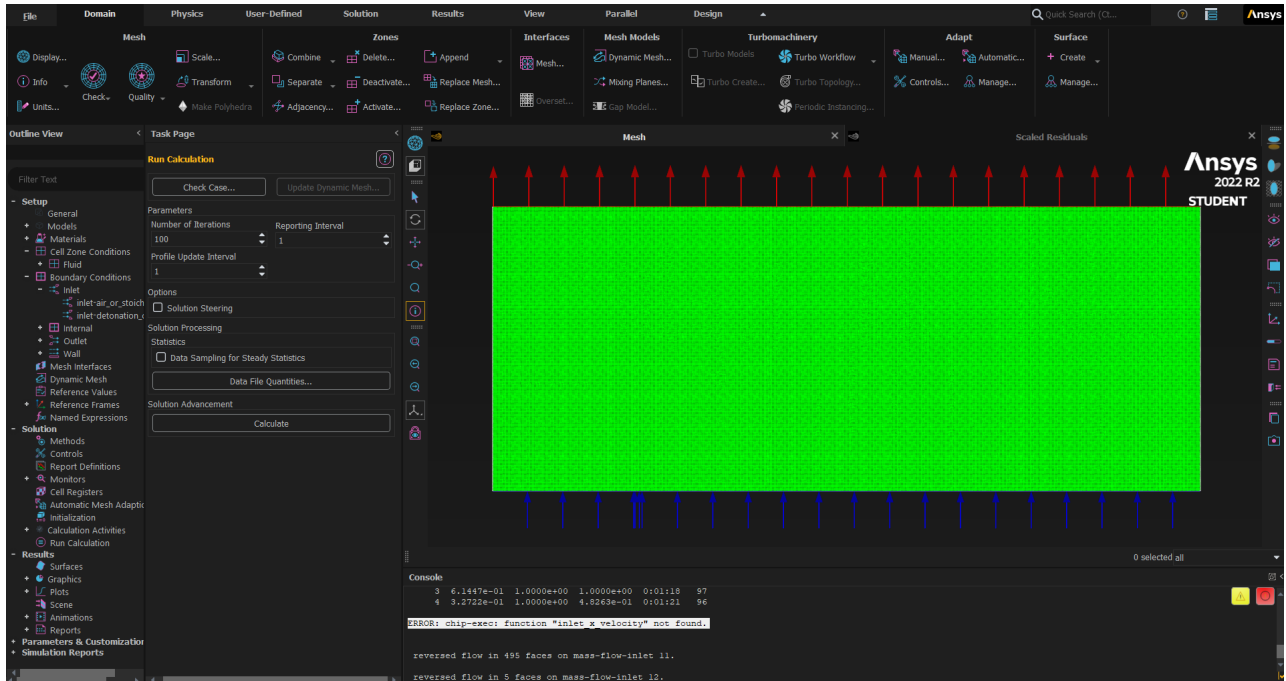


Figure 35 Ansys Fluent RDE mesh [49].

4.4 Initial Results

The first set of initial results came out rough. Here is a look at the rudimentary mesh for a pulse detonation tube example with resulting graphs. Mesh spacing of 0.1 mm was used.

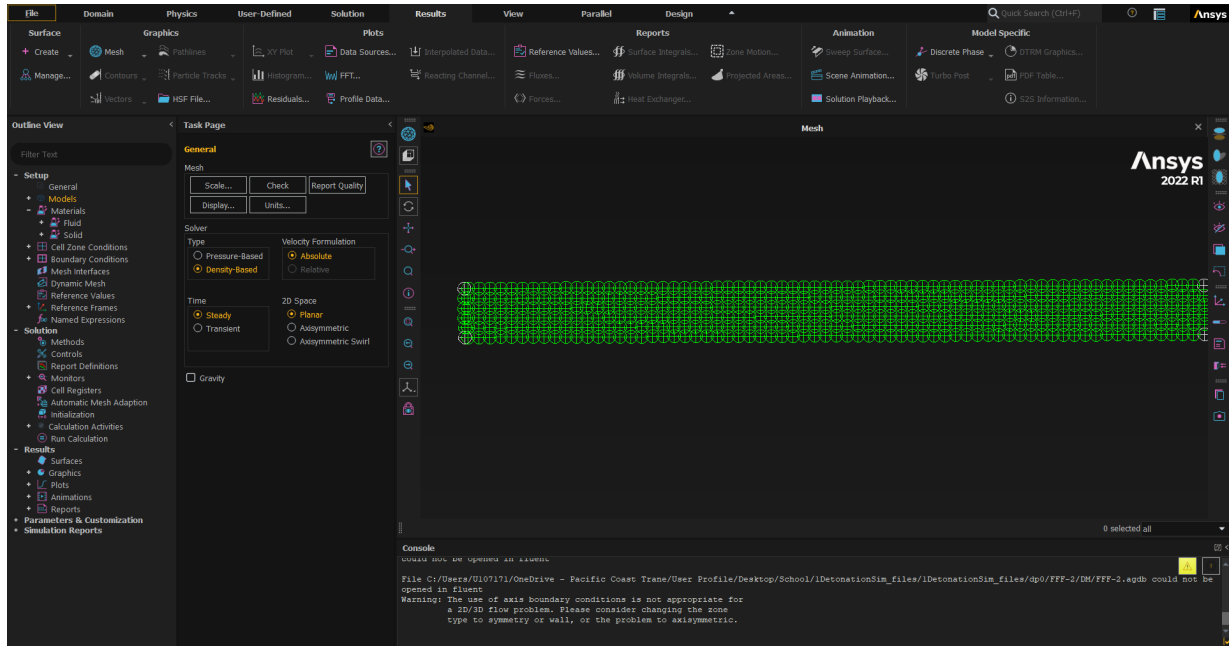


Figure 36 Ansys Fluent pulse detonation tube mesh [49].

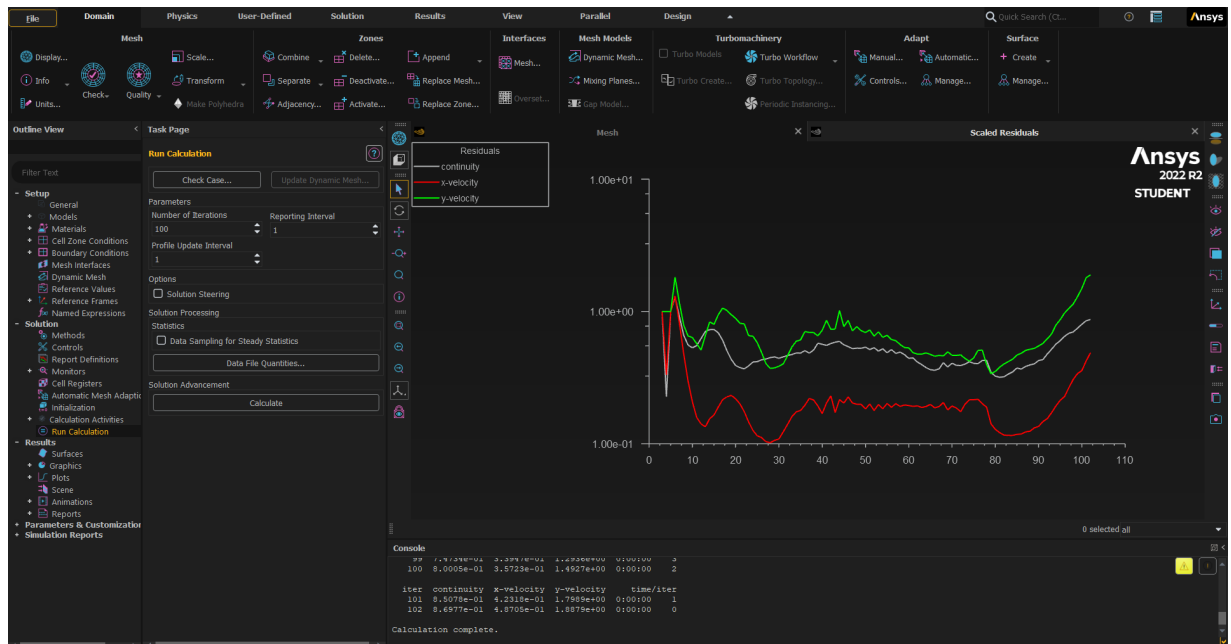


Figure 37 Ansys Fluent pulse detonation tube residuals [49].

Next, is the initial RDE model simulation resulting residuals. This simulation did not converge.

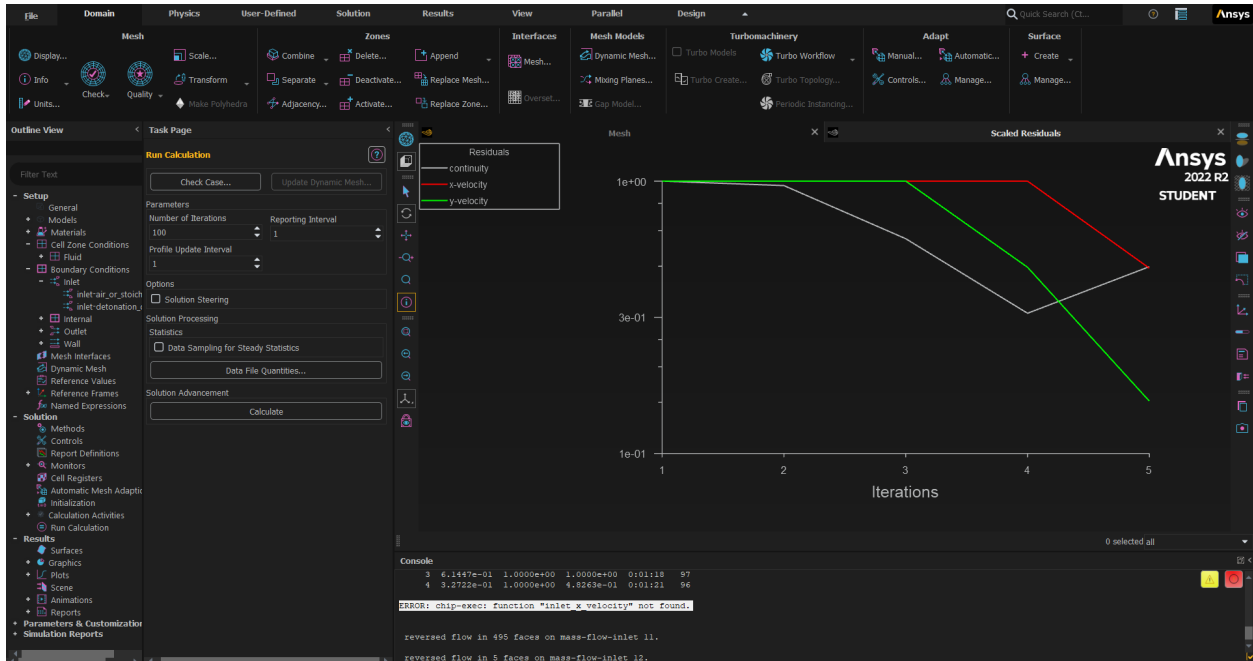


Figure 38 Ansys Fluent RDE initial residuals [49].

Another subsequent simulation was performed and proved to be more successful, producing clearer results. Halfway through the simulation, this is what the results looked like:

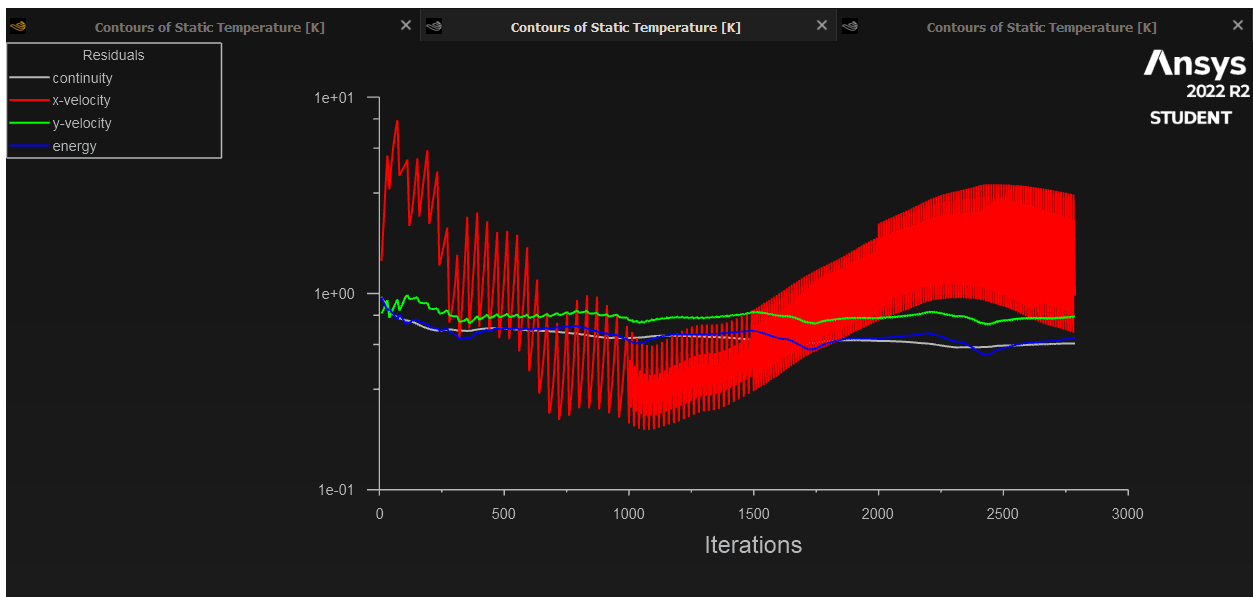


Figure 39 Ansys Fluent 2nd RDE simulation 50% complete residuals [49].

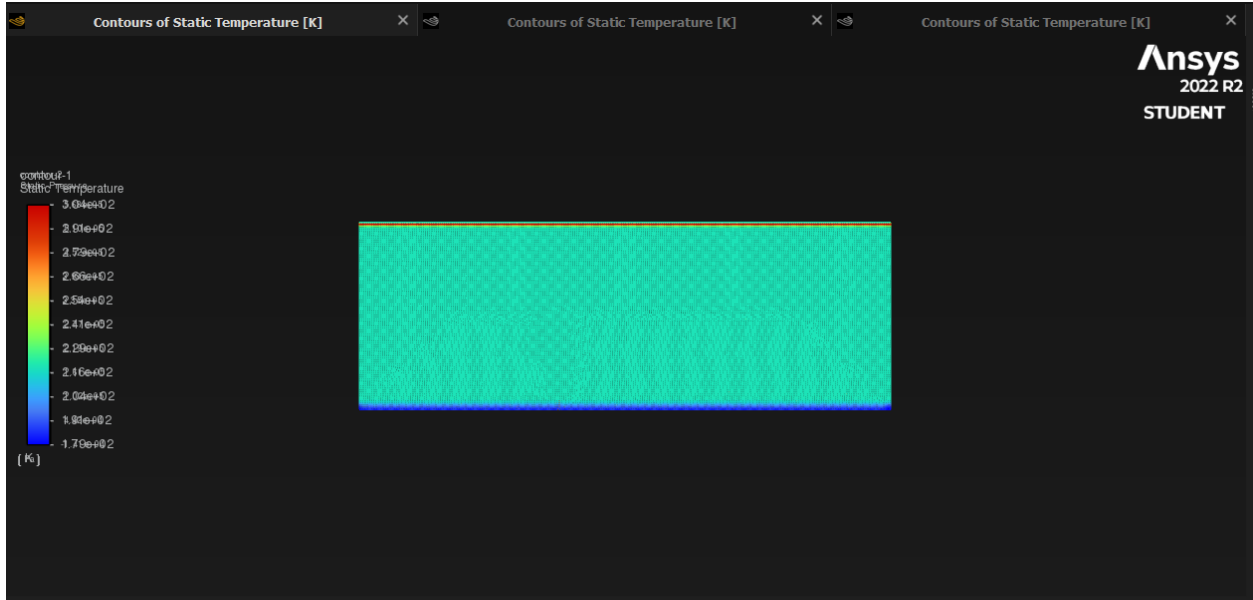


Figure 40 Ansys Fluent 2nd RDE simulation 50% complete temperature [49].

Above, in Figure 40 is the contour created for the Temperature along all mesh surfaces. Further post-processing analysis needs to be done in order to verify the validity of the results received.

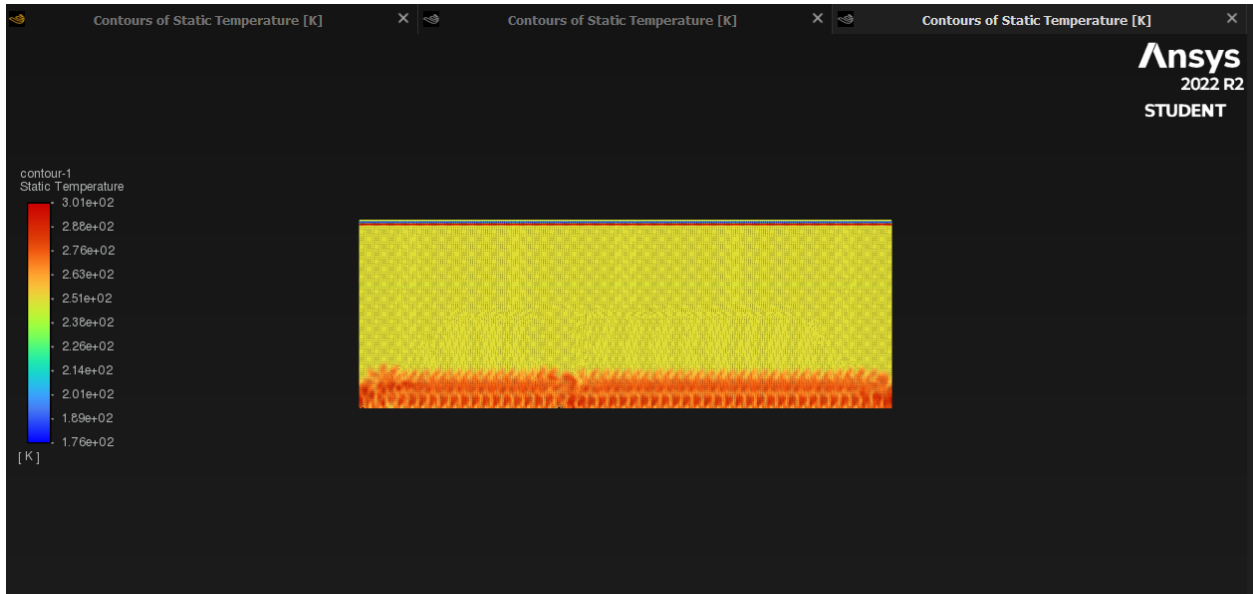


Figure 41 Ansys Fluent 2nd RDE simulation 50% complete pressure [49].

Furthermore, above in Figure 41 is the contour created for the Pressure along all mesh surfaces.

After having completed the simulation, this is what the results looked like. First, in Figure 42 is displayed the residual graph after 100% completion of the simulation.

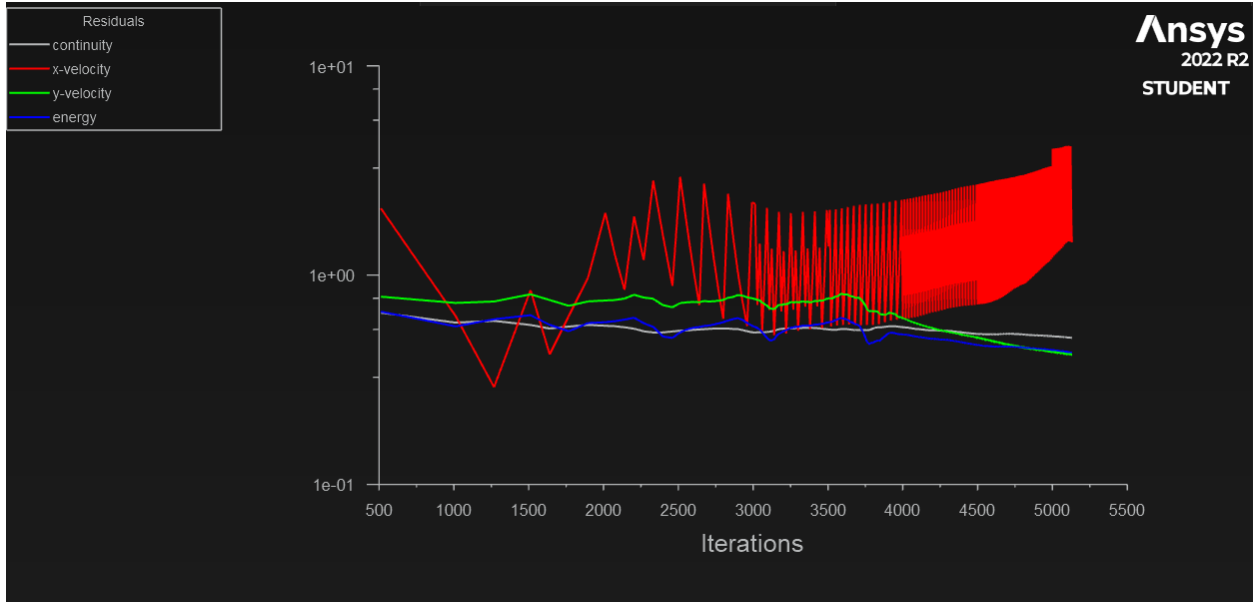


Figure 42 Ansys Fluent 2nd RDE simulation 100% complete residuals [49].

Second, in Figure 43 is displayed the temperature overlay on the mesh after completion.

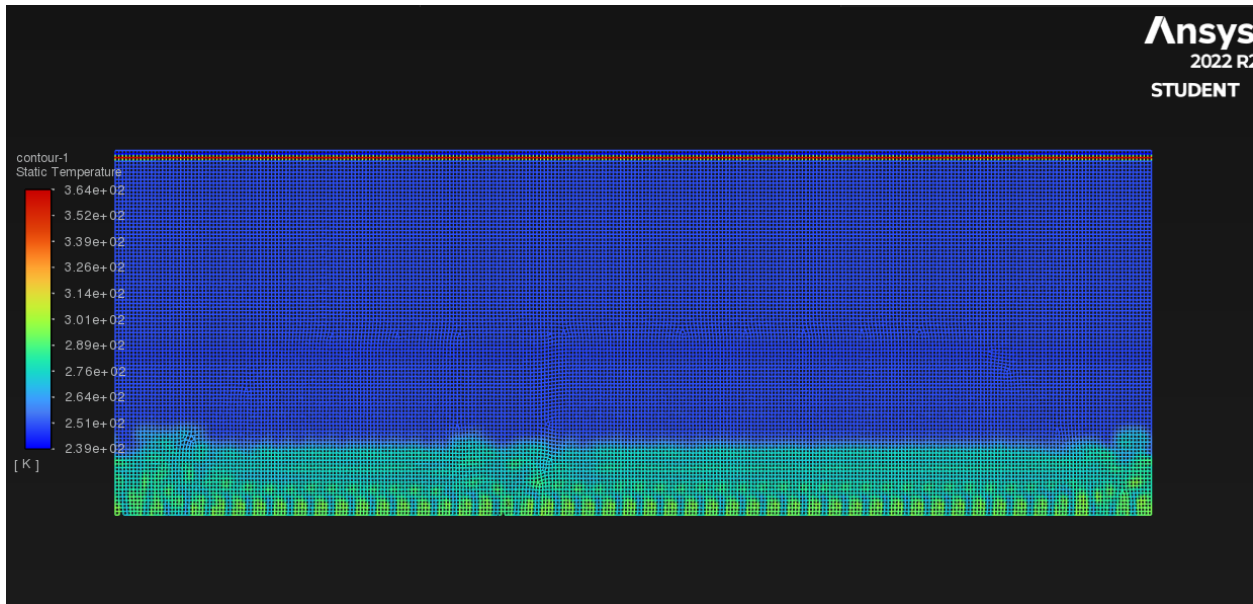


Figure 43 Ansys Fluent 2nd RDE simulation 100% complete temperature [49].

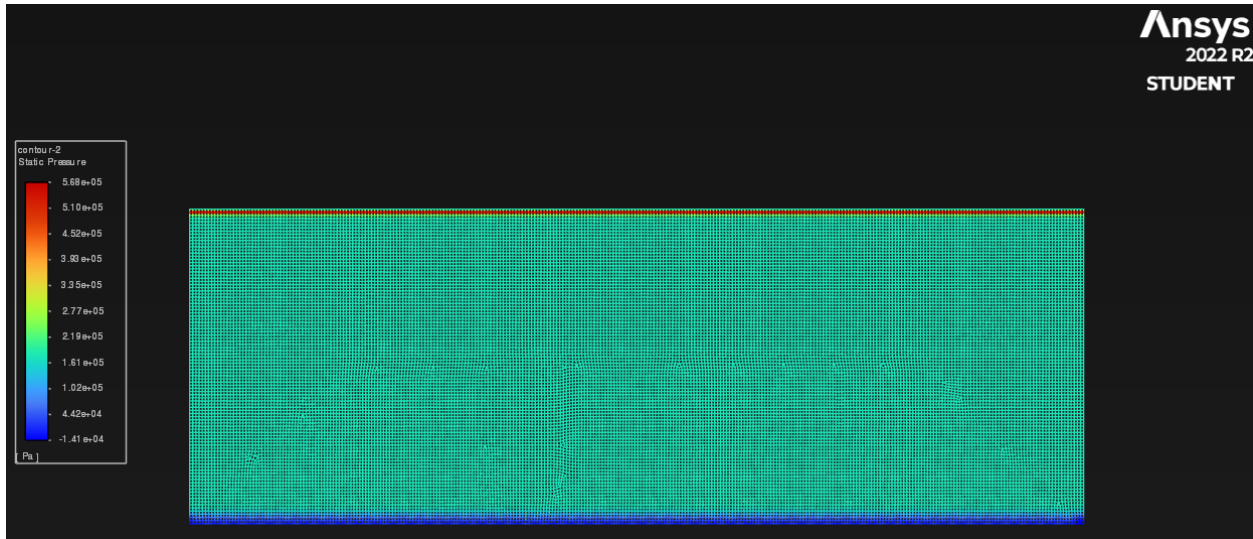


Figure 44 Ansys Fluent 2nd RDE simulation 100% complete pressure [49].

After a closer look, it is clear that the simulation is not capturing the Chapman-Jouguet detonation wave, which should be visibly seen in these simulations.

4.5 Sizing & Scalability Simulations

Next, it is important to explore the term scalability and what exactly it entails in the context of the initial results. Scalability, in technological terms, is defined as: “the measure of a system’s ability to increase or decrease in performance and cost in response to changes in application and system processing demands” [55]. In this particular case, or with scalability and sizing applied to propulsion systems such as an RDE engine, the question is: “Will this RDE exhibit similar performance characteristics, fuel efficiency, and power output if the physical size of the engine is scaled up or down?” This section exists in order to answer that question. As this is a relatively new and emerging technology, not much extensive effort has been made by way of scalability and sizing analysis in the existing literature. Most if not all of the proceeding analysis will be novel in that scalability has not been a focus of RDE’s that currently exist. The purpose

of being able to answer this question is to open the discussion to whether or not these engines (RDE's) can be used in smaller non-rocket based applications, like satellites for example.

Now that initial results have been obtained, it is necessary to next explore the sizing effects and scalability of the rotating detonation engine technology via further Ansys Fluent simulations. The requirements to undertake this deeper step of analysis are quite simple and straightforward. The mesh size needs to be varied, first shrinking the initial mesh size, which was a baseline, and second enlarging the initial mesh size. This will be completed at various sizes, not including only one smaller mesh and one larger mesh. The initial mesh size referenced a height of $Y_{max} = 0.285012\text{m}$ and width or length of $X = 0.1\text{m}$. The mesh size differentiation will be 50% in each direction, that is the larger mesh will be 0.5x larger and the smaller mesh 0.5x smaller. Below is a single example of the effect of mesh scaling:

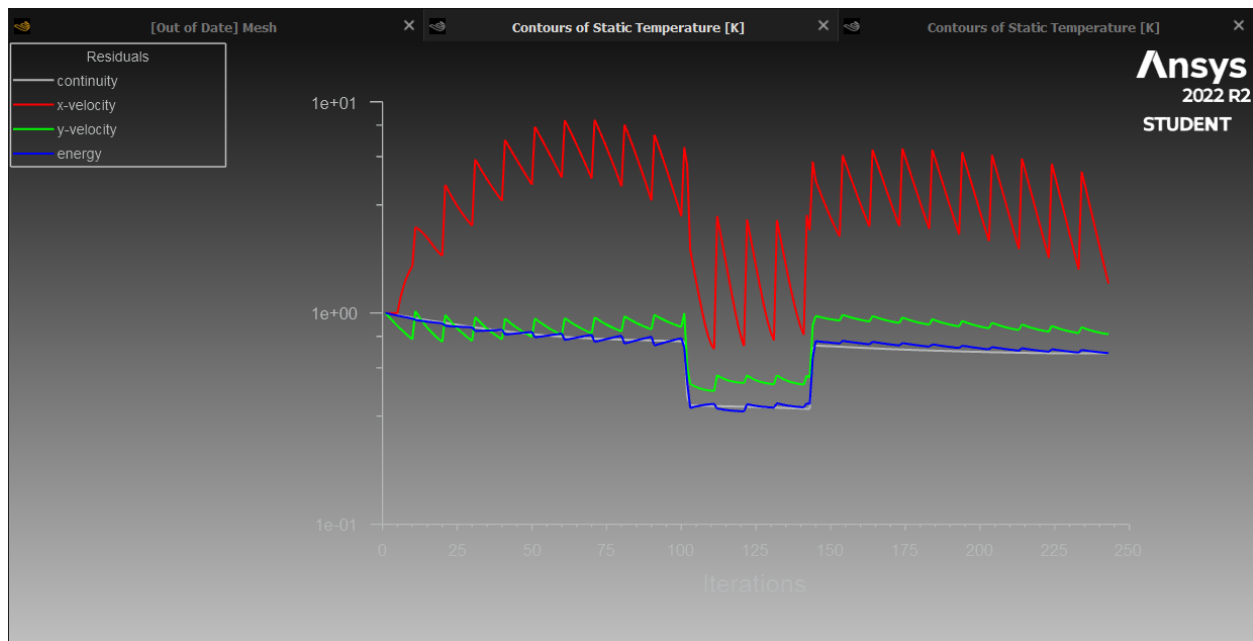


Figure 45 RDE residual graph mesh scaling [49].

The dip in the residuals is seen when the scaling was changed to 2x the starting length and width. After the dip in the residuals was when the scaling was changed to 0.5x the original size.

The results of the RDE combustion chamber mesh that has been scaled down by 0.5x. Displayed below is the residuals plot of the RDE chamber performance during simulation of 0.5x scaling.

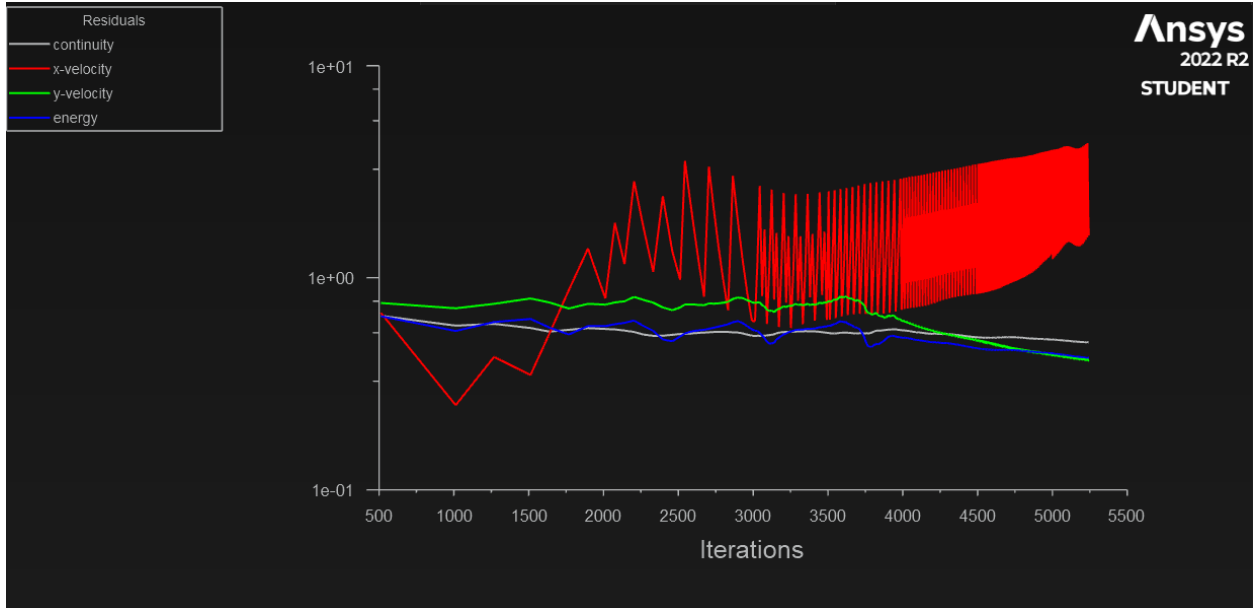


Figure 46 RDE residual graph mesh scaling 0.5x [49].

Below is the residuals plot of the RDE chamber performance during simulation of 2x scaling.

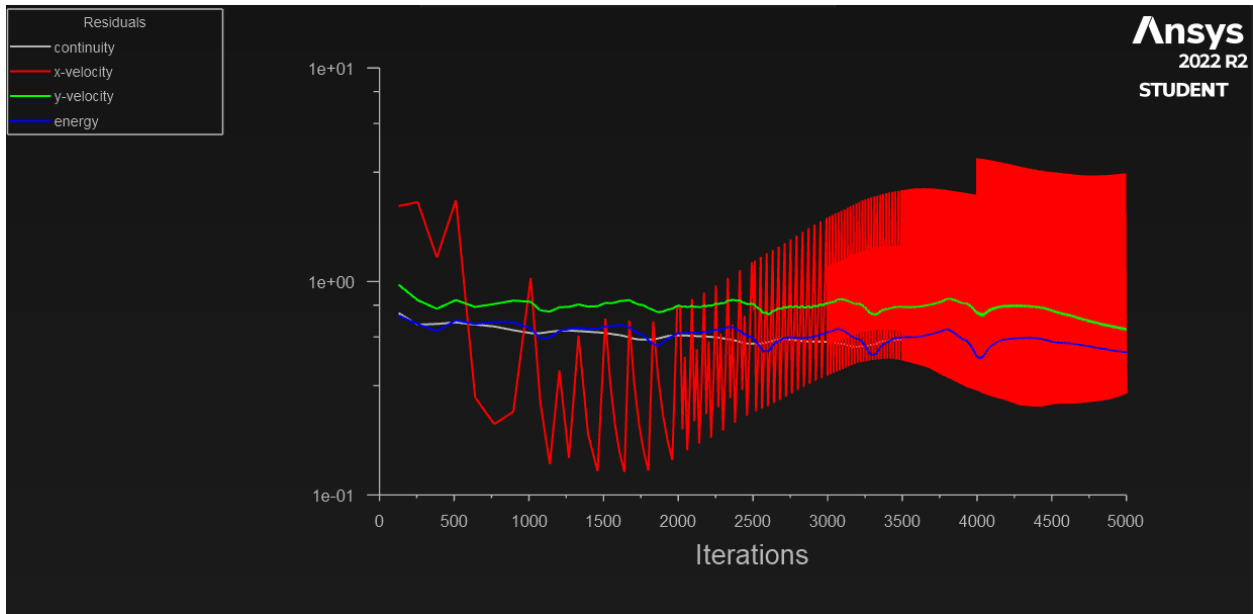


Figure 47 RDE residual graph mesh scaling 2x [49].

Displayed below is the temperature contour plot gradient view of the 2x scaled simulation.

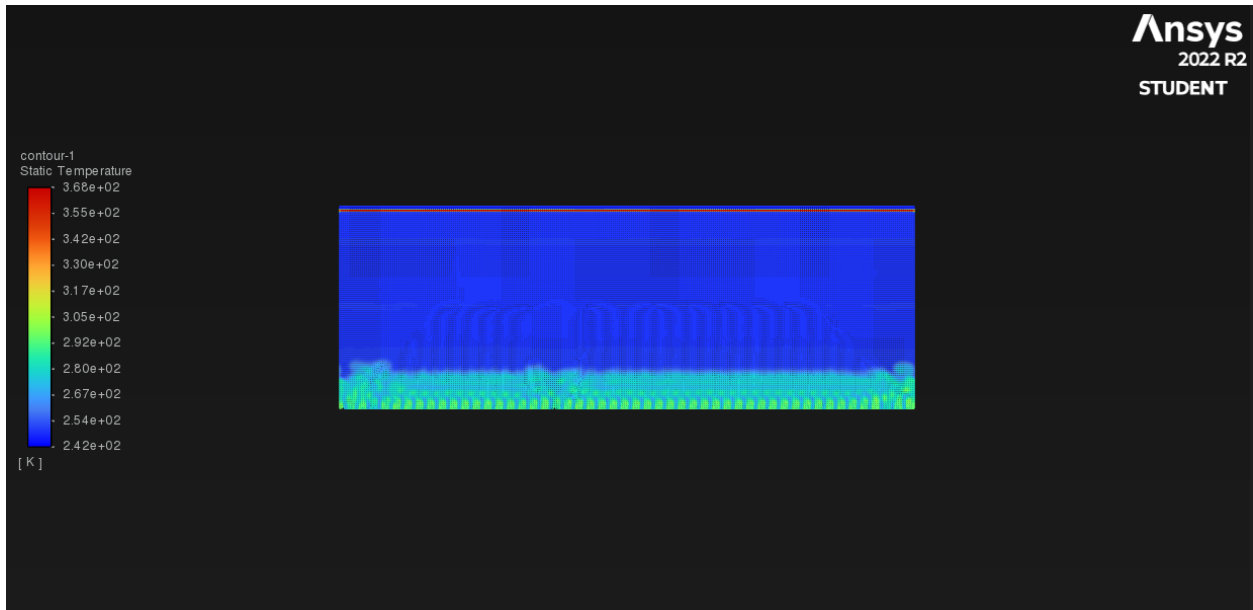


Figure 48 Ansys Fluent RDE scaling 0.5x simulation 100% temperature [49].

Displayed below is the pressure contour plot gradient view of the 2x scaled simulation.



Figure 49 Ansys Fluent RDE scaling 0.5x simulation 100% pressure [49].

Displayed below is the temperature contour plot gradient view of the 0.5x scaled simulation.

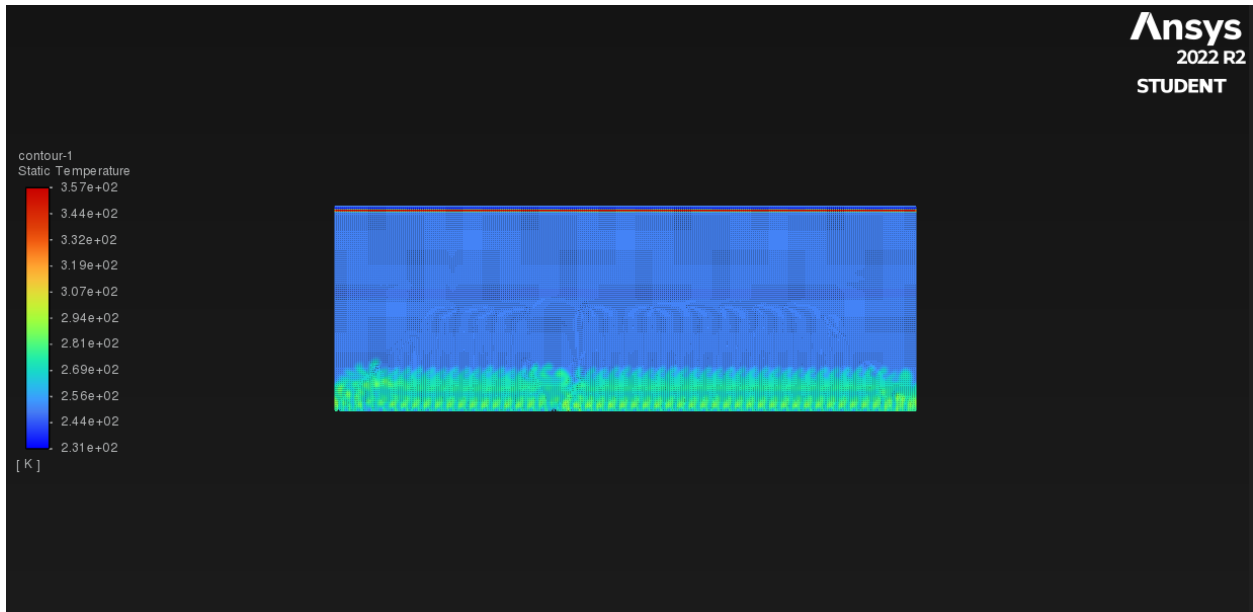


Figure 50 Ansys Fluent RDE scaling 2x simulation 100% temperature [49].

Displayed below is the pressure contour plot gradient view of the 0.5x scaled simulation.

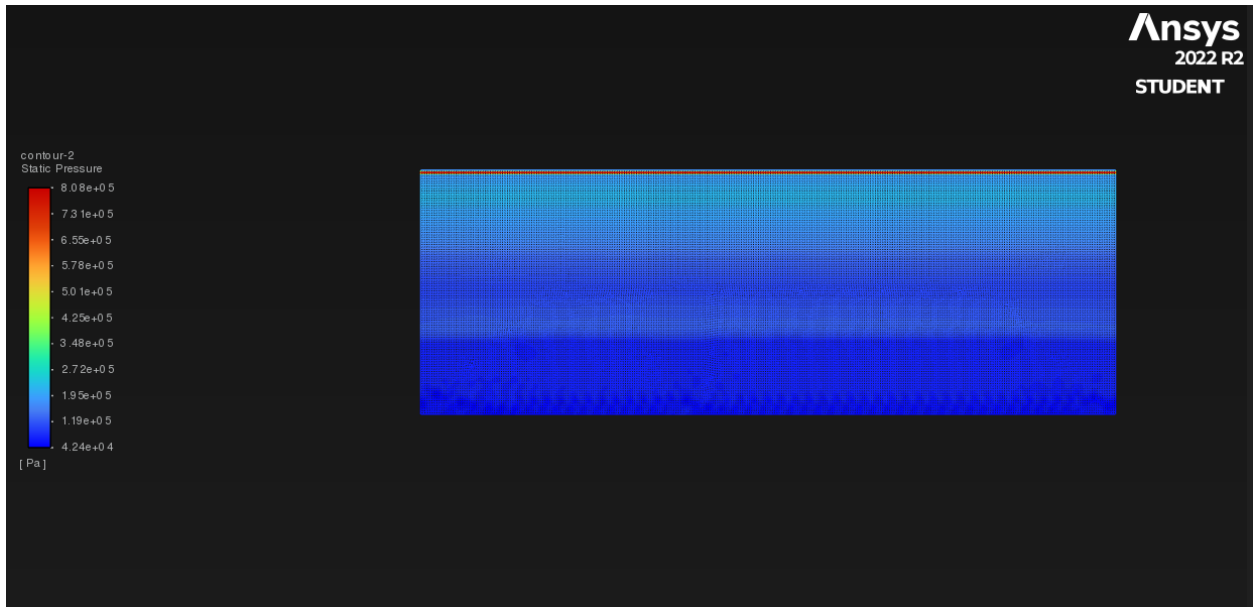


Figure 51 Ansys Fluent RDE scaling 2x simulation 100% pressure [49].

Overall, differences shown here are minimal and difficult to qualify at a first glance. It is clearly seen that there exists a slight variation in the final temperature and pressure gradient view of the mesh. At a visual inspection, it is hypothesized that the 0.5x scaled mesh RDE case performed more efficiently than the 2x scaled mesh RDE case. Higher pressure build-up and further circumferential travel of the detonation waves would be required to maintain the positively scaled case. Further post-processing of the simulation and data exports should be done in the future to arrive at a more specific and exact conclusion. Moreover, this proves that further work must be done to properly qualify ideal engine size and chamber length, depending on the intended application.

5.0 Analysis & Discussion

The results were successfully obtained after running the basic simulation cases mentioned and were successfully completed in Ansys Fluent. After reviewing the initial results produced from Ansys Fluent from the rotating detonation simulations, there is much post-processing work and detailed analysis to be done. Some performance calculations must be done in order to determine how the simulations compare against each other. Performance calculations must be undertaken to provide a baseline for the results received from the initial mesh. It is important to calculate specific impulse (ISP), thrust, and specific fuel consumption to further define the performance of each simulation case. This will be done for the initial RDE unrolled combustion chamber mesh as well as the upsized chamber mesh and the downsized chamber mesh.

Equations for specific impulse, thrust, specific fuel consumption, and finally mass flow rate are seen below:

$$ISP = V_e / g_0 \quad (5.1)$$

$$ISP = Thrust / (\dot{m} * g_0) \quad (5.2)$$

$$Thrust = V_e * (dm/dt) \quad (5.3)$$

$$TSFC = \dot{m} / Thrust \quad (5.4)$$

$$\dot{m} = (m * v_2 - m * v_1) / (t_2 - t_1) \quad (5.5)$$

These equations are the classic rocket equations for determining different performance parameters that relate to the propulsion system. They can be easily adapted for use with rotating detonation engines in order to characterize performance. Below will be a table displaying the specific impulse, thrust, specific fuel consumption, and mass flow rate for the initial RDE chamber size, the scaled down size, and the upscaled chamber size. As is clearly seen, the best performing RDE case is the smaller chamber case, as it allows for higher pressure to be created

in the combustion chamber annulus, by the subsequent detonation waves. Finding balance is key in the quest of discovering the optimal combustion chamber length or engine size. The problem is that most of the key parameters are discovered in alternative methods when the rotating detonation engine enters the equation, some of which are quantified below.

Typical ISP of a realized RDE hovers anywhere between 3500s to 4000s, and theoretically upwards of 10000s. For the case of this discussion, ISP of 3500s will be chosen to calculate the remaining parameters. Using this value and a traditional g_0 of 9.8m/s^2 the exhaust velocity is calculated to be approximately $\sim 34,000\text{m/s}$. From this result, it is possible to determine remaining parameters such as thrust.

It is assumed based on Joseph Dechert's work with the Air Force Institute of Technology, entitled: "Development of a Small Scale Rotating Detonation Engine", that the optimal chamber length is based on h , which is defined as the heat release during the reaction that takes place in the combustion chamber [56]. The equation below used to calculate heat release h is seen as:

$$h = (12 \pm 5)\lambda \quad (5.6)$$

which is directly proportional to the λ , or detonation cell size for a set of reactants.

"Detonation cell size is a critical design parameter for correctly sizing many aspects of an RDE" [56]. The is otherwise defined as the width of a single scale. Based on varying the parameter h , the ideal chamber length was found to be approximately $\sim 4*h$. Applying this principle to the design of an RDE will prove extremely useful in reducing production time of the engine itself and allowing researchers to have access to a baseline when setting up engine parameters in CFD simulations. Although successful RDE simulations were produced in Ansys Fluent during the undertaking of this project, further studies must be conducted in order to find an ideal chamber length that can be tested in simulations as well as in the real world.

6.0 Conclusions & Future Work

In summary, rotating detonation engines prove to be a very promising propulsion system technology in the aerospace industry in the near future. Although currently more of an experimental propulsion system, RDE's have the potential to completely revolutionize the aerospace industry. In order to provide a more sustainable future, this technology must be explored further and more research is a necessity. As space becomes more and more privatized the industry cannot maintain launches and flights that use extreme excessive amounts of fuel. For the sake of financial cost and environmental factors alone RDE's are the next step forward in the field of advanced aerospace propulsion. Research must continue in both the private and public sector, with government funded projects by organizations like the Department of Energy DOE and research institutions like Universities being extremely critical.

The main limitations that stand in the way of successful realization of this technology, that is, reaching flight-proven status or a TRL 9 would have to be the injection schemes and techniques as well as the fuel/oxidizer mixture. Although a number of research papers outlining experiments and numerical studies have been done exploring both of these limitations, the goal still remains to produce a stable *sustained* detonation in an RDE for a prolonged period of time without having to reignite. That is where the potential 25% in efficiency increase will come from as compared to traditional combustion methods and engines.

It is very encouraging to note that there has been a recent development in the area of Rotating Detonation Engines, specifically, long-term stable testing done by NASA Marshall Space Flight Center in Huntsville, Alabama [57]. NASA has recently released details of their findings related to their first full-scale RDE on a test-stand developed at their facility to explore its viability for deep space missions. The differentiating factor from their results is that they

were able to successfully achieve hot-fire tests that totaled close to 10-minutes in duration. This is substantially longer than previous tests that exist in literature up until this point that have only lasted seconds at most in duration and provides hope for classifying what characteristics of the engine (geometry, materials, injection methods, etc) allow for stable sustained detonation of this length. The engine was constructed using additive manufacturing techniques (3-D printing of non-plastic materials), utilizing GRCo-42 a NASA-developed copper alloy, which has contributed to its robust nature. It can operate in very extreme environments for extended periods of time. The most impressive part of these tests is that the engine was able to produce up to 4,000 lbs of thrust (17.8kN), with a 622 lbs/in² pressure in the chamber, both of which are the highest recorded for an RDE design to date. NASA's next milestone outlines developing a fully reusable 10,000 lb class RDE to further examine its benefits over combustion engines.

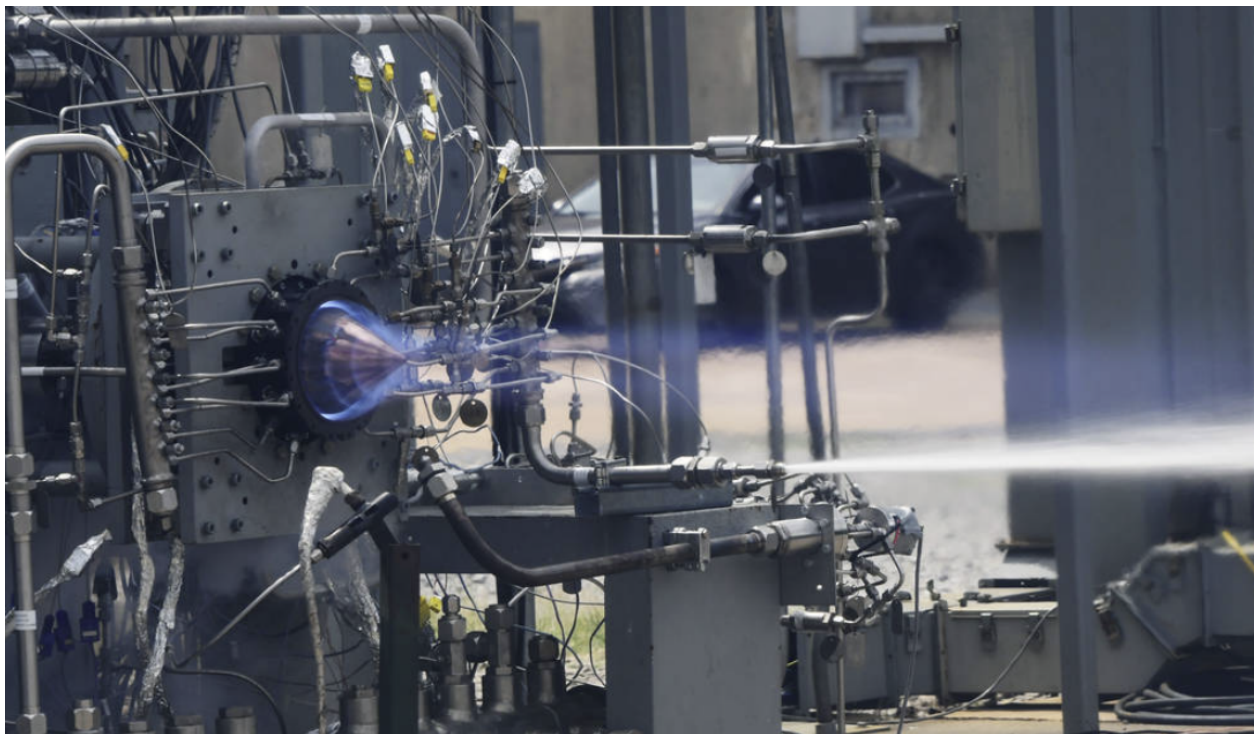


Figure 52 NASA Marshall Space Flight Center RDE hot-fire testing [57].

In conclusion, future work is still necessary and efficient collaboration between multiple entities is key to the success of this technology. More universities and privately-funded research groups need to enter the space of rotating detonation engine development. The upward trend of technological advancement is on an exponential curve, therefore, the literature provides evidence and confidence that RDE technology will officially, one day become a flight-proven propulsion system, potentially one that even transports humans to the outer reaches of the solar system.

References

- [1] Wikipedia, “Specific Impulse,” https://en.wikipedia.org/wiki/Specific_impulse, Sep. 2022.
- [2] Twitter, “Detonation Engines Thread,” <https://twitter.com/drchriscombs/status/1293172198484643840>, Aug. 2022.
- [3] NASA, “Technology Readiness Level,” https://www.nasa.gov/directorates/heo/scan/engineering/technology/technology_readiness_level, Aug. 2022
- [4] Paxson, D., “Pressure Gain Combustion 101,” AIAA 2018, *Propulsion and Energy*, NASA Glenn Research Center, Cincinnati, Ohio, July 2018.
- [5] Wikipedia Commons, “Holzwarth Gas Turbine Prototype,” https://commons.wikimedia.org/wiki/File:Holzwarth_gasturbine_prototype.jpg, “Aug. 2022.
- [6] Caltech Publications, “Fickett-Jacobs Cycle,” <https://shepherd.caltech.edu/EDL/publications/reprints/FickettJacobsCycle.pdf>, Aug. 2022.
- [7] Science Direct, “Deflagration-to-Detonation Transition in Highly Reactive Combustible Mixtures,” <https://www.sciencedirect.com/science/article/abs/pii/S0094576510001906>, Aug. 2022.
- [8] Kailasanath, K., “The Rotating Detonation-Wave Engine Concept: A Brief Status Report,” AIAA 2011-581, *49th AIAA Aerospace Sciences Meeting including the New Horizons Forum and Aerospace Exposition*, Orlando, Florida, Jan. 2011.
- [9] Li, J., “Detonation Control for Propulsion: Pulse Detonation and Rotating Detonation Engines (Shock Wave and High Pressure Phenomena),” *Spring International Publishing*, Aug. 2018.
- [10] Wikipedia, “Humphrey Cycle,” https://en.wikipedia.org/wiki/Humphrey_cycle, Jun. 2020.
- [11] NASA, “Ideal Brayton Cycle,” <https://www.grc.nasa.gov/www/k-12/airplane/brayton.html>, May 2021.

- [12] Intech Open, “A Theoretical Review of Rotating Detonation Engines,” <https://www.intechopen.com/chapters/70511>, Aug 2022.
- [13] Wikipedia, “Chapman-Jouguet Condition,” https://en.wikipedia.org/wiki/Chapman-Jouguet_condition, Sep. 2022.
- [14] Princeton, “Lecture 7 - Detonation Waves,” <https://cefr.princeton.edu/sites/g/files/toruqf1071/files/Files/2013%20Lecture%20Notes/Matalon/Notes-Lecture-7.pdf>, Sep. 2022.
- [15] Wikipedia, “Pulse Detonation Engine,” https://en.wikipedia.org/wiki/Pulse_detonation_engine, Dec. 2021.
- [16] Air Force National Museum, “Scaled Composites Long EZ Borealis,” <https://www.nationalmuseum.af.mil/Visit/Museum-Exhibits/Fact-Sheets/Display/Article/195765/scaled-composites-long-ez-borealis>, Aug. 2022.
- [17] Voitsekhovskiy, B. V., “Stationary spin detonation,” *Soviet Journal of Applied Mechanics and Technical Physics*, vol. 3, 1960, pp. 157–164.
- [18] Liu, S.-J., Lin, Z.-Y., Liu, W.-D., Lin, W., and Sun, M.-B., “Experimental and three-dimensional numerical investigations on H₂/air continuous rotating detonation wave,” *Proceedings of the Institution of Mechanical Engineers, Part G: Journal of Aerospace Engineering*, vol. 227, pp. 326–341, 2012.
- [19] Zheng, Q., Weng, C.-S., and Bai, Q.-D., “Experimental Research on the Propagation Process of Continuous Rotating Detonation Wave,” *Defense Technology*, vol. 9, iss. 4, pp. 201–207, Dec. 2013.
- [20] Wang, Y., Wang, J., Li, Y., and Li, Y., “Induction for multiple rotating detonation waves in the hydrogen–oxygen mixture with tangential flow,” *International Journal of Hydrogen Energy*, vol. 39, 2014, pp. 11792–11797.
- [21] Wolański, P., “Detonative propulsion,” *Proceedings of the Combustion Institute*, vol. 34, pp. 125–158, 2013.
- [22] Boller, S., “Flow Behavior in Radial Rotating Detonation Engines,” Air Force Institute of Technology, Wright-Patterson Air Force Base, Ohio, Mar. 2019.

- [23] Kaemming, T., “Thermodynamic Modeling of a Rotating Detonation Engine Through a Reduced Order Approach,” *Journal of Propulsion and Power*, vol. 33, iss. 5, pp. 1170-1178, Sep. 2017.
- [24] Kaemming, T., “Overview of Performance, Application, and Analysis of Rotating Detonation Engine Technologies,” *Journal of Propulsion and Power*, Vol. 18, Iss. 1, pp. 131-143, Jan. 2017.
- [25] Department of Energy, “NETL Joining with NASA, DOD to Advance Highly Efficient Low-Emission Engine Technology,”
<https://netl.doe.gov/node/9917>, Aug. 2022.
- [26] National Energy Technology Laboratory, “Pressure Gain Combustion,”
<https://netl.doe.gov/node/7553>, Accessed Dec. 2021.
- [27] Koch, J., “Mode-Locked Detonation Waves: Experiments and a Model Equation,” William E. Boeing Department of Aeronautics and Astronautics, University of Washington, Seattle, Nov. 2019.
- [28] Zuniga, S., “Investigation of Detonation Theory and the Continuously Rotating Detonation Engine,” *San Jose State University Department of Aerospace Engineering*, May 2018.
- [29] J. A. Boening, J.D. Heath, T.J. Byrd, J.V. Koch, A.T. Mattick, R. E. Breidenthal, C. Knowlen, and M. Kurosaka, “*Design and Experiments of a Continuous Rotating Detonation Engine: a Spinning Wave Generator and Modulated Fuel/ Oxidizer Mixing*,” Abstract for AIAA Propulsion and Energy 2016.
- [30] Popular Mechanics, “Rotating Detonation Engine,”
<https://www.popularmechanics.com/science/a31000649/rotating-detonation-engine>, Oct. 2022.
- [31] Green Car Congress, “Researchers Demonstrate Continuous Detonation in Rotating Detonation Rocket Engine with H₂/O₂,”
<https://www.greencarcongress.com/2020/05/20200504-rdre.html>, Oct. 2022.
- [32] AIAA Aerospace America, “Increasing Engine Efficiency,”
<https://aerospaceamerica.aiaa.org/departments/increasing-engine-efficiency>, Oct. 2022.
- [33] Gopalakrishnan, S., Ganeshkumar P., “Systematic Reviews and Meta Analysis: Understanding the Best Evidence in Primary Healthcare,” *Journal of Family Medicine and Primary Care*, Vol. 2, Iss. 1, pp. 9-14, Jan. - Mar. 2013.

- [34] Curtin University, “Systematic Reviews,” <https://libguides.library.curtin.edu.au/systematic-reviews>, July 2022.
- [35] Kailasanath, K., “Review of propulsion applications of detonation waves,” *AIAA Journal*, vol. 38, iss. 9, pp. 1698-1708, Sep. 2000.
- [36] Kailasanath, K., “Recent Developments in the Research on Rotating-Detonation-Wave Engines,” AIAA 2017-784, *55th AIAA Aerospace Sciences Meeting*, Grapevine, Texas, Jan. 9-13 2017.
- [37] Kailasanath, K., “Recent Developments in the Research on Rotating-Detonation-Wave Engines,” *55th AIAA Aerospace Sciences Meeting*, May 2017.
- [38] Wikipedia, “Kelvin-Helmholtz Instability,” https://en.wikipedia.org/wiki/Kelvin-Helmholtz_instability, Oct. 2022
- [39] Bykovskii, F. A., Zhdan, S. A., and Vedernikov, E. F., “Continuous Spin Detonations,” *Journal of Propulsion and Power*, vol. 22, 2006, pp. 1204–1216.
- [40] Heiser, W., “Thermodynamic Cycle Analysis of Pulse Detonation Engines,” *Journal of Propulsion and Power*, vol. 18, iss. 1, pp. 68-76, Jan. 2002.
- [41] Ananad, V., Gutmark, E., “Rotating Detonation Combustor Research at the University of Cincinnati,” vol. 101, pp. 869-893, *Journal of Flow Turbulence and Combustion*, May 2018.
- [42] Shi, Z., Kindracki, J., “Numerical Calculation of Rotating Detonation Chamber,” *Journal of Power Technologies*, vol. 97, iss. 4, pp. 314-326, Jan. 2018.
- [43] Leap Australia, “Tips & Tricks: Turbulence Part 2: Wall Functions & Y+ Requirements,” <https://www.computationalfluidynamics.com.au/tips-tricks-turbulence-wall-functions-and-y-requirements>, Nov. 2022.
- [44] Nordeen, C., “Thermodynamics Rotating Detonation Engine,” University of Connecticut, *Doctoral Dissertations*, Dec. 2013.
- [45] Wikipedia, “Rothalpy,” <https://en.wikipedia.org/wiki/Rothalpy>, Nov. 2022.
- [46] Wikipedia, “Heuristic,” <https://en.wikipedia.org/wiki/Heuristic>, Nov. 2022.
- [47] Siemens Blog, “3 Ways to Speed Up CFD Don't Calculate Hard Calculate Smart,”

<https://blogs.sw.siemens.com/simcenter/3-ways-to-cfd-speed-up-dont-calculate-hard-calculate-smart>, Nov. 2022

[48] Yi, T.-H., Lou, J., Turangan, C., Khoo, B. C., and Wolanski, P., “Effect of Nozzle Shapes on the Performance of Continuously-Rotating Detonation Engine,” *48th AIAA Aerospace Sciences Meeting Including the New Horizons Forum and Aerospace Exposition*, Apr. 2010.

[49] Ansys, “Products - Fluent,”
<https://www.ansys.com/products/fluids/ansys-fluent>, Nov. 2022.

[50] Wikipedia, “Navier Stokes Equations,”
https://en.wikipedia.org/wiki/Navier–Stokes_equations, Dec. 2022.

[51] Shao, Y.-T., Liu, M., and Wang, J.-P., “Numerical Investigation of Rotating Detonation Engine Propulsive Performance,” *Combustion Science and Technology*, vol. 182, pp. 1586–1597, Oct. 2010.

[52] NASA Glenn Research Center, “Chemical Equilibrium with Applications,”
<https://www1.grc.nasa.gov/research-and-engineering/ceaweb>, Dec. 2022.

[53] CEARUN, “CEARUN,”
<https://cearun.grc.nasa.gov>, Dec. 2022.

[54] Wikipedia, “Detonation Velocity,”
https://en.wikipedia.org/wiki/Detonation_velocity, Dec. 2022.

[55] Gartner, “Scalability in Technology,”
<https://www.gartner.com/en/information-technology/glossary/scalability>, Nov. 2022.

[56] Dechert, Joseph R., “Development of a Small Scale Rotating Detonation Engine,” Air Force Institute of Technology AFIT Scholar, March 2020.

[57] NASA Marshall, “NASA Validates Revolutionary Propulsion Design for Deep Space Missions,”
<https://www.nasa.gov/centers/marshall/feature/nasa-validates-revolutionary-propulsion-design-for-deep-space-missions>, Feb. 2023.

Appendix A - Structure

Section I Objective:

The primary objective of this project is to explore all current literature regarding rotating detonation engines. More specifically, the goal is to determine the current technological status of RDE's, their limitations, and next steps necessary to implement a viable design.

Section II Objective:

The primary objective of this project is to determine the viability of scaling the rotating detonation engine in order to use it as a propulsion system in smaller (non-rocket based) applications like satellites.

Section I Methodology:

1. Determine inclusive criteria for scientific papers
2. Perform the literature search
3. Screen abstracts to determine viability
4. Extract data, results, and findings from the included papers to include in the review

Section II Methodology:

1. Explore the current literature
2. Examine the technology in terms of successful experiments in the real world
3. Run baseline analysis using ANSYS
4. Run scaled analyses to determine viability on the use of a smaller scale application
5. Compare the results with existing data

Section I Details:

- Include Graph of Systematic review flowchart
- Include criteria for selecting papers and research
- Start with this one and summarize the current status as of 2011: [1] Kailasanath, K., "The Rotating Detonation-Wave Engine Concept: A Brief Status Report," *49th AIAA Aerospace Sciences Meeting including the New Horizons Forum and Aerospace Exposition*, Apr. 2011.
- Then cover this one as of 2015:
 - Progress of Continuously Rotating Detonation Engines by Rui, Dan, Jianping
 - Chinese Journal of Aeronautics
- Include Kailasanath Papers
- Include Kaemming Papers
- Include Heiser Papers
- Include Strakey Papers
- Include Craig Nordeen Papers

Section II Details:

- What is ANSYS FLUENT? (capabilities, uses, etc)
- 2-d analyses versus 3-d
- What RDE simulations have been done (cite papers)
- What is scalability?
- Are RDE's scalable?
- How to scale simulation and analysis
- Baseline simulation (IC's, assumptions, fuel, etc)
- Scaled simulation (IC's, assumptions, fuel, etc)

RDE Computational Model Outline:

- What is Ansys?
- What is scalability?
- What RDE simulations have been done (cite papers)
 - 1-D analyses versus 2-D
 - Advantages vs disadvantages
 - Accuracy
 - 3-D is a ways off
- Ansys Fluent Simulation:
 - Program GUI
 - Entering Parameters
 - Choosing boundary conditions
 - Choosing initial conditions
 - Choosing fuel types
- Are RDE's scalable?
 - How to scale simulation and analysis
 - Baseline simulation
 - Scaled up simulations
 - Scaled down simulations

Appendix B - Outline

- Past:
 - Background
 - Phenomena
 - Concepts
 - Basic Design
 - Historical Development (PDE's, RDE's, OWDE's)

- Present:
 - Systematic Review (PRISMA, flowchart,
 - State of the Art
 - Where is most of the work occurring ?
 - Where do the papers fit in the 3 domains?
 - Stability
 - Injection schemes
 - Fuel Types
 - Where are the current limitations?

- Can this technology be scaled?
 - Where is it primarily used or targeted for application?
 - Can it be shrunk down for use on cubesats or satellites
 - What are the potential downfalls if any for downsizing.

- Future:
 - Innovation Technology
 - Compare to combustion engine timeline development
 - Forecasting progress
 - What area is advancing the quickest?
 - Predictive survey
 - When will the technology be usable?
 - What are the implications of this RDE's?

Appendix C - NASA CEA Results Test I

NASA-GLENN CHEMICAL EQUILIBRIUM PROGRAM CEA2, FEBRUARY 5, 2004
BY BONNIE MCBRIDE AND SANFORD GORDON
REFS: NASA RP-1311, PART I, 1994 AND NASA RP-1311, PART II, 1996

CEA analysis performed on Sat 10-Dec-2022 19:17:10

Problem Type: "Chapman-Jouguet Detonation"

prob case=107171_____3933 det

Pressure (11 values):

p,atm= 80, 82, 84, 86, 88, 90, 92, 94, 96, 98, 100

Temperature (11 values):

t,k= 3000, 3100, 3200, 3300, 3400, 3500, 3600, 3700, 3800, 3900, 4000

You selected the following fuels and oxidizers:

reac

fuel H2 wt%=100.0000

oxid Air wt%=100.0000

You selected these options for output:

short version of output

output short

Proportions of any products will be expressed as Mass Fractions.

output massf

Heat will be expressed as siunits

output siunits

Input prepared by this script:/var/www/sites/cearun.grc.nasa.gov/cgi-bin/CEARU
N/prepareInputFile.cgi

IMPORTANT: The following line is the end of your CEA input file!
end

DETONATION PROPERTIES OF AN IDEAL REACTING GAS
CASE = 107171_____

| REACTANT | | WT FRACTION | ENERGY | TEMP |
|----------|-----|----------------------|--------|-------|
| | | (SEE NOTE) KJ/KG-MOL | K | |
| FUEL | H2 | 1.000000 | 0.000 | 0.000 |
| OXIDANT | Air | 1.000000 | 0.000 | 0.000 |

O/F= 1.00000 %FUEL= 50.000000 R,EQ.RATIO=34.245598 PHI,EQ.RATIO=34.296226

UNBURNED GAS

P1, BAR 81.0600 83.0865 85.1130 87.1395 89.1660 91.1925 93.2190 95.2455
T1, K 3000.00 3000.00 3000.00 3000.00 3000.00 3000.00 3000.00 3000.00
H1, KJ/KG 23620.15 23620.15 23620.15 23620.15 23620.15 23620.15 23620.15 23620.15
M1, (1/n) 3.769 3.769 3.769 3.769 3.769 3.769 3.769 3.769
GAMMA1 1.2888 1.2888 1.2888 1.2888 1.2888 1.2888 1.2888 1.2888
SON VEL1,M/SEC 2920.3 2920.3 2920.3 2920.3 2920.3 2920.3 2920.3 2920.3

BURNED GAS

P, BAR 94.907 97.419 99.934 102.45 104.97 107.49 110.01 112.53
T, K 3145.27 3147.35 3149.36 3151.31 3153.21 3155.04 3156.83 3158.57
RHO, KG/CU M 1.3705 0 1.4060 0 1.4415 0 1.4770 0 1.5125 0 1.5480 0 1.5835 0 1.6191 0
H, KJ/KG 24690.5 24700.6 24710.4 24719.8 24728.8 24737.6 24746.1 24754.3
U, KJ/KG 17765.6 17771.7 17777.7 17783.3 17788.8 17794.1 17799.2 17804.1
G, KJ/KG -121141.6-121056.9-120973.4-120891.2-120810.3-120730.5-120651.8-120574.3
S, KJ/(KG)(K) 46.3655 46.3112 46.2582 46.2065 46.1559 46.1065 46.0582 46.0109

M, (1/n) 3.776 3.777 3.777 3.777 3.778 3.778 3.778 3.779
(dLV/dLP)t -1.00608 -1.00604 -1.00600 -1.00597 -1.00593 -1.00589 -1.00586 -1.00583
(dLV/dLT)p 1.1054 1.1046 1.1038 1.1031 1.1023 1.1016 1.1009 1.1002
Cp, KJ/(KG)(K) 14.0334 13.9998 13.9672 13.9355 13.9046 13.8747 13.8455 13.8170
GAMMA S 1.2279 1.2282 1.2285 1.2288 1.2291 1.2294 1.2297 1.2299
SON VEL,M/SEC 2916.1 2917.3 2918.4 2919.5 2920.6 2921.7 2922.7 2923.7

DETONATION PARAMETERS

P/P1 1.171 1.173 1.174 1.176 1.177 1.179 1.180 1.181
T/T1 1.048 1.049 1.050 1.050 1.051 1.052 1.052 1.053
M/M1 1.0019 1.0019 1.0020 1.0021 1.0022 1.0023 1.0024 1.0024
RHO/RHO1 1.1188 1.1198 1.1207 1.1216 1.1225 1.1233 1.1241 1.1249
DET MACH NUMBER 1.1172 1.1186 1.1200 1.1213 1.1226 1.1238 1.1250 1.1262
DET VEL,M/SEC 3262.5 3266.7 3270.7 3274.6 3278.3 3281.9 3285.4 3288.8

MASS FRACTIONS

*Ar 0.00646 0.00646 0.00646 0.00646 0.00646 0.00646 0.00646 0.00646
*CO 0.00015 0.00015 0.00015 0.00015 0.00015 0.00015 0.00015 0.00015
*H 0.00628 0.00624 0.00619 0.00615 0.00611 0.00607 0.00603 0.00599
*H2 0.47911 0.47915 0.47919 0.47923 0.47927 0.47931 0.47935 0.47938
H2O 0.12898 0.12899 0.12900 0.12901 0.12902 0.12902 0.12903 0.12904
*NH 0.00001 0.00001 0.00001 0.00001 0.00001 0.00001 0.00001 0.00001
NH2 0.00006 0.00006 0.00006 0.00006 0.00006 0.00006 0.00006 0.00006
NH3 0.00051 0.00052 0.00054 0.00055 0.00056 0.00058 0.00059 0.00060

*NO 0.00005 0.00005 0.00005 0.00005 0.00005 0.00005 0.00005 0.00005
 *N2 0.37708 0.37707 0.37706 0.37705 0.37704 0.37703 0.37701 0.37700
 *O 0.00002 0.00002 0.00002 0.00002 0.00002 0.00002 0.00002 0.00002
 *OH 0.00127 0.00127 0.00126 0.00125 0.00124 0.00124 0.00123 0.00122

* THERMODYNAMIC PROPERTIES FITTED TO 20000.K

NOTE. WEIGHT FRACTION OF FUEL IN TOTAL FUELS AND OF OXIDANT IN TOTAL OXIDANTS

DETONATION PROPERTIES OF AN IDEAL REACTING GAS

CASE = 107171_____

| REACTANT | WT FRACTION (SEE NOTE) | ENERGY KJ/KG-MOL | TEMP K |
|-------------|---------------------------|---------------------|-----------|
| FUEL H2 | 1.0000000 | 0.000 | 0.000 |
| OXIDANT Air | 1.0000000 | 0.000 | 0.000 |

O/F= 1.00000 %FUEL= 50.000000 R, EQ. RATIO=34.245598 PHI, EQ. RATIO=34.296226

UNBURNED GAS

P1, BAR 97.2720 99.2985 101.3250 81.0600 83.0865 85.1130 87.1395 89.1660
 T1, K 3000.00 3000.00 3000.00 3100.00 3100.00 3100.00 3100.00 3100.00
 H1, KJ/KG 23620.15 23620.15 23620.15 24607.40 24607.40 24607.40 24607.40 24607.40
 M1, (1/n) 3.769 3.769 3.769 3.769 3.769 3.769 3.769 3.769
 GAMMA1 1.2888 1.2888 1.2888 1.2867 1.2867 1.2867 1.2867 1.2867
 SON VEL1, M/SEC 2920.3 2920.3 2920.3 2966.1 2966.1 2966.1 2966.1 2966.1

BURNED GAS

P, BAR 115.05 117.58 120.10 90.772 93.240 95.708 98.177 100.65
 T, K 3160.26 3161.90 3163.51 3191.96 3194.55 3197.06 3199.48 3201.82
 RHO, KG/CU M 1.6546 0 1.6902 0 1.7257 0 1.2891 0 1.3232 0 1.3573 0 1.3914 0 1.4255 0
 H, KJ/KG 24762.2 24769.9 24777.3 25393.7 25408.9 25423.3 25437.1 25450.4
 U, KJ/KG 17808.8 17813.4 17817.8 18352.3 18362.3 18371.8 18381.0 18389.7
 G, KJ/KG -120497.9-120422.5-120348.1-123624.7-123556.8-123489.4-123422.5-123356.0
 S, KJ/(KG)(K) 45.9646 45.9193 45.8749 46.6856 46.6312 46.5781 46.5262 46.4756

M, (1/n) 3.779 3.779 3.779 3.769 3.769 3.770 3.770 3.770
 (dLV/dLP)t -1.00579 -1.00576 -1.00573 -1.00703 -1.00699 -1.00695 -1.00691 -1.00688
 (dLV/dLT)p 1.0995 1.0988 1.0982 1.1206 1.1198 1.1190 1.1182 1.1174
 Cp, KJ/(KG)(K) 13.7893 13.7623 13.7360 14.5963 14.5612 14.5270 14.4937 14.4612
 GAMMAs 1.2302 1.2304 1.2307 1.2236 1.2239 1.2242 1.2245 1.2248
 SON VEL, M/SEC 2924.7 2925.6 2926.6 2935.3 2936.7 2938.1 2939.4 2940.7

DETONATION PARAMETERS

P/P1 1.183 1.184 1.185 1.120 1.122 1.124 1.127 1.129
T/T1 1.053 1.054 1.055 1.030 1.031 1.031 1.032 1.033
M/M1 1.0025 1.0026 1.0027 0.9999 1.0000 1.0001 1.0002 1.0002
RHO/RHO1 1.1256 1.1263 1.1270 1.0874 1.0890 1.0904 1.0918 1.0931
DET MACH NUMBER 1.1273 1.1284 1.1294 1.0761 1.0782 1.0801 1.0820 1.0838
DET VEL,M/SEC 3292.1 3295.3 3298.4 3192.0 3198.0 3203.8 3209.3 3214.6

MASS FRACTIONS

*Ar 0.00646 0.00646 0.00646 0.00646 0.00646 0.00646 0.00646 0.00646
*CO 0.00015 0.00015 0.00015 0.00015 0.00015 0.00015 0.00015 0.00015
*H 0.00595 0.00591 0.00588 0.00731 0.00726 0.00722 0.00717 0.00713
*H2 0.47942 0.47945 0.47949 0.47811 0.47815 0.47819 0.47824 0.47828
H2O 0.12905 0.12905 0.12906 0.12870 0.12871 0.12871 0.12872 0.12873
*NH 0.00001 0.00001 0.00001 0.00001 0.00001 0.00001 0.00001 0.00001
NH2 0.00006 0.00006 0.00007 0.00006 0.00006 0.00006 0.00006 0.00007
NH3 0.00062 0.00063 0.00064 0.00047 0.00049 0.00050 0.00051 0.00052
*NO 0.00005 0.00005 0.00005 0.00007 0.00007 0.00007 0.00007 0.00007
*N2 0.37699 0.37698 0.37697 0.37710 0.37709 0.37708 0.37707 0.37706
*O 0.00002 0.00002 0.00002 0.00002 0.00002 0.00002 0.00002 0.00002
*OH 0.00122 0.00121 0.00121 0.00153 0.00152 0.00151 0.00151 0.00150

* THERMODYNAMIC PROPERTIES FITTED TO 20000.K

NOTE. WEIGHT FRACTION OF FUEL IN TOTAL FUELS AND OF OXIDANT IN TOTAL OXIDANTS

DETONATION PROPERTIES OF AN IDEAL REACTING GAS

CASE = 107171_____

| REACTANT | WT FRACTION (SEE NOTE) | ENERGY KJ/KG-MOL | TEMP K |
|-------------|---------------------------|---------------------|-----------|
| FUEL H2 | 1.000000 | 0.000 | 0.000 |
| OXIDANT Air | 1.000000 | 0.000 | 0.000 |

O/F= 1.00000 %FUEL= 50.000000 R, EQ. RATIO=34.245598 PHI, EQ. RATIO=34.296226

UNBURNED GAS

P1, BAR 91.1925 93.2190 95.2455 97.2720 99.2985 101.3250
T1, K 3100.00 3100.00 3100.00 3100.00 3100.00 3100.00
H1, KJ/KG 24607.40 24607.40 24607.40 24607.40 24607.40 24607.40
M1, (1/n) 3.769 3.769 3.769 3.769 3.769 3.769
GAMMA1 1.2867 1.2867 1.2867 1.2867 1.2867 1.2867
SON VEL1,M/SEC 2966.1 2966.1 2966.1 2966.1 2966.1 2966.1

BURNED GAS

P, BAR 103.12 105.59 108.07 110.54 113.02 115.49

T, K 3204.09 3206.29 3208.43 3210.50 3212.51 3214.47
 RHO, KG/CU M 1.4595 0 1.4936 0 1.5277 0 1.5618 0 1.5959 0 1.6301 0
 H, KJ/KG 25463.1 25475.4 25487.2 25498.6 25509.5 25520.1
 U, KJ/KG 18398.0 18406.0 18413.6 18421.0 18428.0 18434.9
 G, KJ/KG -123290.1-123224.8-123160.0-123095.8-123032.1-122969.1
 S, KJ/(KG)(K) 46.4260 46.3776 46.3302 46.2839 46.2384 46.1939

M, (1/n) 3.771 3.771 3.771 3.772 3.772 3.772
 (dLV/dLP)t -1.00684 -1.00680 -1.00677 -1.00673 -1.00670 -1.00667
 (dLV/dLT)p 1.1166 1.1159 1.1151 1.1144 1.1137 1.1130
 Cp, KJ/(KG)(K) 14.4296 14.3987 14.3685 14.3391 14.3103 14.2822
 GAMMAS 1.2250 1.2253 1.2255 1.2258 1.2260 1.2263
 SON VEL,M/SEC 2941.9 2943.2 2944.3 2945.5 2946.6 2947.6

DETONATION PARAMETERS

P/P1 1.131 1.133 1.135 1.136 1.138 1.140
 T/T1 1.034 1.034 1.035 1.036 1.036 1.037
 M/M1 1.0003 1.0004 1.0005 1.0006 1.0007 1.0007
 RHO/RHO1 1.0944 1.0956 1.0968 1.0979 1.0990 1.1000
 DET MACH NUMBER 1.0855 1.0871 1.0887 1.0903 1.0917 1.0932
 DET VEL,M/SEC 3219.7 3224.6 3229.3 3233.9 3238.3 3242.5

MASS FRACTIONS

*Ar 0.00646 0.00646 0.00646 0.00646 0.00646 0.00646
 *CO 0.00015 0.00015 0.00015 0.00015 0.00015 0.00015
 *H 0.00709 0.00704 0.00700 0.00696 0.00692 0.00688
 *H2 0.47832 0.47836 0.47839 0.47843 0.47847 0.47850
 H2O 0.12874 0.12875 0.12875 0.12876 0.12877 0.12877
 *NH 0.00001 0.00001 0.00001 0.00001 0.00001 0.00001
 NH2 0.00007 0.00007 0.00007 0.00007 0.00007 0.00007
 NH3 0.00053 0.00055 0.00056 0.00057 0.00058 0.00060
 *NO 0.00007 0.00007 0.00007 0.00007 0.00007 0.00007
 *N2 0.37705 0.37703 0.37702 0.37701 0.37700 0.37699
 *O 0.00002 0.00002 0.00002 0.00002 0.00002 0.00002
 *OH 0.00149 0.00149 0.00148 0.00147 0.00147 0.00146

* THERMODYNAMIC PROPERTIES FITTED TO 20000.K

NOTE. WEIGHT FRACTION OF FUEL IN TOTAL FUELS AND OF OXIDANT IN TOTAL OXIDANTS

Appendix C Continued - NASA CEA Results Test 2

NASA-GLENN CHEMICAL EQUILIBRIUM PROGRAM CEA2, FEBRUARY 5, 2004
BY BONNIE MCBRIDE AND SANFORD GORDON
REFS: NASA RP-1311, PART I, 1994 AND NASA RP-1311, PART II, 1996

CEA analysis performed on Tue 28-Feb-2023 20:05:50

Problem Type: "Chapman-Jouguet Detonation"

prob case= _____ 7236 det

Pressure (11 values):

p,atm= 70, 72, 74, 76, 78, 80, 82, 84, 86, 88, 90

Temperature (11 values):

t,k= 2500, 2600, 2700, 2800, 2900, 3000, 3100, 3200, 3300, 3400, 3500

You selected the following fuels and oxidizers:

reac

fuel H2 wt%=100.0000

oxid Air wt%=100.0000

You selected these options for output:

short version of output

output short

Proportions of any products will be expressed as Mass Fractions.

output massf

Heat will be expressed as siunits

output siunits

Input prepared by this script:/var/www/sites/cearun.grc.nasa.gov/cgi-bin/CEARUN/prepareInputFile.cgi

IMPORTANT: The following line is the end of your CEA input file!

end

DETONATION PROPERTIES OF AN IDEAL REACTING GAS

CASE = _____

| REACTANT | WT FRACTION | ENERGY | TEMP |
|----------|-------------|--------|------|
|----------|-------------|--------|------|

(SEE NOTE) KJ/KG-MOL K

| | | | | |
|---------|-----|----------|-------|-------|
| FUEL | H2 | 1.000000 | 0.000 | 0.000 |
| OXIDANT | Air | 1.000000 | 0.000 | 0.000 |

O/F= 1.00000 %FUEL= 50.000000 R, EQ. RATIO=34.245598 PHI, EQ. RATIO=34.296226

UNBURNED GAS

| | | | | | | | | |
|-----------------|----------|----------|----------|----------|----------|----------|----------|----------|
| P1, BAR | 70.9275 | 72.9540 | 74.9805 | 77.0070 | 79.0335 | 81.0600 | 83.0865 | 85.1130 |
| T1, K | 2500.00 | 2500.00 | 2500.00 | 2500.00 | 2500.00 | 2500.00 | 2500.00 | 2500.00 |
| H1, KJ/KG | 18775.16 | 18775.16 | 18775.16 | 18775.16 | 18775.16 | 18775.16 | 18775.16 | 18775.16 |
| M1, (1/n) | 3.769 | 3.769 | 3.769 | 3.769 | 3.769 | 3.769 | 3.769 | 3.769 |
| GAMMA1 | 1.3013 | 1.3013 | 1.3013 | 1.3013 | 1.3013 | 1.3013 | 1.3013 | 1.3013 |
| SON VEL1, M/SEC | 2678.8 | 2678.8 | 2678.8 | 2678.8 | 2678.8 | 2678.8 | 2678.8 | 2678.8 |

BURNED GAS

| | | | | | | | | |
|--------------------|-----------|-----------|-----------|-----------|-----------|-----------|-----------|-----------|
| P, BAR | 95.107 | 97.868 | 100.63 | 103.39 | 106.15 | 108.92 | 111.68 | 114.45 |
| T, K | 2814.58 | 2815.47 | 2816.32 | 2817.15 | 2817.94 | 2818.71 | 2819.45 | 2820.20 |
| RHO, KG/CU M | 1.5467 | 0 1.5912 | 0 1.6357 | 0 1.6801 | 0 1.7246 | 0 1.7691 | 0 1.8136 | 0 1.8582 |
| H, KJ/KG | 20496.8 | 20499.6 | 20502.4 | 20505.0 | 20507.5 | 20510.0 | 20512.3 | 20514.9 |
| U, KJ/KG | 14347.8 | 14349.0 | 14350.2 | 14351.3 | 14352.4 | 14353.4 | 14354.4 | 14355.6 |
| G, KJ/KG | -106031.7 | -105895.6 | -105762.8 | -105633.2 | -105506.5 | -105382.7 | -105261.6 | -105144.0 |
| S, KJ/(KG)(K) | 44.9547 | 44.8932 | 44.8334 | 44.7752 | 44.7185 | 44.6632 | 44.6093 | 44.5567 |
| M, (1/n) | 3.806 | 3.806 | 3.806 | 3.806 | 3.807 | 3.807 | 3.807 | 3.807 |
| (dLV/dLP)t | -1.00228 | -1.00226 | -1.00224 | -1.00223 | -1.00221 | -1.00219 | -1.00218 | -1.00216 |
| (dLV/dLT)p | 1.0422 | 1.0417 | 1.0413 | 1.0409 | 1.0404 | 1.0400 | 1.0396 | 1.0393 |
| Cp, KJ/(KG)(K) | 11.5384 | 11.5178 | 11.4980 | 11.4789 | 11.4605 | 11.4427 | 11.4254 | 11.4089 |
| GAMMA _s | 1.2553 | 1.2556 | 1.2559 | 1.2562 | 1.2565 | 1.2567 | 1.2570 | 1.2572 |
| SON VEL, M/SEC | 2778.3 | 2779.0 | 2779.7 | 2780.3 | 2780.9 | 2781.5 | 2782.1 | 2782.7 |

DETONATION PARAMETERS

| | | | | | | | | |
|-----------------|--------|--------|--------|--------|--------|--------|--------|--------|
| P/P1 | 1.341 | 1.341 | 1.342 | 1.343 | 1.343 | 1.344 | 1.344 | 1.345 |
| T/T1 | 1.126 | 1.126 | 1.127 | 1.127 | 1.127 | 1.127 | 1.128 | 1.128 |
| M/M1 | 1.0096 | 1.0097 | 1.0098 | 1.0098 | 1.0098 | 1.0099 | 1.0099 | 1.0100 |
| RHO/RHO1 | 1.2025 | 1.2027 | 1.2029 | 1.2031 | 1.2033 | 1.2035 | 1.2037 | 1.2039 |
| DET MACH NUMBER | 1.2472 | 1.2477 | 1.2482 | 1.2487 | 1.2492 | 1.2497 | 1.2501 | 1.2506 |
| DET VEL, M/SEC | 3341.0 | 3342.4 | 3343.8 | 3345.1 | 3346.4 | 3347.6 | 3348.8 | 3350.1 |

MASS FRACTIONS

| | | | | | | | | |
|-----|---------|---------|---------|---------|---------|---------|---------|---------|
| *Ar | 0.00646 | 0.00646 | 0.00646 | 0.00646 | 0.00646 | 0.00646 | 0.00646 | 0.00646 |
| *CO | 0.00015 | 0.00015 | 0.00015 | 0.00015 | 0.00015 | 0.00015 | 0.00015 | 0.00015 |
| *H | 0.00224 | 0.00221 | 0.00219 | 0.00216 | 0.00214 | 0.00212 | 0.00210 | 0.00208 |
| *H2 | 0.48307 | 0.48310 | 0.48312 | 0.48314 | 0.48315 | 0.48317 | 0.48319 | 0.48321 |
| H2O | 0.13000 | 0.13001 | 0.13001 | 0.13001 | 0.13002 | 0.13002 | 0.13003 | 0.13003 |

| | | | | | | | | | |
|-----|---------|---------|---------|---------|---------|---------|---------|---------|---------|
| NH2 | 0.00002 | 0.00003 | 0.00003 | 0.00003 | 0.00003 | 0.00003 | 0.00003 | 0.00003 | 0.00003 |
| NH3 | 0.00066 | 0.00068 | 0.00070 | 0.00072 | 0.00074 | 0.00075 | 0.00077 | 0.00079 | |
| *NO | 0.00001 | 0.00001 | 0.00001 | 0.00001 | 0.00001 | 0.00001 | 0.00001 | 0.00001 | 0.00001 |
| *N2 | 0.37702 | 0.37700 | 0.37699 | 0.37697 | 0.37696 | 0.37694 | 0.37692 | 0.37691 | |
| *OH | 0.00035 | 0.00035 | 0.00035 | 0.00034 | 0.00034 | 0.00034 | 0.00033 | 0.00033 | |

* THERMODYNAMIC PROPERTIES FITTED TO 20000.K

NOTE. WEIGHT FRACTION OF FUEL IN TOTAL FUELS AND OF OXIDANT IN TOTAL OXIDANTS

DETONATION PROPERTIES OF AN IDEAL REACTING GAS

CASE = _____

| | REACTANT | WT FRACTION (SEE NOTE) | ENERGY KJ/KG-MOL | TEMP K |
|---------|----------|---------------------------|---------------------|-----------|
| FUEL | H2 | 1.0000000 | 0.000 | 0.000 |
| OXIDANT | Air | 1.0000000 | 0.000 | 0.000 |

O/F= 1.00000 %FUEL= 50.000000 R, EQ. RATIO=34.245598 PHI, EQ. RATIO=34.296226

UNBURNED GAS

| | | | | | | | | |
|-----------------|----------|----------|----------|----------|----------|----------|----------|----------|
| P1, BAR | 87.1395 | 89.1660 | 91.1925 | 70.9275 | 72.9540 | 74.9805 | 77.0070 | 79.0335 |
| T1, K | 2500.00 | 2500.00 | 2500.00 | 2600.00 | 2600.00 | 2600.00 | 2600.00 | 2600.00 |
| H1, KJ/KG | 18775.16 | 18775.16 | 18775.16 | 19731.19 | 19731.19 | 19731.19 | 19731.19 | 19731.19 |
| M1, (1/n) | 3.769 | 3.769 | 3.769 | 3.769 | 3.769 | 3.769 | 3.769 | 3.769 |
| GAMMA1 | 1.3013 | 1.3013 | 1.3013 | 1.2985 | 1.2985 | 1.2985 | 1.2985 | 1.2985 |
| SON VEL1, M/SEC | 2678.8 | 2678.8 | 2678.8 | 2728.9 | 2728.9 | 2728.9 | 2728.9 | 2728.9 |

BURNED GAS

| | | | | | | | | |
|---------------|-----------|-----------|-----------|-----------|-----------|-----------|-----------|-----------|
| P, BAR | 117.21 | 119.98 | 122.74 | 92.995 | 95.708 | 98.422 | 101.14 | 103.85 |
| T, K | 2820.90 | 2821.57 | 2822.23 | 2888.46 | 2889.59 | 2890.68 | 2891.72 | 2892.73 |
| RHO, KG/CU M | 1.9027 | 0 1.9472 | 0 1.9917 | 0 1.4718 | 0 1.5142 | 0 1.5567 | 0 1.5991 | 0 1.6416 |
| H, KJ/KG | 20517.1 | 20519.2 | 20521.3 | 21373.0 | 21376.9 | 21380.6 | 21384.2 | 21387.6 |
| U, KJ/KG | 14356.6 | 14357.5 | 14358.3 | 15054.5 | 15056.3 | 15058.0 | 15059.6 | 15061.2 |
| G, KJ/KG | -105028.0 | -104914.4 | -104803.0 | -109506.4 | -109375.6 | -109247.9 | -109123.1 | -109001.2 |
| S, KJ/(KG)(K) | 44.5054 | 44.4552 | 44.4062 | 45.3111 | 45.2495 | 45.1896 | 45.1314 | 45.0746 |

| | | | | | | | | |
|----------------|----------|----------|----------|----------|----------|----------|----------|----------|
| M, (1/n) | 3.807 | 3.807 | 3.808 | 3.801 | 3.801 | 3.801 | 3.802 | 3.802 |
| (dLV/dLP)t | -1.00215 | -1.00213 | -1.00212 | -1.00291 | -1.00288 | -1.00286 | -1.00283 | -1.00281 |
| (dLV/dLT)p | 1.0389 | 1.0385 | 1.0382 | 1.0533 | 1.0528 | 1.0522 | 1.0517 | 1.0512 |
| Cp, KJ/(KG)(K) | 11.3928 | 11.3772 | 11.3620 | 12.0115 | 11.9870 | 11.9633 | 11.9404 | 11.9184 |

GAMMAS 1.2575 1.2577 1.2579 1.2487 1.2490 1.2493 1.2496 1.2499
 SON VEL,M/SEC 2783.3 2783.8 2784.3 2808.9 2809.7 2810.5 2811.3 2812.0

DETONATION PARAMETERS

P/P1 1.345 1.346 1.346 1.311 1.312 1.313 1.313 1.314
 T/T1 1.128 1.129 1.129 1.111 1.111 1.112 1.112 1.113
 M/M1 1.0100 1.0101 1.0101 1.0083 1.0084 1.0085 1.0085 1.0086
 RHO/RHO1 1.2041 1.2042 1.2044 1.1900 1.1903 1.1906 1.1909 1.1912
 DET MACH NUMBER 1.2510 1.2514 1.2518 1.2249 1.2256 1.2262 1.2269 1.2275
 DET VEL,M/SEC 3351.2 3352.3 3353.4 3342.7 3344.5 3346.3 3348.0 3349.7

MASS FRACTIONS

*Ar 0.00646 0.00646 0.00646 0.00646 0.00646 0.00646 0.00646 0.00646
 *CO 0.00015 0.00015 0.00015 0.00015 0.00015 0.00015 0.00015 0.00015
 *H 0.00206 0.00204 0.00202 0.00291 0.00288 0.00285 0.00282 0.00279
 *H2 0.48322 0.48324 0.48325 0.48242 0.48245 0.48248 0.48250 0.48253
 H2O 0.13003 0.13003 0.13004 0.12986 0.12986 0.12987 0.12987 0.12988
 NH2 0.00003 0.00003 0.00003 0.00003 0.00003 0.00003 0.00003 0.00003
 NH3 0.00081 0.00083 0.00085 0.00061 0.00062 0.00064 0.00066 0.00068
 *NO 0.00001 0.00001 0.00001 0.00002 0.00002 0.00002 0.00002 0.00002
 *N2 0.37689 0.37688 0.37686 0.37705 0.37704 0.37703 0.37701 0.37700
 *OH 0.00033 0.00032 0.00032 0.00049 0.00048 0.00048 0.00047 0.00047

* THERMODYNAMIC PROPERTIES FITTED TO 20000.K

NOTE. WEIGHT FRACTION OF FUEL IN TOTAL FUELS AND OF OXIDANT IN TOTAL OXIDANTS

DETONATION PROPERTIES OF AN IDEAL REACTING GAS

CASE = _____

| REACTANT | WT FRACTION (SEE NOTE) | ENERGY KJ/KG-MOL | TEMP K |
|-------------|---------------------------|---------------------|-----------|
| FUEL H2 | 1.000000 | 0.000 | 0.000 |
| OXIDANT Air | 1.000000 | 0.000 | 0.000 |

O/F= 1.00000 %FUEL= 50.000000 R,EQ.RATIO=34.245598 PHI,EQ.RATIO=34.296226

UNBURNED GAS

P1, BAR 81.0600 83.0865 85.1130 87.1395 89.1660 91.1925 70.9275 72.9540
 T1, K 2600.00 2600.00 2600.00 2600.00 2600.00 2600.00 2700.00 2700.00

H1, KJ/KG 19731.19 19731.19 19731.19 19731.19 19731.19 19731.19 20693.97 20693.97
M1, (1/n) 3.769 3.769 3.769 3.769 3.769 3.769 3.769 3.769
GAMMA1 1.2985 1.2985 1.2985 1.2985 1.2985 1.2985 1.2959 1.2959
SON VEL1,M/SEC 2728.9 2728.9 2728.9 2728.9 2728.9 2728.9 2778.1 2778.1

BURNED GAS

P, BAR 106.57 109.29 112.00 114.72 117.44 120.16 90.723 93.387
T, K 2893.71 2894.66 2895.57 2896.46 2897.32 2898.16 2957.75 2959.14
RHO, KG/CU M 1.6840 0 1.7265 0 1.7690 0 1.8115 0 1.8539 0 1.8964 0 1.4001 0 1.4406 0
H, KJ/KG 21391.0 21394.2 21397.3 21400.3 21403.2 21406.0 22232.0 22237.2
U, KJ/KG 15062.8 15064.3 15065.7 15067.1 15068.4 15069.7 15752.2 15754.8
G, KJ/KG -108881.8-108765.0-108650.7-108538.7-108428.9-108321.2-112816.0-112692.0
S, KJ/(KG)(K) 45.0193 44.9653 44.9127 44.8613 44.8110 44.7619 45.6591 45.5974

M, (1/n) 3.802 3.802 3.802 3.803 3.803 3.803 3.795 3.796
(dLV/dLP)t -1.00279 -1.00277 -1.00275 -1.00273 -1.00271 -1.00269 -1.00363 -1.00360
(dLV/dLT)p 1.0507 1.0502 1.0497 1.0493 1.0489 1.0484 1.0659 1.0652
Cp, KJ/(KG)(K) 11.8971 11.8765 11.8565 11.8372 11.8185 11.8003 12.5234 12.4948
GAMMAs 1.2502 1.2505 1.2507 1.2510 1.2513 1.2515 1.2424 1.2427
SON VEL,M/SEC 2812.7 2813.4 2814.1 2814.8 2815.4 2816.0 2837.3 2838.3

DETONATION PARAMETERS

P/P1 1.315 1.315 1.316 1.317 1.317 1.318 1.279 1.280
T/T1 1.113 1.113 1.114 1.114 1.114 1.115 1.095 1.096
M/M1 1.0086 1.0087 1.0087 1.0088 1.0088 1.0089 1.0068 1.0069
RHO/RHO1 1.1915 1.1917 1.1920 1.1922 1.1924 1.1926 1.1756 1.1761
DET MACH NUMBER 1.2281 1.2286 1.2292 1.2297 1.2302 1.2307 1.2007 1.2015
DET VEL,M/SEC 3351.3 3352.8 3354.3 3355.8 3357.2 3358.5 3335.7 3338.0

MASS FRACTIONS

*Ar 0.00646 0.00646 0.00646 0.00646 0.00646 0.00646 0.00646 0.00646
*CO 0.00015 0.00015 0.00015 0.00015 0.00015 0.00015 0.00015 0.00015
*H 0.00276 0.00274 0.00271 0.00269 0.00266 0.00264 0.00368 0.00364
*H2 0.48255 0.48257 0.48259 0.48261 0.48263 0.48265 0.48167 0.48170
H2O 0.12988 0.12988 0.12989 0.12989 0.12990 0.12990 0.12967 0.12968
NH2 0.00003 0.00003 0.00003 0.00003 0.00003 0.00003 0.00004 0.00004
NH3 0.00069 0.00071 0.00073 0.00075 0.00076 0.00078 0.00056 0.00058
*NO 0.00002 0.00002 0.00002 0.00002 0.00002 0.00002 0.00002 0.00002
*N2 0.37698 0.37697 0.37695 0.37694 0.37692 0.37691 0.37708 0.37707
*O 0.00000 0.00000 0.00000 0.00000 0.00000 0.00000 0.00001 0.00001
*OH 0.00047 0.00046 0.00046 0.00045 0.00045 0.00045 0.00065 0.00065

* THERMODYNAMIC PROPERTIES FITTED TO 20000.K

NOTE. WEIGHT FRACTION OF FUEL IN TOTAL FUELS AND OF OXIDANT IN TOTAL OXIDANTS

DETONATION PROPERTIES OF AN IDEAL REACTING GAS

CASE = _____

| REACTANT | | WT FRACTION | | ENERGY | TEMP |
|----------|-----|-------------|-------|-----------|------|
| | | (SEE NOTE) | | KJ/KG-MOL | K |
| FUEL | H2 | 1.000000 | 0.000 | 0.000 | |
| OXIDANT | Air | 1.000000 | 0.000 | 0.000 | |

O/F= 1.00000 %FUEL= 50.000000 R, EQ. RATIO=34.245598 PHI, EQ. RATIO=34.296226

UNBURNED GAS

| | | | | | | | | |
|-----------------|----------|----------|----------|----------|----------|----------|----------|----------|
| P1, BAR | 74.9805 | 77.0070 | 79.0335 | 81.0600 | 83.0865 | 85.1130 | 87.1395 | 89.1660 |
| T1, K | 2700.00 | 2700.00 | 2700.00 | 2700.00 | 2700.00 | 2700.00 | 2700.00 | 2700.00 |
| H1, KJ/KG | 20693.97 | 20693.97 | 20693.97 | 20693.97 | 20693.97 | 20693.97 | 20693.97 | 20693.97 |
| M1, (1/n) | 3.769 | 3.769 | 3.769 | 3.769 | 3.769 | 3.769 | 3.769 | 3.769 |
| GAMMA1 | 1.2959 | 1.2959 | 1.2959 | 1.2959 | 1.2959 | 1.2959 | 1.2959 | 1.2959 |
| SON VEL1, M/SEC | 2778.1 | 2778.1 | 2778.1 | 2778.1 | 2778.1 | 2778.1 | 2778.1 | 2778.1 |

BURNED GAS

| | | | | | | | | |
|---------------|-----------|-----------|-----------|-----------|-----------|-----------|-----------|-----------|
| P, BAR | 96.052 | 98.718 | 101.38 | 104.05 | 106.72 | 109.39 | 112.06 | 114.74 |
| T, K | 2960.49 | 2961.78 | 2963.04 | 2964.25 | 2965.43 | 2966.57 | 2967.67 | 2968.74 |
| RHO, KG/CU M | 1.4812 | 1.5217 | 1.5623 | 1.6028 | 1.6434 | 1.6840 | 1.7246 | 1.7651 |
| H, KJ/KG | 22242.1 | 22246.9 | 22251.5 | 22255.9 | 22260.2 | 22264.3 | 22268.3 | 22272.2 |
| U, KJ/KG | 15757.3 | 15759.6 | 15761.9 | 15764.1 | 15766.2 | 15768.3 | 15770.2 | 15772.1 |
| G, KJ/KG | -112570.9 | -112452.4 | -112336.4 | -112222.9 | -112111.8 | -112002.8 | -111896.0 | -111791.2 |
| S, KJ/(KG)(K) | 45.5374 | 45.4791 | 45.4222 | 45.3669 | 45.3128 | 45.2601 | 45.2086 | 45.1583 |

| | | | | | | | | |
|--------------------|----------|----------|----------|----------|----------|----------|----------|----------|
| M, (1/n) | 3.796 | 3.796 | 3.796 | 3.797 | 3.797 | 3.797 | 3.797 | 3.797 |
| (dLV/dLP)t | -1.00357 | -1.00354 | -1.00351 | -1.00349 | -1.00346 | -1.00344 | -1.00341 | -1.00339 |
| (dLV/dLT)p | 1.0645 | 1.0639 | 1.0633 | 1.0627 | 1.0622 | 1.0616 | 1.0611 | 1.0605 |
| Cp, KJ/(KG)(K) | 12.4672 | 12.4406 | 12.4149 | 12.3900 | 12.3659 | 12.3426 | 12.3200 | 12.2980 |
| GAMMA _s | 1.2431 | 1.2434 | 1.2437 | 1.2440 | 1.2443 | 1.2446 | 1.2448 | 1.2451 |
| SON VEL, M/SEC | 2839.2 | 2840.1 | 2841.0 | 2841.8 | 2842.6 | 2843.4 | 2844.1 | 2844.9 |

DETONATION PARAMETERS

| | | | | | | | | |
|----------|--------|--------|--------|--------|--------|--------|--------|--------|
| P/P1 | 1.281 | 1.282 | 1.283 | 1.284 | 1.284 | 1.285 | 1.286 | 1.287 |
| T/T1 | 1.096 | 1.097 | 1.097 | 1.098 | 1.098 | 1.099 | 1.099 | 1.100 |
| M/M1 | 1.0070 | 1.0071 | 1.0071 | 1.0072 | 1.0073 | 1.0073 | 1.0074 | 1.0074 |
| RHO/RHO1 | 1.1765 | 1.1769 | 1.1773 | 1.1776 | 1.1780 | 1.1783 | 1.1787 | 1.1790 |

DET MACH NUMBER 1.2024 1.2031 1.2039 1.2046 1.2053 1.2060 1.2067 1.2073
 DET VEL,M/SEC 3340.3 3342.4 3344.5 3346.6 3348.5 3350.4 3352.3 3354.0

MASS FRACTIONS

*Ar 0.00646 0.00646 0.00646 0.00646 0.00646 0.00646 0.00646 0.00646
 *CO 0.00015 0.00015 0.00015 0.00015 0.00015 0.00015 0.00015 0.00015
 *H 0.00361 0.00357 0.00354 0.00351 0.00348 0.00345 0.00342 0.00339
 *H2 0.48173 0.48176 0.48179 0.48182 0.48185 0.48188 0.48190 0.48193
 H2O 0.12969 0.12969 0.12970 0.12970 0.12971 0.12972 0.12972 0.12973
 NH2 0.00004 0.00004 0.00004 0.00004 0.00004 0.00004 0.00004 0.00004
 NH3 0.00059 0.00061 0.00063 0.00064 0.00066 0.00067 0.00069 0.00071
 *NO 0.00002 0.00002 0.00002 0.00002 0.00002 0.00002 0.00002 0.00002
 *N2 0.37706 0.37704 0.37703 0.37701 0.37700 0.37699 0.37697 0.37696
 *O 0.00001 0.00001 0.00000 0.00000 0.00000 0.00000 0.00000 0.00000
 *OH 0.00064 0.00064 0.00063 0.00062 0.00062 0.00061 0.00061 0.00061

* THERMODYNAMIC PROPERTIES FITTED TO 20000.K

NOTE. WEIGHT FRACTION OF FUEL IN TOTAL FUELS AND OF OXIDANT IN TOTAL OXIDANTS

CONSERVATION EQNS NOT SATISFIED IN 8 ITERATIONS (DETON)

DETONATION PROPERTIES OF AN IDEAL REACTING GAS

CASE = _____

| REACTANT | | WT FRACTION | ENERGY | TEMP |
|----------|-----|-------------|-----------|-------|
| | | (SEE NOTE) | KJ/KG-MOL | K |
| FUEL | H2 | 1.0000000 | 0.000 | 0.000 |
| OXIDANT | Air | 1.0000000 | 0.000 | 0.000 |

O/F= 1.00000 %FUEL= 50.000000 R,EQ.RATIO=34.245598 PHI,EQ.RATIO=34.296226

UNBURNED GAS

P1, BAR 91.1925 70.9275 72.9540 74.9805 79.0335 81.0600 83.0865 85.1130
 T1, K 2700.00 2800.00 2800.00 2800.00 2800.00 2800.00 2800.00 2800.00
 H1, KJ/KG 20693.97 21663.22 21663.22 21663.22 21663.22 21663.22 21663.22 21663.22
 M1, (1/n) 3.769 3.769 3.769 3.769 3.769 3.769 3.769 3.769
 GAMMA1 1.2959 1.2934 1.2934 1.2934 1.2934 1.2934 1.2934 1.2934
 SON VEL1,M/SEC 2778.1 2826.3 2826.3 2826.3 2826.3 2826.3 2826.3 2826.3

BURNED GAS

P, BAR 117.41 88.251 90.863 93.476 98.709 101.32 103.94 106.56
T, K 2969.78 3022.11 3023.80 3025.44 3028.56 3030.03 3031.46 3032.85
RHO, KG/CU M 1.8057 0 1.3307 0 1.3694 0 1.4082 0 1.4857 0 1.5245 0 1.5632 0 1.6020 0
H, KJ/KG 22275.9 23068.4 23075.2 23081.7 23094.1 23099.8 23105.5 23110.9
U, KJ/KG 15774.0 16436.5 16440.1 16443.6 16450.3 16453.3 16456.2 16459.1
G, KJ/KG -111688.5-115946.7-115831.2-115718.1-115499.2-115392.6-115288.4-115186.1
S, KJ/(KG)(K) 45.1092 45.9994 45.9376 45.8775 45.7622 45.7067 45.6526 45.5998

M, (1/n) 3.798 3.789 3.789 3.790 3.790 3.790 3.791 3.791
(dLV/dLP)t -1.00337 -1.00445 -1.00441 -1.00438 -1.00431 -1.00428 -1.00425 -1.00422
(dLV/dLT)p 1.0600 1.0796 1.0789 1.0781 1.0767 1.0760 1.0754 1.0747
Cp, KJ/(KG)(K) 12.2767 13.0678 13.0353 13.0038 12.9441 12.9157 12.8881 12.8615
GAMMAS 1.2454 1.2365 1.2369 1.2372 1.2379 1.2382 1.2385 1.2388
SON VEL,M/SEC 2845.6 2863.7 2864.8 2865.8 2867.8 2868.7 2869.7 2870.6

DETONATION PARAMETERS

P/P1 1.287 1.244 1.245 1.247 1.249 1.250 1.251 1.252
T/T1 1.100 1.079 1.080 1.081 1.082 1.082 1.083 1.083
M/M1 1.0075 1.0052 1.0052 1.0053 1.0055 1.0056 1.0056 1.0057
RHO/RHO1 1.1793 1.1587 1.1593 1.1599 1.1610 1.1615 1.1620 1.1625
DET MACH NUMBER 1.2079 1.1740 1.1751 1.1761 1.1781 1.1789 1.1798 1.1807
DET VEL,M/SEC 3355.8 3318.3 3321.2 3324.1 3329.6 3332.1 3334.6 3337.0

MASS FRACTIONS

*Ar 0.00646 0.00646 0.00646 0.00646 0.00646 0.00646 0.00646 0.00646
*CO 0.00015 0.00015 0.00015 0.00015 0.00015 0.00015 0.00015 0.00015
*H 0.00336 0.00455 0.00451 0.00447 0.00439 0.00435 0.00432 0.00428
*H2 0.48195 0.48081 0.48085 0.48089 0.48096 0.48100 0.48103 0.48106
H2O 0.12973 0.12946 0.12947 0.12947 0.12949 0.12950 0.12950 0.12951
*NH 0.00000 0.00001 0.00001 0.00001 0.00001 0.00001 0.00001 0.00001
NH2 0.00004 0.00004 0.00004 0.00004 0.00004 0.00004 0.00005 0.00005
NH3 0.00072 0.00052 0.00053 0.00055 0.00058 0.00059 0.00061 0.00062
*NO 0.00002 0.00003 0.00003 0.00003 0.00003 0.00003 0.00003 0.00003
*N2 0.37695 0.37711 0.37709 0.37708 0.37705 0.37704 0.37703 0.37702
*O 0.00000 0.00001 0.00001 0.00001 0.00001 0.00001 0.00001 0.00001
*OH 0.00060 0.00085 0.00084 0.00083 0.00082 0.00081 0.00081 0.00080

* THERMODYNAMIC PROPERTIES FITTED TO 20000.K

NOTE. WEIGHT FRACTION OF FUEL IN TOTAL FUELS AND OF OXIDANT IN TOTAL OXIDANTS

DETONATION PROPERTIES OF AN IDEAL REACTING GAS

CASE = _____

| REACTANT | WT FRACTION (SEE NOTE) | ENERGY KJ/KG-MOL | TEMP K |
|-------------|---------------------------|---------------------|-----------|
| FUEL H2 | 1.000000 | 0.000 | 0.000 |
| OXIDANT Air | 1.000000 | 0.000 | 0.000 |

O/F= 1.00000 %FUEL= 50.000000 R, EQ. RATIO=34.245598 PHI, EQ. RATIO=34.296226

UNBURNED GAS

| | | | | | | | | |
|-----------------|----------|----------|----------|----------|----------|----------|----------|----------|
| P1, BAR | 87.1395 | 89.1660 | 91.1925 | 70.9275 | 72.9540 | 74.9805 | 77.0070 | 79.0335 |
| T1, K | 2800.00 | 2800.00 | 2800.00 | 2900.00 | 2900.00 | 2900.00 | 2900.00 | 2900.00 |
| H1, KJ/KG | 21663.22 | 21663.22 | 21663.22 | 22638.69 | 22638.69 | 22638.69 | 22638.69 | 22638.69 |
| M1, (1/n) | 3.769 | 3.769 | 3.769 | 3.769 | 3.769 | 3.769 | 3.769 | 3.769 |
| GAMMA1 | 1.2934 | 1.2934 | 1.2934 | 1.2910 | 1.2910 | 1.2910 | 1.2910 | 1.2910 |
| SON VEL1, M/SEC | 2826.3 | 2826.3 | 2826.3 | 2873.7 | 2873.7 | 2873.7 | 2873.7 | 2873.7 |

BURNED GAS

| | | | | | | | | |
|--------------------|-----------|-----------|-----------|-----------|-----------|-----------|-----------|-----------|
| P, BAR | 109.18 | 111.81 | 114.43 | 85.512 | 88.069 | 90.629 | 93.190 | 95.753 |
| T, K | 3034.19 | 3035.50 | 3036.77 | 3081.09 | 3083.13 | 3085.10 | 3087.00 | 3088.84 |
| RHO, KG/CU M | 1.6408 | 1.6796 | 1.7184 | 1.2624 | 1.2994 | 1.3365 | 1.3735 | 1.4106 |
| H, KJ/KG | 23116.2 | 23121.3 | 23126.2 | 23874.0 | 23883.0 | 23891.6 | 23900.0 | 23908.0 |
| U, KJ/KG | 16461.9 | 16464.6 | 16467.1 | 17100.3 | 17105.4 | 17110.4 | 17115.1 | 17119.7 |
| G, KJ/KG | -115085.8 | -114987.3 | -114890.6 | -118881.0 | -118775.7 | -118672.6 | -118571.4 | -118472.1 |
| S, KJ/(KG)(K) | 45.5482 | 45.4978 | 45.4486 | 46.3326 | 46.2707 | 46.2106 | 46.1520 | 46.0950 |
| M, (1/n) | 3.791 | 3.791 | 3.792 | 3.782 | 3.782 | 3.783 | 3.783 | 3.783 |
| (dLV/dLP)t | -1.00419 | -1.00416 | -1.00413 | -1.00535 | -1.00530 | -1.00526 | -1.00522 | -1.00519 |
| (dLV/dLT)p | 1.0741 | 1.0735 | 1.0729 | 1.0944 | 1.0936 | 1.0927 | 1.0919 | 1.0911 |
| Cp, KJ/(KG)(K) | 12.8356 | 12.8105 | 12.7861 | 13.6366 | 13.6004 | 13.5653 | 13.5314 | 13.4986 |
| GAMMA _s | 1.2391 | 1.2393 | 1.2396 | 1.2312 | 1.2315 | 1.2319 | 1.2322 | 1.2325 |
| SON VEL, M/SEC | 2871.4 | 2872.3 | 2873.1 | 2887.8 | 2889.1 | 2890.2 | 2891.4 | 2892.5 |

DETONATION PARAMETERS

| | | | | | | | | |
|-----------------|--------|--------|--------|--------|--------|--------|--------|--------|
| P/P1 | 1.253 | 1.254 | 1.255 | 1.206 | 1.207 | 1.209 | 1.210 | 1.212 |
| T/T1 | 1.084 | 1.084 | 1.085 | 1.062 | 1.063 | 1.064 | 1.064 | 1.065 |
| M/M1 | 1.0058 | 1.0058 | 1.0059 | 1.0033 | 1.0034 | 1.0035 | 1.0036 | 1.0037 |
| RHO/RHO1 | 1.1629 | 1.1634 | 1.1638 | 1.1385 | 1.1394 | 1.1402 | 1.1409 | 1.1417 |
| DET MACH NUMBER | 1.1815 | 1.1823 | 1.1831 | 1.1441 | 1.1454 | 1.1467 | 1.1479 | 1.1491 |
| DET VEL, M/SEC | 3339.3 | 3341.6 | 3343.7 | 3287.9 | 3291.7 | 3295.4 | 3298.9 | 3302.3 |

MASS FRACTIONS

| | | | | | | | | | |
|-----|---------|---------|---------|---------|---------|---------|---------|---------|---------|
| *Ar | 0.00646 | 0.00646 | 0.00646 | 0.00646 | 0.00646 | 0.00646 | 0.00646 | 0.00646 | 0.00646 |
| *CO | 0.00015 | 0.00015 | 0.00015 | 0.00015 | 0.00015 | 0.00015 | 0.00015 | 0.00015 | 0.00015 |
| *H | 0.00425 | 0.00421 | 0.00418 | 0.00551 | 0.00546 | 0.00542 | 0.00537 | 0.00533 | |
| *H2 | 0.48109 | 0.48112 | 0.48115 | 0.47987 | 0.47992 | 0.47996 | 0.48001 | 0.48005 | |
| H2O | 0.12951 | 0.12952 | 0.12953 | 0.12921 | 0.12922 | 0.12923 | 0.12924 | 0.12925 | |
| *NH | 0.00001 | 0.00001 | 0.00001 | 0.00001 | 0.00001 | 0.00001 | 0.00001 | 0.00001 | |
| NH2 | 0.00005 | 0.00005 | 0.00005 | 0.00005 | 0.00005 | 0.00005 | 0.00005 | 0.00005 | |
| NH3 | 0.00064 | 0.00065 | 0.00067 | 0.00048 | 0.00050 | 0.00051 | 0.00052 | 0.00054 | |
| *NO | 0.00003 | 0.00003 | 0.00003 | 0.00004 | 0.00004 | 0.00004 | 0.00004 | 0.00004 | |
| *N2 | 0.37700 | 0.37699 | 0.37698 | 0.37712 | 0.37711 | 0.37710 | 0.37709 | 0.37708 | |
| *O | 0.00001 | 0.00001 | 0.00001 | 0.00001 | 0.00001 | 0.00001 | 0.00001 | 0.00001 | |
| *OH | 0.00080 | 0.00079 | 0.00079 | 0.00107 | 0.00106 | 0.00105 | 0.00105 | 0.00104 | |

* THERMODYNAMIC PROPERTIES FITTED TO 20000.K

NOTE. WEIGHT FRACTION OF FUEL IN TOTAL FUELS AND OF OXIDANT IN TOTAL OXIDANTS

DETONATION PROPERTIES OF AN IDEAL REACTING GAS

CASE = _____

| REACTANT | WT FRACTION (SEE NOTE) | ENERGY KJ/KG-MOL | TEMP K |
|-------------|---------------------------|---------------------|-----------|
| FUEL H2 | 1.0000000 | 0.000 | 0.000 |
| OXIDANT Air | 1.0000000 | 0.000 | 0.000 |

O/F= 1.00000 %FUEL= 50.000000 R, EQ. RATIO=34.245598 PHI, EQ. RATIO=34.296226

UNBURNED GAS

| | | | | | | | | |
|-----------------|----------|----------|----------|----------|----------|----------|----------|----------|
| P1, BAR | 81.0600 | 83.0865 | 85.1130 | 87.1395 | 89.1660 | 91.1925 | 70.9275 | 72.9540 |
| T1, K | 2900.00 | 2900.00 | 2900.00 | 2900.00 | 2900.00 | 2900.00 | 3000.00 | 3000.00 |
| H1, KJ/KG | 22638.69 | 22638.69 | 22638.69 | 22638.69 | 22638.69 | 22638.69 | 23620.15 | 23620.15 |
| M1, (1/n) | 3.769 | 3.769 | 3.769 | 3.769 | 3.769 | 3.769 | 3.769 | 3.769 |
| GAMMA1 | 1.2910 | 1.2910 | 1.2910 | 1.2910 | 1.2910 | 1.2910 | 1.2888 | 1.2888 |
| SON VEL1, M/SEC | 2873.7 | 2873.7 | 2873.7 | 2873.7 | 2873.7 | 2873.7 | 2920.3 | 2920.3 |

BURNED GAS

| | | | | | | | | |
|--------------|---------|----------|----------|----------|----------|----------|----------|----------|
| P, BAR | 98.318 | 100.88 | 103.45 | 106.02 | 108.59 | 111.16 | 82.370 | 84.874 |
| T, K | 3090.62 | 3092.35 | 3094.02 | 3095.64 | 3097.21 | 3098.74 | 3133.76 | 3136.23 |
| RHO, KG/CU M | 1.4476 | 0 1.4847 | 0 1.5218 | 0 1.5589 | 0 1.5960 | 0 1.6331 | 0 1.1933 | 0 1.2287 |
| H, KJ/KG | 23915.7 | 23923.1 | 23930.3 | 23937.3 | 23944.0 | 23950.5 | 24633.4 | 24645.8 |
| U, KJ/KG | 17124.1 | 17128.3 | 17132.3 | 17136.2 | 17140.0 | 17143.7 | 17730.5 | 17738.2 |

G, KJ/KG -118374.6-118278.9-118184.9-118092.6-118001.8-117912.5-121585.9-121494.2
 S, KJ/(KG)(K) 46.0394 45.9852 45.9323 45.8806 45.8302 45.7809 46.6593 46.5973

M, (1/n) 3.784 3.784 3.784 3.785 3.785 3.785 3.775 3.775
 (dLV/dLP)t -1.00515 -1.00511 -1.00508 -1.00504 -1.00501 -1.00498 -1.00630 -1.00625
 (dLV/dLT)p 1.0904 1.0896 1.0889 1.0882 1.0875 1.0868 1.1098 1.1089
 Cp, KJ/(KG)(K) 13.4669 13.4361 13.4062 13.3772 13.3491 13.3217 14.2178 14.1785
 GAMMAs 1.2328 1.2331 1.2334 1.2337 1.2340 1.2343 1.2263 1.2267
 SON VEL,M/SEC 2893.6 2894.6 2895.6 2896.6 2897.6 2898.5 2909.5 2910.9

DETONATION PARAMETERS

P/P1 1.213 1.214 1.215 1.217 1.218 1.219 1.161 1.163
 T/T1 1.066 1.066 1.067 1.067 1.068 1.069 1.045 1.045
 M/M1 1.0038 1.0039 1.0039 1.0040 1.0041 1.0042 1.0014 1.0015
 RHO/RHO1 1.1424 1.1431 1.1437 1.1443 1.1450 1.1455 1.1133 1.1145
 DET MACH NUMBER 1.1503 1.1514 1.1524 1.1535 1.1545 1.1554 1.1091 1.1109
 DET VEL,M/SEC 3305.6 3308.7 3311.8 3314.8 3317.6 3320.4 3239.1 3244.2

MASS FRACTIONS

*Ar 0.00646 0.00646 0.00646 0.00646 0.00646 0.00646 0.00646 0.00646
 *CO 0.00015 0.00015 0.00015 0.00015 0.00015 0.00015 0.00015 0.00015
 *H 0.00528 0.00524 0.00520 0.00516 0.00513 0.00509 0.00653 0.00648
 *H2 0.48009 0.48012 0.48016 0.48020 0.48023 0.48027 0.47888 0.47893
 H2O 0.12925 0.12926 0.12927 0.12928 0.12928 0.12929 0.12894 0.12895
 *NH 0.00001 0.00001 0.00001 0.00001 0.00001 0.00001 0.00001 0.00001
 NH2 0.00005 0.00005 0.00005 0.00005 0.00005 0.00005 0.00005 0.00005
 NH3 0.00055 0.00057 0.00058 0.00059 0.00061 0.00062 0.00045 0.00046
 *NO 0.00004 0.00004 0.00004 0.00004 0.00004 0.00004 0.00006 0.00006
 *N2 0.37706 0.37705 0.37704 0.37703 0.37702 0.37700 0.37714 0.37713
 *O 0.00001 0.00001 0.00001 0.00001 0.00001 0.00001 0.00002 0.00002
 *OH 0.00103 0.00102 0.00102 0.00101 0.00101 0.00100 0.00131 0.00131

* THERMODYNAMIC PROPERTIES FITTED TO 20000.K

NOTE. WEIGHT FRACTION OF FUEL IN TOTAL FUELS AND OF OXIDANT IN TOTAL OXIDANTS

DETONATION PROPERTIES OF AN IDEAL REACTING GAS

CASE = _____

REACTANT WT FRACTION ENERGY TEMP
 (SEE NOTE) KJ/KG-MOL K

| | | | | |
|---------|-----|----------|-------|-------|
| FUEL | H2 | 1.000000 | 0.000 | 0.000 |
| OXIDANT | Air | 1.000000 | 0.000 | 0.000 |

O/F= 1.00000 %FUEL= 50.000000 R,EQ.RATIO=34.245598 PHI,EQ.RATIO=34.296226

UNBURNED GAS

| | | | | | | | | |
|----------------|----------|----------|----------|----------|----------|----------|----------|----------|
| P1, BAR | 74.9805 | 77.0070 | 79.0335 | 81.0600 | 83.0865 | 85.1130 | 87.1395 | 89.1660 |
| T1, K | 3000.00 | 3000.00 | 3000.00 | 3000.00 | 3000.00 | 3000.00 | 3000.00 | 3000.00 |
| H1, KJ/KG | 23620.15 | 23620.15 | 23620.15 | 23620.15 | 23620.15 | 23620.15 | 23620.15 | 23620.15 |
| M1, (1/n) | 3.769 | 3.769 | 3.769 | 3.769 | 3.769 | 3.769 | 3.769 | 3.769 |
| GAMMA1 | 1.2888 | 1.2888 | 1.2888 | 1.2888 | 1.2888 | 1.2888 | 1.2888 | 1.2888 |
| SON VEL1,M/SEC | 2920.3 | 2920.3 | 2920.3 | 2920.3 | 2920.3 | 2920.3 | 2920.3 | 2920.3 |

BURNED GAS

| | | | | | | | | |
|---------------|-----------|-----------|-----------|-----------|-----------|-----------|-----------|-----------|
| P, BAR | 87.379 | 89.887 | 92.396 | 94.907 | 97.419 | 99.934 | 102.45 | 104.97 |
| T, K | 3138.61 | 3140.90 | 3143.12 | 3145.27 | 3147.35 | 3149.36 | 3151.31 | 3153.21 |
| RHO, KG/CU M | 1.2641 0 | 1.2996 0 | 1.3350 0 | 1.3705 0 | 1.4060 0 | 1.4415 0 | 1.4770 0 | 1.5125 0 |
| H, KJ/KG | 24657.7 | 24669.1 | 24680.0 | 24690.5 | 24700.6 | 24710.4 | 24719.8 | 24728.8 |
| U, KJ/KG | 17745.5 | 17752.5 | 17759.2 | 17765.6 | 17771.7 | 17777.7 | 17783.3 | 17788.8 |
| G, KJ/KG | -121403.9 | -121315.1 | -121227.7 | -121141.6 | -121056.9 | -120973.4 | -120891.2 | -120810.3 |
| S, KJ/(KG)(K) | 46.5371 | 46.4784 | 46.4212 | 46.3655 | 46.3112 | 46.2582 | 46.2065 | 46.1559 |

| | | | | | | | | |
|--------------------|----------|----------|----------|----------|----------|----------|----------|----------|
| M, (1/n) | 3.775 | 3.776 | 3.776 | 3.776 | 3.777 | 3.777 | 3.777 | 3.778 |
| (dLV/dLP)t | -1.00621 | -1.00616 | -1.00612 | -1.00608 | -1.00604 | -1.00600 | -1.00597 | -1.00593 |
| (dLV/dLT)p | 1.1080 | 1.1071 | 1.1063 | 1.1054 | 1.1046 | 1.1038 | 1.1031 | 1.1023 |
| Cp, KJ/(KG)(K) | 14.1405 | 14.1037 | 14.0680 | 14.0334 | 13.9998 | 13.9672 | 13.9355 | 13.9046 |
| GAMMA _s | 1.2270 | 1.2273 | 1.2276 | 1.2279 | 1.2282 | 1.2285 | 1.2288 | 1.2291 |
| SON VEL,M/SEC | 2912.2 | 2913.6 | 2914.8 | 2916.1 | 2917.3 | 2918.4 | 2919.5 | 2920.6 |

DETONATION PARAMETERS

| | | | | | | | | |
|-----------------|--------|--------|--------|--------|--------|--------|--------|--------|
| P/P1 | 1.165 | 1.167 | 1.169 | 1.171 | 1.173 | 1.174 | 1.176 | 1.177 |
| T/T1 | 1.046 | 1.047 | 1.048 | 1.048 | 1.049 | 1.050 | 1.050 | 1.051 |
| M/M1 | 1.0016 | 1.0017 | 1.0018 | 1.0019 | 1.0019 | 1.0020 | 1.0021 | 1.0022 |
| RHO/RHO1 | 1.1156 | 1.1168 | 1.1178 | 1.1188 | 1.1198 | 1.1207 | 1.1216 | 1.1225 |
| DET MACH NUMBER | 1.1126 | 1.1142 | 1.1157 | 1.1172 | 1.1186 | 1.1200 | 1.1213 | 1.1226 |
| DET VEL,M/SEC | 3249.0 | 3253.7 | 3258.2 | 3262.5 | 3266.7 | 3270.7 | 3274.6 | 3278.3 |

MASS FRACTIONS

| | | | | | | | | |
|-----|---------|---------|---------|---------|---------|---------|---------|---------|
| *Ar | 0.00646 | 0.00646 | 0.00646 | 0.00646 | 0.00646 | 0.00646 | 0.00646 | 0.00646 |
| *CO | 0.00015 | 0.00015 | 0.00015 | 0.00015 | 0.00015 | 0.00015 | 0.00015 | 0.00015 |
| *H | 0.00643 | 0.00638 | 0.00633 | 0.00628 | 0.00624 | 0.00619 | 0.00615 | 0.00611 |
| *H2 | 0.47897 | 0.47902 | 0.47907 | 0.47911 | 0.47915 | 0.47919 | 0.47923 | 0.47927 |
| H2O | 0.12896 | 0.12897 | 0.12897 | 0.12898 | 0.12899 | 0.12900 | 0.12901 | 0.12902 |
| *NH | 0.00001 | 0.00001 | 0.00001 | 0.00001 | 0.00001 | 0.00001 | 0.00001 | 0.00001 |

| | | | | | | | | | |
|-----|---------|---------|---------|---------|---------|---------|---------|---------|---------|
| NH2 | 0.00005 | 0.00005 | 0.00006 | 0.00006 | 0.00006 | 0.00006 | 0.00006 | 0.00006 | 0.00006 |
| NH3 | 0.00047 | 0.00049 | 0.00050 | 0.00051 | 0.00052 | 0.00054 | 0.00055 | 0.00056 | 0.00056 |
| *NO | 0.00006 | 0.00006 | 0.00006 | 0.00005 | 0.00005 | 0.00005 | 0.00005 | 0.00005 | 0.00005 |
| *N2 | 0.37712 | 0.37711 | 0.37709 | 0.37708 | 0.37707 | 0.37706 | 0.37705 | 0.37704 | 0.37704 |
| *O | 0.00002 | 0.00002 | 0.00002 | 0.00002 | 0.00002 | 0.00002 | 0.00002 | 0.00002 | 0.00002 |
| *OH | 0.00130 | 0.00129 | 0.00128 | 0.00127 | 0.00127 | 0.00126 | 0.00125 | 0.00124 | 0.00124 |

* THERMODYNAMIC PROPERTIES FITTED TO 20000.K

NOTE. WEIGHT FRACTION OF FUEL IN TOTAL FUELS AND OF OXIDANT IN TOTAL OXIDANTS

DETONATION PROPERTIES OF AN IDEAL REACTING GAS

CASE = _____

| REACTANT | WT FRACTION | ENERGY | TEMP |
|-------------|-------------|-----------|-------|
| | (SEE NOTE) | KJ/KG-MOL | K |
| FUEL H2 | 1.0000000 | 0.000 | 0.000 |
| OXIDANT Air | 1.0000000 | 0.000 | 0.000 |

O/F= 1.00000 %FUEL= 50.000000 R, EQ. RATIO=34.245598 PHI, EQ. RATIO=34.296226

UNBURNED GAS

| | | | | | | | | |
|-----------------|----------|----------|----------|----------|----------|----------|----------|----------|
| P1, BAR | 91.1925 | 70.9275 | 72.9540 | 74.9805 | 77.0070 | 79.0335 | 81.0600 | 83.0865 |
| T1, K | 3000.00 | 3100.00 | 3100.00 | 3100.00 | 3100.00 | 3100.00 | 3100.00 | 3100.00 |
| H1, KJ/KG | 23620.15 | 24607.40 | 24607.40 | 24607.40 | 24607.40 | 24607.40 | 24607.40 | 24607.40 |
| M1, (1/n) | 3.769 | 3.769 | 3.769 | 3.769 | 3.769 | 3.769 | 3.769 | 3.769 |
| GAMMA1 | 1.2888 | 1.2867 | 1.2867 | 1.2867 | 1.2867 | 1.2867 | 1.2867 | 1.2867 |
| SON VEL1, M/SEC | 2920.3 | 2966.1 | 2966.1 | 2966.1 | 2966.1 | 2966.1 | 2966.1 | 2966.1 |

BURNED GAS

| | | | | | | | | |
|---------------|-----------|-----------|-----------|-----------|-----------|-----------|-----------|-----------|
| P, BAR | 107.49 | 78.445 | 80.910 | 83.375 | 85.840 | 88.306 | 90.772 | 93.240 |
| T, K | 3155.04 | 3177.39 | 3180.55 | 3183.57 | 3186.47 | 3189.27 | 3191.96 | 3194.55 |
| RHO, KG/CU M | 1.5480 | 0 1.1186 | 0 1.1527 | 0 1.1868 | 0 1.2209 | 0 1.2550 | 0 1.2891 | 0 1.3232 |
| H, KJ/KG | 24737.6 | 25305.8 | 25325.3 | 25343.8 | 25361.3 | 25377.9 | 25393.7 | 25408.9 |
| U, KJ/KG | 17794.1 | 18293.1 | 18306.4 | 18318.8 | 18330.6 | 18341.7 | 18352.3 | 18362.3 |
| G, KJ/KG | -120730.5 | -123968.3 | -123899.4 | -123830.4 | -123761.6 | -123693.0 | -123624.7 | -123556.8 |
| S, KJ/(KG)(K) | 46.1065 | 46.9801 | 46.9179 | 46.8575 | 46.7987 | 46.7414 | 46.6856 | 46.6312 |

| | | | | | | | | |
|------------|----------|----------|----------|----------|----------|----------|----------|----------|
| M, (1/n) | 3.778 | 3.767 | 3.768 | 3.768 | 3.768 | 3.769 | 3.769 | 3.769 |
| (dLV/dLP)t | -1.00589 | -1.00725 | -1.00720 | -1.00716 | -1.00712 | -1.00707 | -1.00703 | -1.00699 |
| (dLV/dLT)p | 1.1016 | 1.1251 | 1.1242 | 1.1233 | 1.1224 | 1.1215 | 1.1206 | 1.1198 |

Cp, KJ/(KG)(K) 13.8747 14.7868 14.7466 14.7075 14.6694 14.6324 14.5963 14.5612
 GAMMAS 1.2294 1.2221 1.2224 1.2227 1.2230 1.2233 1.2236 1.2239
 SON VEL,M/SEC 2921.7 2927.4 2929.1 2930.8 2932.4 2933.9 2935.3 2936.7

DETONATION PARAMETERS

P/P1 1.179 1.106 1.109 1.112 1.115 1.117 1.120 1.122
 T/T1 1.052 1.025 1.026 1.027 1.028 1.029 1.030 1.031
 M/M1 1.0023 0.9994 0.9995 0.9996 0.9997 0.9998 0.9999 1.0000
 RHO/RHO1 1.1233 1.0784 1.0804 1.0823 1.0841 1.0858 1.0874 1.0890
 DET MACH NUMBER 1.1238 1.0644 1.0670 1.0694 1.0718 1.0740 1.0761 1.0782
 DET VEL,M/SEC 3281.9 3157.0 3164.8 3172.1 3179.1 3185.7 3192.0 3198.0

MASS FRACTIONS

*Ar 0.00646 0.00646 0.00646 0.00646 0.00646 0.00646 0.00646 0.00646
 *CO 0.00015 0.00015 0.00015 0.00015 0.00015 0.00015 0.00015 0.00015
 *H 0.00607 0.00755 0.00750 0.00745 0.00740 0.00735 0.00731 0.00726
 *H2 0.47931 0.47788 0.47792 0.47797 0.47802 0.47806 0.47811 0.47815
 H2O 0.12902 0.12866 0.12867 0.12867 0.12868 0.12869 0.12870 0.12871
 *NH 0.00001 0.00001 0.00001 0.00001 0.00001 0.00001 0.00001 0.00001
 NH2 0.00006 0.00005 0.00006 0.00006 0.00006 0.00006 0.00006 0.00006
 NH3 0.00058 0.00041 0.00042 0.00044 0.00045 0.00046 0.00047 0.00049
 *NO 0.00005 0.00007 0.00007 0.00007 0.00007 0.00007 0.00007 0.00007
 *N2 0.37703 0.37716 0.37715 0.37713 0.37712 0.37711 0.37710 0.37709
 *O 0.00002 0.00003 0.00003 0.00003 0.00002 0.00002 0.00002 0.00002
 *OH 0.00124 0.00156 0.00156 0.00155 0.00154 0.00153 0.00153 0.00152

* THERMODYNAMIC PROPERTIES FITTED TO 20000.K

NOTE. WEIGHT FRACTION OF FUEL IN TOTAL FUELS AND OF OXIDANT IN TOTAL OXIDANTS

DETONATION PROPERTIES OF AN IDEAL REACTING GAS

CASE = _____

| REACTANT | WT FRACTION (SEE NOTE) | ENERGY KJ/KG-MOL | TEMP K |
|-------------|---------------------------|---------------------|-----------|
| FUEL H2 | 1.000000 | 0.000 | 0.000 |
| OXIDANT Air | 1.000000 | 0.000 | 0.000 |

O/F= 1.00000 %FUEL= 50.000000 R, EQ. RATIO=34.245598 PHI, EQ. RATIO=34.296226

UNBURNED GAS

P1, BAR 85.1130 87.1395 89.1660 91.1925
 T1, K 3100.00 3100.00 3100.00 3100.00
 H1, KJ/KG 24607.40 24607.40 24607.40 24607.40
 M1, (1/n) 3.769 3.769 3.769 3.769

GAMMA1 1.2867 1.2867 1.2867 1.2867
SON VEL,M/SEC 2966.1 2966.1 2966.1 2966.1

BURNED GAS

P, BAR 95.708 98.177 100.65 103.12
T, K 3197.06 3199.48 3201.82 3204.09
RHO, KG/CU M 1.3573 0 1.3914 0 1.4255 0 1.4595 0
H, KJ/KG 25423.3 25437.1 25450.4 25463.1
U, KJ/KG 18371.8 18381.0 18389.7 18398.0
G, KJ/KG -123489.4-123422.5-123356.0-123290.1
S, KJ/(KG)(K) 46.5781 46.5262 46.4756 46.4260

M, (1/n) 3.770 3.770 3.770 3.771
(dLV/dLP)t -1.00695 -1.00691 -1.00688 -1.00684
(dLV/dLT)p 1.1190 1.1182 1.1174 1.1166
Cp, KJ/(KG)(K) 14.5270 14.4937 14.4612 14.4296
GAMMA_s 1.2242 1.2245 1.2248 1.2250
SON VEL,M/SEC 2938.1 2939.4 2940.7 2941.9

DETONATION PARAMETERS

P/P1 1.124 1.127 1.129 1.131
T/T1 1.031 1.032 1.033 1.034
M/M1 1.0001 1.0002 1.0002 1.0003
RHO/RHO1 1.0904 1.0918 1.0931 1.0944
DET MACH NUMBER 1.0801 1.0820 1.0838 1.0855
DET VEL,M/SEC 3203.8 3209.3 3214.6 3219.7

MASS FRACTIONS

*Ar 0.00646 0.00646 0.00646 0.00646
*CO 0.00015 0.00015 0.00015 0.00015
*H 0.00722 0.00717 0.00713 0.00709
*H2 0.47819 0.47824 0.47828 0.47832
H2O 0.12871 0.12872 0.12873 0.12874
*NH 0.00001 0.00001 0.00001 0.00001
NH2 0.00006 0.00006 0.00007 0.00007
NH3 0.00050 0.00051 0.00052 0.00053
*NO 0.00007 0.00007 0.00007 0.00007
*N2 0.37708 0.37707 0.37706 0.37705
*O 0.00002 0.00002 0.00002 0.00002
*OH 0.00151 0.00151 0.00150 0.00149

* THERMODYNAMIC PROPERTIES FITTED TO 20000.K

NOTE. WEIGHT FRACTION OF FUEL IN TOTAL FUELS AND OF OXIDANT IN TOTAL OXIDANTS